NTNU

Norwegian University of
Science and Technology

# Hyperspectral Analysis of Plastic Particles in the Ocean

**Silja Bogfjellmo**

Master of Science in Electronics
Submission date: June 2016
Supervisor: Lise Lyngsnes Randeberg, IET
Co-supervisor: Astrid Aksnes, IET

Norwegian University of Science and Technology
Department of Electronics and Telecommunications

# Problem Description

Plastics in the ocean is an increasing environmental problem. One problem is to collect the plastics floating around, another is to characterize and map where the plastics are. Previously different methods have been used with varying effect.

The thesis should investigate the method of characterizing plastics in water using hyperspectral imaging and three different analysis tools.

The thesis should contain these elements:

1. A theoretical introduction to hyperspectral imaging, environmental concerns, optical properties, material characteristics and analyzing methods.

2. Perform introductory hyperspectral imaging of plastics in water in a laboratory setup.

3. Analyze the laboratory results with three different statistical tools, such as principal component analysis, as well as identifying the main absorption features.

4. Presentation and discussion of the achieved results. Comparison of the results to literature, and comparison of the different analyses.

# Abstract

Huge amounts of plastics end up in the ocean each year. Some of the plastics are eaten by fish and birds, and can cause death. It is important to find an easy, fast and reliable method to detect the plastics, as a first step towards a solution for removing these from the ocean.

Hydrocarbons (C-H bindings) are found in all types of plastics, and their absorption properties are significant in the short wave infrared (SWIR) region between 1000 nm to 2300 nm. A hyperspectral camera operating in the SWIR region was chosen to record these optical properties.

Samples of plastic have been collected and imaged in a laboratory setup. The plastics were imaged alone and together with seawater. The hyperspectral images have been inspected and analyzed to find the main spectral features and to identify the plastics and the water correctly. The analyzing methods used were spectral angle mapper (SAM), principal component analysis (PCA) and partial least squares-discriminant analysis (PLS-DA).

The absorption peaks of the plastic types were found to match the absorption peaks for C-H-bindings reported in the literature. The absorption peaks were found at 1100 nm–1225 nm, 1300 nm–1420 nm, 1650 nm–1800 nm and 2200 nm–2450 nm.

SAM proved to be the most consistent method for identification of the different types of plastics, and was able to correctly identify the materials in the images. The analysis using PCA showed an inconsistency between the images, and was not always able to distinguish between plastic and water. PLS-DA worked well for some samples. The data basis acquired was too small to achieve a training set for PLS-DA that were big enough to get consistently good predictions.

To make hyperspectral imaging of plastics in the ocean more applicable, the mentioned analysis methods were also used to analyze images made up of three spectral bands (instead of the original 256). Four bands were chosen from the mean spectral features observed for the different plastics, and were found at 1162 nm, 1392 nm, 1684 nm and 2281 nm. Using the band at 1392 nm and two of the mentioned bands, the analysis showed promising results to identify the plastics from the water.

In the ocean and on the shoreline, other materials like seaweed, vegetation, glass and cardboard are found. These spectra have been compared to the plastics, which have significantly different features than the other materials. Therefore, hyperspectral imaging is an applicable method to detect plastics in the ocean.

# Sammendrag

Store mengder med plast havner i sjøen hvert år. Noe av plasten blir spist av fisk og fugl, noe som kan medføre død. Det er viktig å finne en enkel, rask og pålitelig måte for å detektere plasten i havet, som det første steget mot en løsning for å fjerne plasten fra havet.

Hydrokarboner (C-H-bindinger) finnes i alle typer plast, og de har tydlige absorpsjonsegenskaper for bølgelengder i området 1000 nm–2300 nm, som er kortbølget infrarødt lys (SWIR). For å måle disse absorpsjonsegenskapene er det valgt å bruke et hyperspektralt kamera som operer i SWIR-området.

Plastprøver ble samlet in og avbildet i et laboratorium. Plasten ble avbildet alene og sammen med havvann. De hyperspektrale bildene ble analyserte for å finne de viktigste absorpsjonsegenskapene i spektrene og for å kunne identifisere plasten og vannet fra hverandre. Analysemedone som ble brukt i oppgaven var spektralvinkelkartlegging (SAM), prinsipalkomponentsanalyse (PCA) og partiell minstekvadrats-diskiminantsanalyse (PLS-DA).

De observerte absorpsjonstoppene for plast stemte overens med absorpsjonstoppene funnet i litteraturen for C-H-bindinger. Absorpsjonstoppene ble funnet ved 1100 nm–1225 nm, 1300 nm–1420 nm, 1650 nm–1800 nm og 2200 nm–2450 nm.

SAM viste seg å være den mest konsistente analysemetoden for å identifisere de ulike typene plast, og ga korrekt klassifisering av materialene i bildene. Analysen med PCA var ukonsistent fra bilde til bilde og i enkelte tilfeller klarte den ikke å skille mellom vann og plast. PLS-DA fungerte godt for enkelte bilder. Datagrunnlaget brukt i treningssettet til PLS-DAen var for lite for å få konsistent gode predikerte resultater.

For å få hyperspektral avbilding av plast i havet mer anvendelig, ble de ovennevnte analysemetodene brukt til å analysere bilder med kun tre bånd (istedenfor de 256 originale). Gjennomsnittet til absjorbsjonstoppene for de ulike spektrene ble funnet ved 1162 nm, 1392 nm, 1684 nm and 2281 nm. Ved å bruke båndet ved 1392 nm og to andre av disse båndene viste det seg å gi lovende resultater for å identifisere plast fra vann.

I havet og ved strandlinjen finner man også andre materialer, slik som tang, tare, vegetasjon, glass og papp. Spektrene til disse materialene ble sammenlignet med plastens spektre, og de spektrale forskjellene var signifikante. Hyperspektral avbildning kan derfor brukes til å detektere plast i havet.

# Preface

This master thesis has been performed during the spring semester of 2016 at the Department of Electronics and Telecommunications (IET), Norwegian University of Science and Technology (NTNU). The master thesis is designed to take all of the work load of the $10^{th}$ semester at NTNU.

The work in this thesis is loosely based on previous work performed by me.[1] Some parts of the project thesis has been reused in the theory and methods section with different levels of modification. This includes the background of hyperspectral imaging, the theory of absorption and scattering, the analyses, and the experimental setup. This includes several of the images included in the above-mentioned

I have appreciated being able to work with something I care about: the environment. Being able do to that in combination with working with the interesting technology of hyperspectral imaging were the motivations behind choosing this topic for my master thesis. Being in contact with "Bellona", "Miljøvernforbundet" and "NIVA" increased the engagement for the environment.

There have been some struggles during the project. Collecting enough plastics from all the material types were more difficult than expected, especially since some types of plastics were not flat enough and some were too light and got blown away by the cooling fan of the lamp. Handling data of big volumes gave my computer some difficulties, due to lack of RAM.

I would like to thank my supervisor Lise Lyngsnes Randeberg for the theoretical help with the hyperspectral analysis, optical properties and help with the laboratory work. I would also like to thank my other supervisor Astrid Aksnes for the work she has done to keep me on track. She has helped me set up meetings, structuring my report, as well as correcting the language of parts of this thesis. Lukasz Paluchowski, a PhD student at NTNU has taught me how the MNF works, step by step. Asgeir Bjørgan, a scientist at NTNU that has helped me perform the MNF and inverse MNF for all the images acquired. Thank you!

Last but not least I would like to thank my significant other, Jonas Agentoft Eggen for mental support, discussions and my go-to for MATLAB-problems.

Trondheim, June 2016

Silja Bogfjellmo

# Contents


**1 Introduction** **1**
1.1 Environmental Perspective . . . 1
1.1.1 Microplastic . . . 1
1.1.2 Chemical Absorption by Plastics . . . 2
1.2 Hyperspectral Imaging . . . 3
1.3 State of the Art . . . 3
1.4 Overview of the Thesis . . . 4

**2 Theory** **5**
2.1 Hyperspectral Imaging . . . 5
2.1.1 Basic Operational Principle . . . 6
2.1.2 Advantages and Disadvantages . . . 6
2.1.3 Acquisition Methods . . . 7
2.1.4 Focal Plane Arrays and tunable Filters . . . 8
2.1.5 Image processing . . . 9
2.2 Optical Properties . . . 12
2.2.1 Absorption . . . 12
2.2.2 Scattering . . . 13
2.2.3 Absorption and Scattering . . . 14
2.2.4 Optical Properties of Plastic . . . 14
2.3 Materials . . . 15
2.3.1 Polyethylene . . . 15
2.3.2 Polypropylene . . . 16
2.3.3 Polyvinyl Chloride . . . 17
2.3.4 Polyethylene Terephthalate . . . 17
2.3.5 Polystyrene . . . 17
2.3.6 Water . . . 18
2.3.7 Plastic Fillers . . . 18
2.3.8 Material Characteristics . . . 18
2.3.9 Chemical Structure . . . 19
2.3.10 Absorption Characteristics . . . 19
2.4 Analysis . . . 21
2.4.1 Principal Component Analysis (PCA) . . . 21
2.4.2 Minimum Noise Fraction (MNF) . . . 24
2.4.3 Spectral Angle Mapper (SAM) . . . 25

2.4.4 Partial Least Squares-Discriminant Analysis . . . . . 26
2.4.5 Comparison of the Three Models . . . . . 27

**3 Methods** **29**
3.1 Collection of Materials . . . . . 29
3.2 Test . . . . . 29
3.2.1 Test 1 . . . . . 30
3.2.2 Test 2 . . . . . 30
3.2.3 Test 3 . . . . . 32
3.3 Experimental Setup . . . . . 32
3.4 Analysis . . . . . 36
3.4.1 MATLAB and Evince . . . . . 38

**4 Results and Discussion** **39**
4.1 Collection of Samples . . . . . 39
4.2 Results of Pre-Process Correction . . . . . 40
4.3 Spectral Analysis . . . . . 41
4.3.1 Absorption in Water . . . . . 41
4.3.2 Comparison of NaCl-Water and Seawater . . . . . 42
4.3.3 Comparison of PE, PP, PET, PVC, and PS Spectra for Wavelengths between 1000nm and 2000nm . . . . . 43
4.3.4 Effect of the Thickness of Water Layer . . . . . 44
4.3.5 Spectral Features . . . . . 45
4.3.6 Low Reflectance Materials . . . . . 45
4.4 Spectral Angle Mapper . . . . . 48
4.4.1 White Plastic Fragments on Black Cardboard . . . . . 48
4.4.2 Different Types of Plastic on Glass . . . . . 49
4.4.3 Plastics with Added Water . . . . . 50
4.4.4 Effect of the Changing Thickness of Water Layer . . . . . 51
4.4.5 PP from Different Sources . . . . . 52
4.5 Principal Component Analysis . . . . . 54
4.5.1 White Plastic Fragments on Black Cardboard . . . . . 54
4.5.2 Plastics with Added Water . . . . . 55
4.5.3 Effect of the Changing Thickness of Water Layer . . . . . 56
4.5.4 PP from Different Sources . . . . . 58
4.6 Partial Least Squares-Discriminant Analysis . . . . . 58
4.6.1 White Plastic Fragments on Black Cardboard . . . . . 58
4.6.2 Plastics with Added Water . . . . . 59
4.6.3 Effect of the Changing Thickness of Water Layer . . . . . 60
4.6.4 PP from Different Sources . . . . . 61
4.7 Accuracy . . . . . 62

4.8 Three Band Analysis . . . . . 63
4.9 Discussion . . . . . 64

**5 Conclusion** **69**
5.1 Recommendations for Further Work . . . . . 70

**A Attachments** **83**
A.1 Matlab-files . . . . . 83
A.1.1 Image Viewer . . . . . 83
A.1.2 Spectral Angle Mapper . . . . . 87
A.1.3 Principal Component Analysis . . . . . 90
A.1.4 Partial Least Squares-Discriminant Analysis . . . . . 96
A.1.5 Joiner . . . . . 99
A.1.6 Crop Image . . . . . 100
A.1.7 Mean Plotter . . . . . 100
A.2 Instrumentation . . . . . 102
A.2.1 Petri Dish . . . . . 102
A.2.2 HySpex SWIR-320m-e . . . . . 102
A.2.3 Salt Water . . . . . 103
A.2.4 Versalight$^{TM}$Polarizer IR . . . . . 104

# List of Figures


1.1 Dead albatross with plastics in stomach. . . . . 2

2.1 Hyperspectral imaging cube . . . . . 5
2.2 Different acquisition methods . . . . . 7
2.3 Contrast comparison . . . . . 10
2.4 Pseudo-coloring . . . . . 11
2.5 Vibration and rotation of atoms, absorption . . . . . 13
2.6 Electromagnetic spectrum . . . . . 13
2.7 Effect of Thickness of Plastic Layer in Water . . . . . 16
2.8 Chemical structure of materials . . . . . 19
2.9 Material Spectra . . . . . 20
2.10 PCA, two-dimensional . . . . . 21
2.11 Principal component variance . . . . . 24
2.12 Spectral Angle Mapper . . . . . 25

3.1 Plastic recycling symbol . . . . . 29
3.2 Plastic-matrix . . . . . 33
3.3 Laboratory setup . . . . . 34
3.4 Light source spectra, uncalibrated . . . . . 34
3.5 RGB-image of the placement of the sample and the white standard. 35
3.6 Flowchart of the image chain . . . . . 36
3.7 Correction of light distribution . . . . . 37

4.1 Collected plastic and seawater . . . . . 39
4.2 Calibration . . . . . 40
4.3 Light source reflectance . . . . . 41
4.4 Reflectance spectra of salt water . . . . . 42
4.5 Spectra of NaCl-water and seawater . . . . . 42
4.6 Comparison of mean-spectra . . . . . 43
4.7 Different levels of water . . . . . 44
4.8 Spectral Features of Plastic . . . . . 46
4.9 Comparison of different color plastic spectra . . . . . 47
4.10 Comparing the reflectance spectra of PP from different sources . . . 48
4.11 SAM of plastic-matrix on cardboard . . . . . 49
4.12 SAM of the different types of plastic, $t = 0.05$ . . . . . 50
4.13 SAM of the different types of plastic, $t = 0.10$ . . . . . 50

4.14 SAM of plastics with 20 ml added water. $t = 0.05$ . . . . . 51
4.15 SAM of plastics with 20 ml added water. $t = 0.10$ . . . . . 51
4.16 SAM of PE with changing water thickness $t = 0.05$ . . . . . 52
4.17 SAM of PE with changing water thickness $t = 0.10$ . . . . . 52
4.18 SAM of seven types of PP from different sources . . . . . 53
4.19 PCA of cardboard-matrix . . . . . 55
4.21 PCA of PE with changing level of water . . . . . 56
4.20 PCA of the samples with 20 ml added water . . . . . 57
4.22 PCA of PP from seven different sources . . . . . 58
4.23 PLS-DA of plastic on cardboard . . . . . 59
4.24 PLS-DA of plastics in 20 ml added water . . . . . 60
4.25 PLS-DA of PE with 20 ml, 30 ml, 40 ml and 50 ml water . . . . . 60
4.26 PLS-DA of seven different types of PP, and PLS-DA of different types of plastics in water . . . . . 61
4.27 SAM, PCA and PLS-DA, three bands . . . . . 63
4.28 SAM, PCA and PLS-DA, three bands . . . . . 64
4.29 SAM, PCA and PLS-DA of plastics with 20 ml added water . . . . 65
4.30 Spectra of glass, cardboard, seaweed, water, soil, grass, and vegetation. . . . . 66

A.1 Image Viewer . . . . . 87
A.2 SAM threshold . . . . . 90
A.3 PCA GUI . . . . . 96
A.4 PLS-DA as shown in evince . . . . . 98
A.5 Salt Water . . . . . 104

# List of Tables


2.1 Material parameters . . . . . 18
2.2 Wavelength Properties . . . . . 20
2.3 Pros of the three methods. PCA,[2] SAM,[3] and PLS-DA[4] . . . . . 27
2.4 Cons PCA,[3] SAM,[2] and PLS-DA[4] . . . . . 27

3.1 Test matrix scheme 1 . . . . . 30
3.2 Test matrix scheme 2 . . . . . 31
3.3 Test matrix scheme 3 . . . . . 32

4.1 Plastic collection . . . . . 40
4.2 Observed Absorption Peaks . . . . . 45
4.3 Classified pixels by SAM . . . . . 49
4.4 SAM between the samples . . . . . 53
4.5 SAM between the PP's . . . . . 54
4.6 Classified pixels by PCA . . . . . 55
4.7 Classified pixels by PLS-DA . . . . . 59
4.8 Accuracy table . . . . . 62
4.9 Classification-percentage of SAM, PCA and PLS-DA . . . . . 62
4.10 Comparison of SAM, PCA, and PLS-DA . . . . . 67

A.1 Petri Dish Specifications . . . . . 102
A.2 HySpex SWIR-320m-e Main Specifications . . . . . 103
A.3 Versalight$^{TM}$Polarizer . . . . . 104

# Acronyms

| | |
|---|---|
| **HSI** | Hyperspectral Imaging |
| **IR** | Infrared |
| **NIR** | Near Infrared |
| **PC** | Principal Component |
| **PCA** | Principal Component Analysis |
| **PE** | Polyethylene |
| **PET** | Polyethylene Terephthalate |
| **PLS-DA** | Partial Least-Squares Discriminant Analysis |
| **PP** | Polypropylene |
| **PS** | Polystyrene |
| **PVC** | Polyvinyl Chloride |
| **RGB** | Red Green Blue |
| **ROI** | Region of Interest |
| **SAM** | Spectral Angle Mapper |
| **SNR** | Signal to Noise Ratio |
| **SWIR** | Short Wave Infrared |
| **TIR** | Total Internal Reflection |
| **UV** | Ultraviolet |
| **VIS** | Visible region |

# Chapter 1: Introduction

In today's process of recycling plastics, a common technique for sorting the plastics is hyperspectral imaging (HSI). Plastics are imaged by a hyperspectral camera and classified through image analysis before it is sorted according to chemical composition/type of plastic. This is the reason for choosing hyperspectral imaging as a possible technique for analyzing and distinguishing plastics in the ocean.

## 1.1 Environmental Perspective

One of the main focuses of this master thesis is the environmental aspect. To be able to map the plastics floating around in the ocean, which again breaks down to microplastics is an important step to fight the environmental damages observed in the oceans.

Over the past decades the production of plastic has increased drastically, and some of the plastic ends up in the ocean. An estimated 20 million metric tons of plastic enters the ocean every year.[5] The plastic floating around has been found in the digestive systems of organisms of all sizes, from small marine invertebrates to whales.[6] Ingestion of plastics might cause choking, starvation (due to no space left for food), internal injuries or digestive tract blockage.[7–9] See Figure 1.1 for illustration.

Lost fishing nets and fishing lines keep on "ghost fishing" in the ocean, and often entangles wildlife. An entangled creature might drown, get wounded, have decreased ability to catch food and avoid predators.[11,12] This also yields for fishing nets on the seafloor, that might cause harm to the living creatures and plants and the seafloor.

Different types of plastics have different densities, and can be both denser and less dense than water. Due to density difference, plastics are found throughout the ocean column. In addition, the growth of marine organisms on floating plastic might change the overall density and make it sink.

### 1.1.1 Microplastic

Microplastics, also known as microbeads, are generally defined as plastic particles smaller than 5 mm. According to a report stating the amount of primary source microplastics in Norway, most of the microplastic comes from unintentional wear and tear of vehicle tires, approximately contributing 2250 metric tons out of a

Figure 1.1: Dead albatross with plastics in stomach.[10]

total of 4000 metric tons.[13] Several articles and blogs have through the last years exposed this new environmental threat, and often focused on the microplastic in cosmetic and personal care items, which according to the study only contributes to 4 metric tons out of 4000 in Norway.[13–16]

In the United States of America, a ban on microplastic in cosmetic products was announced in 2015, and will take effect from 2017 and by July 2019 the distribution will be completely halted. The daily release of microbeads in the U.S. is estimated to eight trillion particles that comes from cosmetic products.[16]

### 1.1.2 Chemical Absorption by Plastics

Plastic is in addition a potential carrier of chemicals. Several studies have characterized and measured the amount of chemicals in plastic. Plastic products with and without bisphenol A (BPA) have both been characterized to have estrogenic activity (EA), which might cause adverse health effects.[17] In birds, higher-brominated congeners (flame retardant) has been detected in the fatty tissue, a chemical not present in natural prey. In the birds where polybrominated diphenyl ether (PBDE) was detected, PBDE was also detected in the plastic found in their stomachs. This study suggests that the detection of PBDE in the birds can be explained by the ingestion of plastic.[18]

Filter feeders are at high risk of ingesting microplastic, as it is similar in size to phytoplankton. One study has looked at the effect of oyster's ingesting polystyrene microplastic. The study showed a clear impact on the oyster's ability to reproduce, due to the intake of PS microplastic.[19]

Plastics can absorb contaminants already present in the ocean, such as polychlorinated biphenyls (PCB), dichlorodiphenyltrichloroethane DDT) and aqueous metals. It has been shown that these contaminants are linked to health impacts

such as disease and reproduction abnormalities.[20,21]

## 1.2 Hyperspectral Imaging

Different material compositions have different spectral fingerprints, and can be identified by their spectral signature. The ability to distinguish between materials and their placement is one of the advantages of hyperspectral imaging. This project thesis has looked into the possibility to use hyperspectral imaging to identify plastics in the ocean.

Hyperspectral imaging is a non-contact method and does not disturb the organisms at sea. In earlier experiments for measuring the amount (and type) of plastics at sea, a boat mission collecting plastics with a following analysis with i.e. Fourier transform IR back at the mainland laboratory has been the performed.[22,23] That is a slow process. HSI on the other hand gives results relatively fast after the images are taken. This means actions could be initiated quicker. In earlier experiments for test

In this thesis, which is an introductory study, the experiments have been done in a laboratory. Known samples have been imaged to obtain spectral information, and further analyzed with different statistical tools.

## 1.3 State of the Art

The implementation of different algorithms to process and handle the large amount of data generated for each image in HSI is important for the success of HSI. Different samples and different purposes have led to many multivariate and statistical methods to analyze hyperspectral data. They all have their advantages and disadvantages, which makes it important to choose the correct method for the purpose.[24]

One study, published in 2015, mainly used partial least squares-discriminant analysis (PLS-DA) on hyperspectral images in the near-infrared region to differentiate between several types of plastic. Other algorithms were used beforehand to prepare the image for analysis (e.g. principal component analysis (PCA), manual selections and clustering).[24]

Magnetic density separation (MDS) is a technique differentiating between material densities. To verify the separation between polyethylene (PE) and polypropylene (PP) by MDS, HSI was used. By using the PCA and PLS-DA algorithms, it was found that MDS showed promising results. MDS was able separate the PE and PP products to generate high quality products when recycled.[25]

There is an ongoing study in Germany, which studies microplastics in water. Estimation of plastic debris loads in ecosystems from water samples using hyper-

spectral imaging, and monitoring of contamination by plastic debris in aquatic ecosystems are two of the topics from conferences. None of the information is public yet, and the work is still in progress. The researcher was not able to give any details or descriptions through contact with him.[26]

HSI is well developed within the field of quality control and sorting of food. This field is evolving, due to several reasons, including non-invasive, non-destructive analysis that can reduce the waste of food. One study performed at NTNU looked into the possibility of using HSI in an automated sorting system for roe, milt and liver from the Atlantic cod. The sorting was done using spectral angle mapping (SAM) and two wavelength bands. The implementation of the system can reduce the loss of raw material.[27]

Taking airborne hyperspectral images has been done from airplanes for biomass characterization and detection of oil spills. Small unmanned air vehicles like drones have been made with a hyperspectral camera in the mid-IR range. The camera was light weight, only 1.7 kg and was mounted on a drone. It has been tested and proven to work. The cost was small, which makes hyperspectral imaging more available. Environmental measurements will be performed in future works.[28] This technology might be a part of future farming, where the images taken can help to characterize the state of the crops.

## 1.4 Overview of the Thesis

The background theory for this master thesis is given in chapter 2, it presents the background theory for this master thesis, and includes theory about hyperspectral imaging, optical properties, analyzing methods and the properties of the materials used for testing. chapter 3 describes the methods used for collecting the materials, the laboratory/experimental setup and tests as well as how the analysis was performed. The results of the measurements and the discussion and results of the analysis are presented in chapter 4. The chapter include the results by the analyzing algorithms PCA, SAM, and PLS-DA. The conclusions drawn from chapter 4 are found in chapter 5, together with the proposals for future work.

# Chapter 2: Theory

This chapter represents the theory behind this thesis. The principles of hyperspectral imaging, the characteristics of different plastic materials, the algorithms used for analysis and the optical properties of materials will be presented. Section 2.1, section 2.2 and section 2.4 are taken and altered from the project report "Field-Deployable Hyperspectral Analysis".[1]

## 2.1 Hyperspectral Imaging

Hyperspectral imaging is a type of imaging which collects information from a number of electromagnetic bands. In hyperspectral imaging the information collected per image is great, since the spectral dimension contains a large number (several hundreds) of bands. Thus, it can give useful information, since different molecules will give different spectral fingerprints. Figure 2.1 shows a hyperspectral image cube and the reflectance spectra of a given pixel.

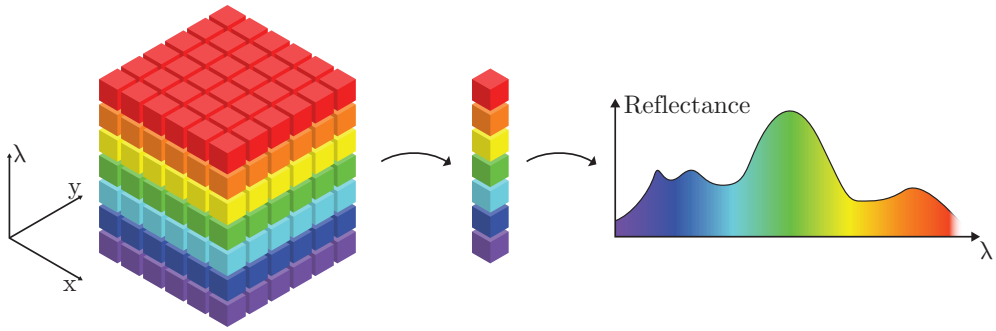


Figure 2.1: Hyperspectral imaging cube, with $x$ and $y$ representing the spatial dimensions, while $\lambda$ represents the wavelength in the spectral dimension.

Hyperspectral imaging combines two mature technologies, spectroscopy and imaging. In this technology, an image is acquired over a chosen region of wavelengths to describe each pixel in the image. These pixels are spectral pixels, and correspond to the spectral signature of that spatial region.[29]

Spectroscopy is an established technique for determining the chemical composition of materials. It gives a detailed fingerprint from the interaction between

the electromagnetic spectra and the atoms and molecules. They provide both qualitative and quantitative measurements of the sample. This could be measured in transmittance, reflectance, absorbance, phosphorescence, fluorescence and/or radioactive decay.[30] In Figure 2.1, the rightmost part of the figure shows the reflectance-wavelength spectra of one pixel in the image.

The material inspected needs to be illuminated by a light source that emits in the wavelength regions of interest (ROI). This could be in the near infrared (NIR) region, the infrared (IR) region, the visible (VIS) region, other regions or a combination of them.

### 2.1.1 Basic Operational Principle

A lens and an aspheric mirror focuses the incoming light from the area imaged. The light is focused into a slit that defines the field of view (FOV). Behind the slit is another aspherical mirror that collimates the light onto a grating for dispersion (different wavelengths are refracted in different angles, and it "splits" the light). The grating is followed by an objective lens that focuses the light onto a charge couple device (CCD). The CCD is the detecting array where the amount of incoming light is measured.[31]

### 2.1.2 Advantages and Disadvantages

Hyperspectral imaging has numerous advantages. Due to the large amount of information, the identification capabilities of hyperspectral imaging can be used in several applications. Once the model is built and validated, it is simple to use and economic, as time and labor is saved. It is a flexible method, the region of interest can be changed, and gives both qualitative and quantitative measurements. It is non-invasive and therefore a nondestructive method, such that the sample can be used for further analysis. One of the most important advantages is the possibility to extract the spectral signatures of each pixel, and therefore identify exactly where the components of interest are located.[30]

There are also a few disadvantages, but for many purposes the advantages outweigh the disadvantages. One of the main problems is the huge amount of data. Especially when space and weight is limited, the computational power and storage needed are substantial. It is a real-time instrument with the aid of real-time-specified algorithms, but is generally not real-time, as the amount of data is substantial.[32] Another problem is overlapping bands, which can make it difficult to identify a specific chemical compound. Therefore, it is important to be able to discriminate the object's characteristic absorption features.

Another disadvantage is multicollinearity. Multicollinearity exists when two or more predictor variables in a regression model are highly correlated. This might

result in strange results, but in general it can cause wide confidence intervals and prediction for independent values. To mitigate these problems, further analysis is needed, which again slows down the process.[30,33]

### 2.1.3 Acquisition Methods

There are several methods of acquisition, and two of them are spatial scanning and spectral scanning. Spatial scanning generates hyperspectral images by acquiring the whole spectrum for a pixel or a line, and then spatially scans through a scene.[34] Spectral scanning freezes the position and scans through the different wavelengths. See Figure 2.2, showing the different acquisition methods.

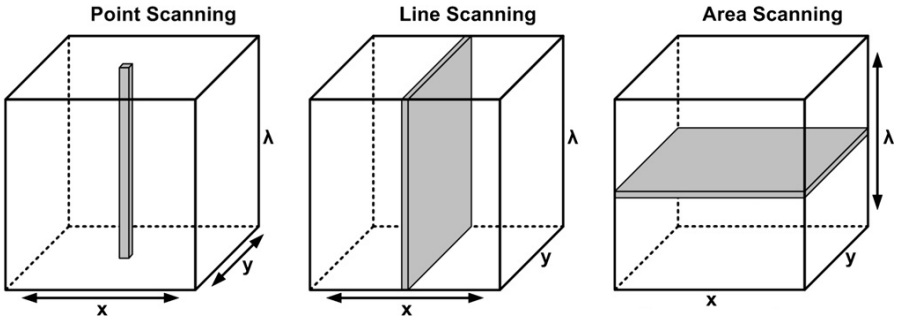


Figure 2.2: Different acquisition methods. From left to right: Point-scanning (whiskbroom), line-scanning (pushbroom) and area-scanning. The three dimensions are as shown in the image, $x$ and $y$ are the spatial dimensions, while $\lambda$ is the spectral dimension.[35]

#### Whiskbroom

Whiskbroom, also known as point-scan imaging, scans an area one pixel at a time while the scanning element moves continuously. The light coming from the object (from that particular pixel) is dispersed by a dispersing element (e.g. a prism or a diffraction grating). Then, there is a detection element for each wavelength to be recorded. This method gives a stable high resolution spectrum, but the method is very time consuming. This method is common in microscopic imaging, as its resolution is more important than speed.[30]

#### Pushbroom

Pushbroom, also known as line-scan imaging is the most common method and is used in this project. A row of pixels is imaged simultaneously, and linear scanning provides the last spatial dimension.[36] The principle for this method is partially

the same as for whiskbroom, where a dispersing element is used. The difference is that this method uses a two-dimensional dispersion element and a two-dimensional detection array. The speed of this type of acquisition is faster than the whiskbroom, and is mainly limited by the camera read-out speed.[30]

#### Area Scanning

Area scanning is as the name proposes, a method that scans a fixed spatial area in the spectral dimension. Single band images are acquired with the use of filters and stacked on top of each other.[30]

#### Single Shot

The single shot or one-shot camera acquires both the spectral and spatial information at once, with no scanning involved. To do this, more advanced optics and a software reconstruction algorithm are used. To capture fast moving objects, such as an explosion, one-shot images are needed.[37]

#### Fourier Transform IR

Fourier Transform IR (FT-IR) acquires an interferogram instead of a spectrum. For a mono-pixel FT-IR spectrometer, each pixel has a recorded interferogram for a specific location in the scene.[38] The interferogram consists of a sum of cosines. The cosine components are created by interference of monochromatic light. The data will then be processed by a Fourier transform to get the spectra. Since the detected signal contains a combination of cosines of all wavelengths, the FT-IR method can achieve a high spectral resolution.[39] It is also a method with high signal to noise ratio (SNR) which partly comes from the higher energy throughput (higher detected signal) and partly due to the reason of higher spectral resolution.[40] Multi-pixel FT-IR provides more accurate spatial characterization.[38]

### 2.1.4 Focal Plane Arrays and tunable Filters

Focal plane array (FPA), is an array of light-sensing pixels at the focal plane of a lens. The development in material science, optics, and electronics have made high-performance and high-sensitivity cooled and uncooled IR FPAs. InGaAs FPAs are able to operate at room temperature at short wave IR (SWIR) wavelengths.[41]

tunable filters are filters that can separate a narrow band of frequency from a broadband source. Two of the common tunable filters are acousto-optic tunable filters (AOTFs) and electronically tunable filters (ETFs).[42]

One type of ETFs are liquid crystal tunable filters (LCTFs). An LCTF is built using a stack of polarizers and birefringent liquid crystal plates. The LCTF

polarization is sensitive. The switching speed is limited by the relaxation time of the crystal. Normally the relaxation time is in the order of 50 ms. For a short sequence of wavelengths, the relaxation time can be down to 5 ms. The spectral resolution is in the order of several nm.[42]

In AOTFs, a radio frequency is applied to a transducer that generate acoustic waves that propagate through a crystal. The propagating acoustic waves will create a periodic grating that can diffract portions of the incident light beam. It can separate a very narrow band of frequencies out of a broadband source. By changing the frequency of the radio waves, large optical regions can be tuned over. The great tuning range gives AOTFs the advantage of having a wide spectral tuning range. The scanning speed is in the order of µs, and the spectral range of the AOTF depends on the wavelength of the light.[41]

### 2.1.5 Image processing

After acquiring the data, image processing is important to extract the useful information. Normally a hyperspectral image contains hundreds of spectral pixels, where each pixel stores the information of all the recorded spectral bands. The hyperspectral images therefore tend to be very large (in amount of data), as well as being multidimensional. Visual interpretation is difficult without any form of processing. Enhancing features, like removing noise, enhancing edges and sharpening, are some of the processing steps which make interpretation easier.

#### Image Enhancement

The goal of image enhancement is to improve the visibility of certain image features for further analysis and image display. The enhancement should emphasize the image characteristics of interest. Image enhancement includes contrast and edge enhancement, noise filtering, pseudo-coloring, sharpening, and magnification.[29]

Filters are used for blurring and reducing noise. Blurring is used to remove small details, and bridge small gaps in lines. Filters in a matrix-form are used to filter out noise. One can use linear filters, such as low-pass and high-pass filters, or nonlinear filters such as a mean filter.[29]

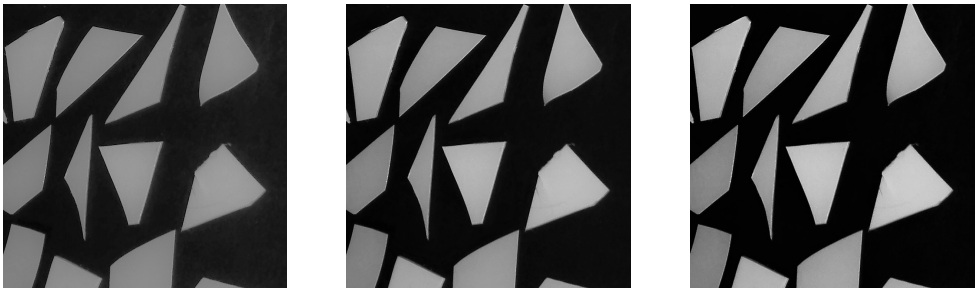

(a) Decreased contrast (b) Original (c) Increased contrast

Figure 2.3: Comparison of different contrast. (a) is a low-passed image (smoothed), (b) the original image, and (c) high-pass filtered, high contrast image.

A mean filter uses a mask made up of the neighboring pixels (which can be the whole image) to find a mean/average grey-level (using the intensity-level of a specific wavelength). The filter then replaces the level of the pixel by the mean of the grey-levels. This can increase or decrease the contrast and brightness. This type of filter gives excellent noise-reduction and reduces the blurring edges in the image. It is therefore important to choose the correct neighboring pixels in terms of spatial distribution and the number of neighbors. A low-pass filter is used to remove the components with higher frequency. This is done in the frequency domain, and over a given frequency components are attenuated. The high frequency components are often image noise or edge components. Low-pass filtering causes smoothing of the image. High-pass filtering on the other hand, sharpens the image by high-pass filtering in the frequency domain, and can enhance the edge components.[43] See Figure 2.3 for image enhancement by filtering.

Pseudo-coloring is a tool that helps to visualize the image, see Figure 2.4. It often simplifies the identification of objects. It is common to use RGB (red, green, blue), which are three colors seen by the human eye. By combining these three colors with different magnitude, most of the wavelengths in the visible region are covered. The colors can relate to the intensity of the signal, where intensity could be measured in for example reflectance or transmittance. By choosing the wavelengths that give the most information, one might be able to classify the different objects in the image. Instead of RGB one could use hue, saturation, and intensity. Different colors in the pseudo-colored image correspond to different features. The coloring aids the human visualization and interpretation of grey-scale images, since hue, saturation, and intensity can be discerned by humans much better than the shades of grey alone.[29]

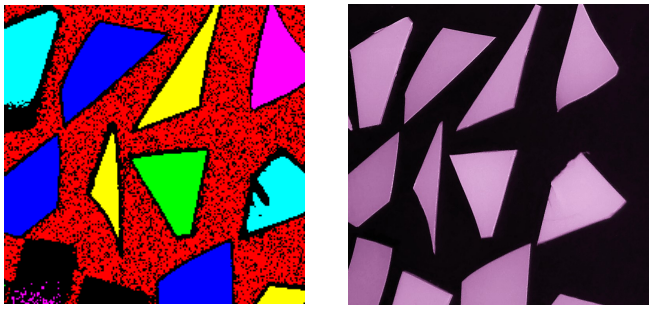

(a) Pseudo-colored (b) Pseudo-colored

Figure 2.4: Psedo-coloring of images. (a) RGB, the different regions have been colored with areas with similar spectra, (b) hue, saturation, and intensity, high hue and high saturation.

Minimum Noise Fraction (MNF) is another method used to remove noise. This method is explained more thoroughly in subsection 2.4.2. MNF in combination with the inverse MNF removes the bands containing the most noise, and has been used in this project.[32]

### Image Segmentation

Image segmentation divides the image into smaller sections/objects. The sections are either found by "similar" image characteristics or by dissimilarities, such as edges. The purpose of image segmentation is to reduce data (the number of sections are smaller than the number of pixels) and extract features (building blocks for recognition).[44]

### Dark Current

Dark current is the current that flows in the detectors when no photons are entering the photosensitive part of the device. Ideally this current would be zero, but in reality it needs to be accounted for. Dark current is normally generated by thermal excitation of the electrons in the detector, and the voltage applied across the detector. The dark current is fluctuating and contributing to the total noise of the image. To correct for the dark current Equation 2.1 is used.[30,34]

$$I_{ref} = \frac{I_{raw} - I_{dark}}{I_{white} - I_{dark}} \tag{2.1}$$

where $I_{ref}$ is the relative reflectance level, $I_{raw}$ is the raw reflectance image, $I_{dark}$ and $I_{white}$ are the dark current and the white reference intensity, respectively. This effect is corrected by the camera software.

## 2.2 Optical Properties

The optical properties affecting the spectra of a material are absorption and scattering. The amount of absorption and scattering changes according to wavelength and depend on the material composition. A material, especially a mixture of materials, will have a complex spectra consisting of both absorption and scattering. In this section they are explained separately for simplicity.

### 2.2.1 Absorption

Electrons are bound to atoms, and can be excited by incoming photons, see Figure 2.5 (G). For the electron to be excited from one energy level to another, the energy of the photon needs to match the gap between the energy levels, where the energy of the photon is given by Equation 2.2. Absorption happens when electrons absorb the energy of the photon, and the frequency $\nu$ matches the natural frequency of the atom.[45]

$$E = h\nu \tag{2.2}$$

where $E$ is the energy of the photon, $h$ is Planck's constant, and $\nu$ is the frequency.

The energy absorbed from the photon that matches the natural frequency is transformed into internal energy, and leads to vibration, stretching or bending, as shown in Figure 2.5 (A-F). The absorption of photons depend on the composition of the material. Different materials and their composition will determine their fundamental vibration (at the natural frequency).

When two quanta of energy are absorbed, the first overtone is excited and has approximately the double frequency of the natural frequency. The second overtone is excited by three quanta of energy. Another phenomenon is combination bands. Combination bands are observed when two or more fundamental vibrations are excited simultaneously. By scanning over a frequency range one can obtain the absorption spectra of that particular material.[46,47]

In an ideally absorbing medium, a medium with no scattering, one can use Beer's law for ideally absorbing media:

$$I(x) = I_0 e^{-\mu_a x} \tag{2.3}$$

where $I$ is the intensity, $x$ the distance in the direction of propagation, $I_0$ the intensity at $x = 0$, and $\mu_a$ is the absorption coefficient. Beer's law then gives an exponential relationship between the intensity, the absorption coefficient, and the distance propagated through the medium. $\mu_a$ is set by the medium.[48]

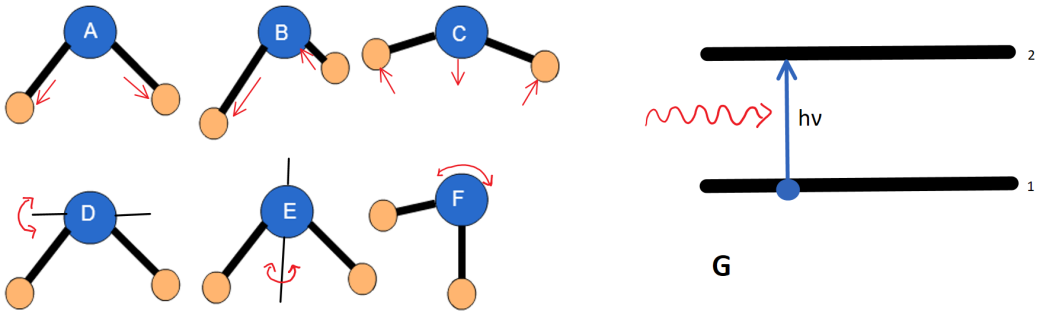


Figure 2.5: Stretching, bending, and vibration of atoms. (A) Symmetric stretch, (B) asymmetric stretch, (C) bend, (D-F) vibration in different directions ((D) $\hat{x}$, (E) $\hat{y}$, (F) $\hat{z}$). (G) Photon with energy $h\nu$ absorbed by an electron.

The electromagnetic spectrum can be seen in Figure 2.6. It shows the relation between the wavelength $\lambda$, the frequency $f$, and the categories they are divided into.

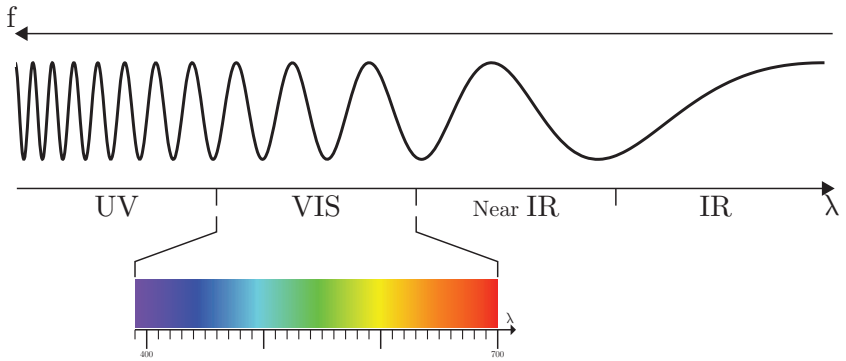


Figure 2.6: The electromagnetic spectrum, divided into categories and labeled $f$ for frequency and $\lambda$ for wavelength. The categories are UV (ultraviolet), VIS (visible region), Near IR (near infrared) and IR (infrared).

### 2.2.2 Scattering

Scattering is the process where light deviating from a straight optical path due to a non-uniform medium.[49] The scattering process involves re-emitting of a photon after absorption, where the re-emitted photon has a different direction. How

photons are scattered, and in what directions they are scattered depend on the wavelength and the material composition and size.

In an ideally scattering medium, with no absorption, one can use Beer's law for ideally scattering media:

$$I(x) = I_0 e^{-\mu_s x} \tag{2.4}$$

where $I$ is the intensity, $x$ the distance in the direction of propagation, $I_0$ the intensity at $x = 0$, and $\mu_s$ the scattering coefficient. Beer's law then gives an exponential relationship between the intensity out and the scattering coefficient and distance propagated through the medium. $\mu_s$ is set by the medium.[48]

### 2.2.3 Absorption and Scattering

Combining both scattering and absorption, we obtain Beer's law for absorbing and scattering media:

$$I(x) = I_0 e^{-\mu_t x} \tag{2.5}$$

where $I$ is the intensity, $x$ the distance in the direction of propagation, $I_0$ the intensity at $x = 0$, and $\mu_t$ is the extinction coefficient, $\mu_t = \mu_s + \mu_a$. Beer's law then gives an exponential relationship between the intensity out and the extinction coefficient and distance propagated through the medium. $\mu_t$ is set by the medium.[48]

### 2.2.4 Optical Properties of Plastic

The observed optical properties of plastic can change from several factors. When plastic floats on water, the reflected spectrum can be affected, due to interaction between the media (different refractive indices). The general rule is that waves at media interfaces (air-plastic and plastic-water) are summed.[50] For one plastic material (e.g. PE), the reflectance will depend on several factors that will be presented in this section.

The enhanced properties plastic fillers can give plastics (see subsection 2.3.7), cause them to often be incorporated in plastic products. Pure plastics (e.g. PE) are homogeneous and will be glossier and cause less scattering.[51] The incorporation of heterogeneous fillers make the material inhomogeneous. This causes light to be scattered rather than transmitted or reflected.[52]

When a material scatters more of the light, it becomes more opaque. Depending on the use of the material and the criteria for its appearance, this might or might not be desired. Adding a coating on top of the plastic can reduce the scattering and increase the reflection to make it appear shinier/glossier.

For the optical properties of plastic composites, two observations are the most important. Smaller particles scatter more light than larger particles, and that decreasing the refractive index contrast between the particle and the surroundings tends to reduce the amount of scattered light by a particle.[52]

Another factor to take into account is the roughness of the surface. If the surface is straight and smooth, compared to the wavelength of the light, the reflected light will be reflected with the same angle to the normal of the surface as the incident light had. For surface roughness the reflection is diffuse, and the reflection depends on the structure of the surface and will be scattered in several directions.[53]

For the case of plastic in water, plastic has a higher refractive index than water. Snell's law states that if the refractive index of the incident (first) material is higher than the second material, the light can experience total internal reflection for angles greater than the critical angle. Therefore the reflectance and transmission properties will change at the boundaries between the materials.[54] Water has a refractive index around 1.33, while the plastic materials tested lays higher at 1.49-1.59. The refractive indices are listed in Table 2.1, and are as follows; PE 1.51-1.54, PP 1.49, PET 1.58, PVC 1.54, and PS 1.59.[55]

Some light will be scattered by the water and can further be transmitted through the plastic.[54] Due to the high absorption of light in water for longer wavelengths (above 1900 nm for thin layers of water and above 1400 nm for thicker layers), this scattering effect will decrease for longer wavelengths.

The thickness of the plastic on a thick water layer is taken into account in Figure 2.7.

All in all, the thickness of the plastic sample, the spectral absorption features, the plastic fillers (color, texture, opacity), the surface roughness, and the scattering within the media all contribute to the shape of the observed absorption bands.

## 2.3 Materials

The five most common plastics, according to production statistics, were chosen for analysis and characteristics.[56–60] Those five types of plastics are polyethylene, polypropylene, polyethylene terephthalate, polyvinyl chloride and polystyrene. One thing the five materials have in common is a C-H binding. In this section a further description of the materials is given.

### 2.3.1 Polyethylene

Polyethylene, PE, is the most common plastic, with an annual global production of 82 million tonnes in 2013.[56] Polyethylene is found in many consumer products,

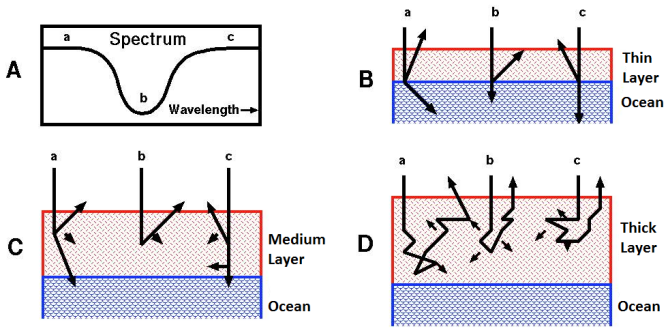


Figure 2.7: Illustration of how light scatters in plastic on water. (A) Shows an example spectrum(black line), with three example wavelengths, a, b, and c. A thin layer of plastic will let all three wavelengths penetrate through the layer in (B). A medium layer in (C) will absorb and scatter the wavelengths in the absorption bands, in this case b. At less absorbing wavelengths, a and c, the light will penetrate deeper. For a thick layer of plastic (D) all the wavelengths will be scattered within the plastic and none will penetrate. The figure is taken and modified from the literature.[54]

like food wrapping, plastic bags and bottles. Polyethylene is made up of ethylene-molecules. The ethylene molecule has the chemical formula $C_2H_4$.[61]

Polyethylene has a melting point of 115–130 °C, and a density of 0.91–0.96 g/cm$^3$. There are different categories of polyethylene, depending on the density. LDPE (low density PE) and HDPE (high density PE) are in the opposite ends of the scale.[62] LDPE has a refractive index of 1.51, while HDPE has a refractive index of 1.54.[55]

HDPE has a low degree of branching and therefore stacks more tightly. Less branching leads to stronger intermolecular forces and makes the material stronger. LDPE on the other hand has a higher degree of branching, and the packing of the structure is less dense, giving weaker intermolecular forces and a weaker material than HDPE.[62]

### 2.3.2 Polypropylene

Polypropylene, PP, is the second most common plastic, with an annual global production of 55 million tonnes in 2013. Polypropylene is found in many products, including food packaging, clothing, reusable containers and ropes.[57]

Polypropylene has a chemical formula $C_3H_6$. The density of polypropylene is typically 0.9 g/cm$^3$ and it has a melting point around 142–163 °C. Due to a higher melting point, plastic made out of polypropylene can withstand higher heat for a longer duration than many other types of plastic.[63] The refractive index of PP is

1.49.[55] In addition polypropylene has a great resistance to fatigue.[64]

### 2.3.3 Polyvinyl Chloride

Polyvinyl chloride, PVC, is the third most widely produced plastic with an annual production of 39 million tonnes in 2013.[58] Polyvinyl chloride is found in payment and membership cards, as insulation in electrical cables and in sewage pipes. Many products containing PVC have added plasticizers to achieve the desired properties.

The chemical formula of polyvinyl chloride is $C_2H_3Cl$. It has a density of $1.38\,g/cm^3$ and a melting point of 121 °C.[65] It has a refractive index of 1.54.[55]

### 2.3.4 Polyethylene Terephthalate

Polyethylene terephthalate, PET, placed fourth in 2012 with an annual production of 20 million tonnes.[59] Polyethylene terephthalate is found in plastic bottles (PET bottles), and is also found as fibers in clothing. In clothing PET is commonly listed as polyester.

Polyethylene terephthalate has a more complex chemical formula than PE and PP, with the chemical formula $C_{10}H_8O_4$. It has a density of $1.30\,g/cm^3$, a melting point around 212 °C,[66] and a refractive index of 1.58.[55]

### 2.3.5 Polystyrene

Polystyrene, PS, had an annual production of approximately 15 million tonnes in 2013.[60] Polystyrene is used in a broad range of food packaging, like yogurt-containers, disposable/takeout food containers (also in the form of Styrofoam), and disposable cutlery.

Polystyrene has the chemical formula $C_8H_8$. It has a density of $1.06\,g/cm^3$, and a melting point at 240 °C.[67] When polystyrene is in the form of Styrofoam, which is polystyrene with up to 98 % air, the density is much lower and it is positively buoyant in water. Polystyrene is brittle and easily breaks into smaller pieces.[68] PS has the highest refractive index of the materials described here, with a refractive index of 1.59.[55]

Polystyrene in the form of single-use Styrofoam has been banned in several cities, such as New York. The Styrofoam is lightweight and easily blows around and often ends up in the ocean. The environmental issue of using a single-use container that is made up of a material that can last a century as well as problems with recycling the material caused the band.[68]

### 2.3.6 Water

The ocean covers around 70% of the earth's surface, and a lot of the waste that is not handled properly after use ends up in the ocean. The ocean is the home of billions of living creatures; for them keeping the ocean clean is crucial.

Water has the chemical formula $H_2O$, and a density of $1.0\,g/cm^3$. The melting point of ice is $0\,°C$, and the refractive index is 1.33.

### 2.3.7 Plastic Fillers

Fillers or additives are added to plastic materials to enhance performance and reduce manufacturing costs. Calcium carbonate, kaolin and alumina trihydrate are some of the fillers. Some of the enhanced properties the fillers can give the plastics are increased resistance to chemicals and corrosion, fire retardancy, greater shrink resistance and more durability for temperature.[69] Other benefits from fillers can give are better particle dispersion in the polymer, improved effectiveness of light scattering, protection from outside influences and color enhancement.[70]

### 2.3.8 Material Characteristics

A summary of the material characteristics is shown in Table 2.1. The time the different types of plastics use to decay vary between different material compositions and environment. In general plastic has a long decay time. Plastic has only been around the last century, which makes it hard to estimate a decay time, but 400-500 years is a general estimate.[71,72]

Table 2.1: Table listing the parameters of the materials. The annual global production given, is given in either 2012 or 2013. Polystyrene is often found as Styrofoam, where the density will be much lower than listed in the table.

| Material | Chemical formula | Production [$10^9$ kg/year] | Melting point [°C] | Density [g/cm$^3$] | Refractive index |
|---|---|---|---|---|---|
| PE | $C_2H_4$ | 82 (2013) | 115-130 | 0.91-0.96 | 1.51-1.54 |
| PP | $C_3H_6$ | 55 (2013) | 142-163 | 0.9 | 1.49 |
| PVC | $C_2H_3Cl$ | 39 (2013) | 212 | 1.45 | 1.58 |
| PET | $C_{10}H_8O_4$ | 20 (2012) | 250 | 1.3 | 1.54 |
| PS | $C_8H_8$ | 15 (2013) | 240 | 1.06 | 1.59 |
| Water | $H_2O$ | | 0 | 1.0 | 1.33 |

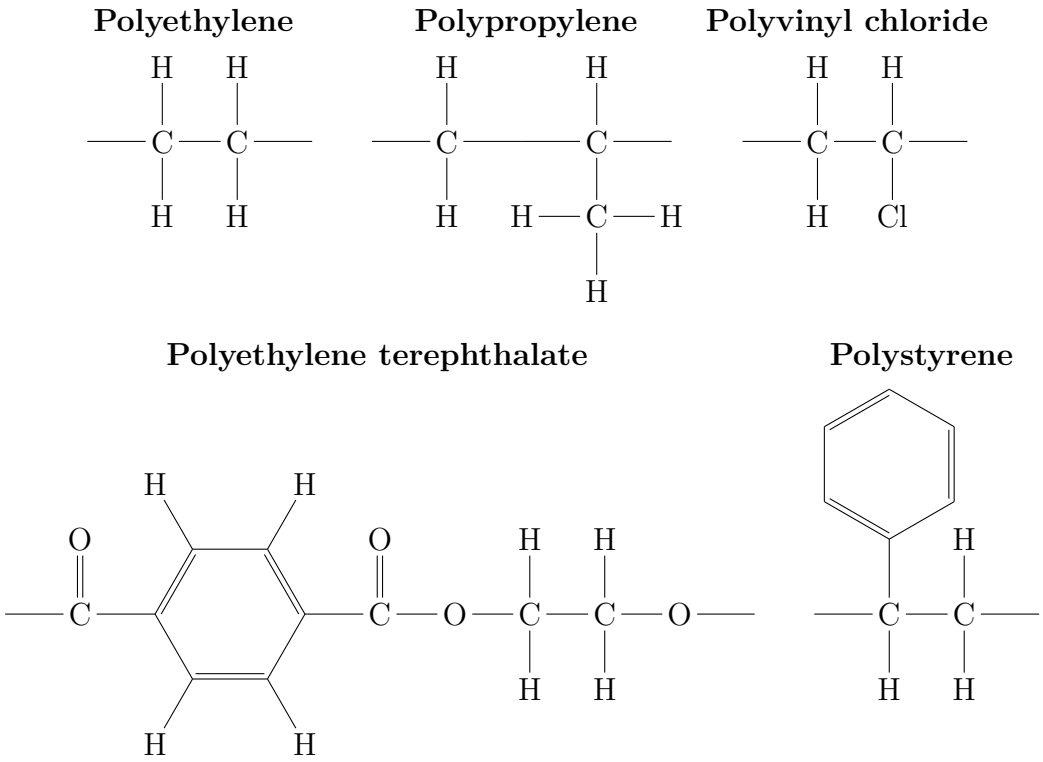


Figure 2.8: The chemical structures of ethylene, propylene, vinyl chloride, ethylene terephthalate and styrene, as named in the plural form in the figure. By combining a single structure together with other similar structures, the poly-form is achieved.

### 2.3.9 Chemical Structure

The chemical structure of the plastics are shown in Figure 2.8.

### 2.3.10 Absorption Characteristics

The absorption peaks for the materials are given in Table 2.2. The absorption features are results of vibrational transitions involving various overtones and combination of the fundamental vibrational transitions.[73]

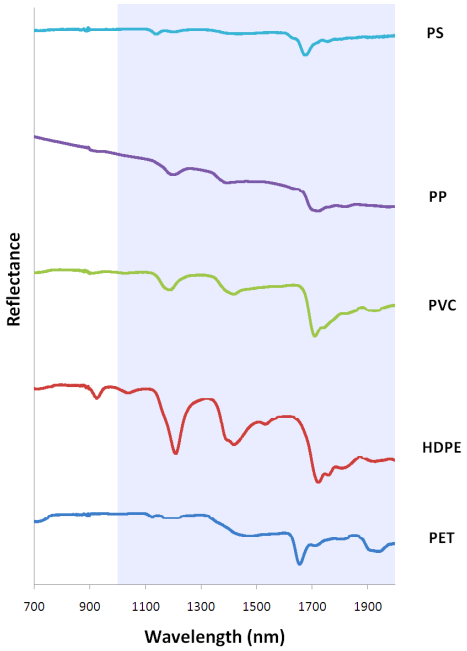


Figure 2.9: Spectra of the plastic materials, PS, PP, PVC, HDPE (PE) and PET. The shaded area indicates the wavelengths coinciding with the recorded wavelengths in this project.[76]

Table 2.2: Absorption properties of the different wavelengths for plastic (C-H)[74,75] and water (H-O-H).[73] Asym. is short for asymmetric, and sym. short for symmetric.

| Wavelength [nm] | Assignment |
|---|---|
| 1100-1225 | Second overtone C-H stretching |
| 1300-1420 | Combination C-H stretching |
| 1650-1800 | First overtone C-H stretching |
| 2200-2450 | Combination C-H stretching |
| 970 | Combination H-O-H asym. stretch and sym. stretch |
| 1200 | Combination H-O-H asym. stretch, sym. stretch and bend |
| 1450 | Combination H-O-H asym. and sym. stretch |
| 1950 | Combination H-O-H bending and asym. stretch |

The spectra of the materials between 700 nm and 2000 nm is shown in Figure 2.9.[76] The data were acquired during an experiment aiming to identify and classify plastics with NIR spectroscopy for the waste sorting industry.

## 2.4 Analysis

The hyperspectral setup used for the experimental part is not real-time, and the analyzing and computation is mostly done afterwards. Minimal Noise Fraction and noise reduction has been done using ENVI 4.8 (Environment for Visualizing Images, ITT Exelis, Tysons Corner, Virginia, USA), while the characterization of the different materials has been done with MATLAB (Mathworks, Kista, Sweden).

### 2.4.1 Principal Component Analysis (PCA)

Principal component analysis, PCA, is a widely used statistical tool. It is a technique to reduce the dimensionality of a data set based on the fact that neighboring bands in hyperspectral imaging often are correlated and contain some of the same information about the object. The analysis is used to transform the original data into equal or fewer bands, by removing the correlation between the original bands.[77]

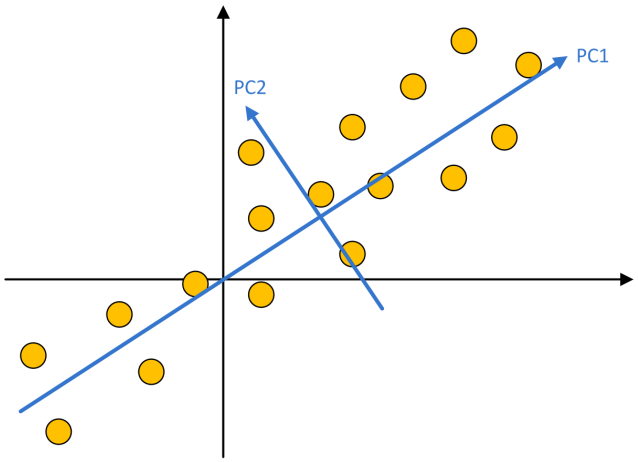


Figure 2.10: PC 1 points in the direction with the greatest variance. PC 2 points in the direction of the greatest variance orthogonal to PC 1. The data is represented by circles. The plot is taken from the literature.[78]

PCA is a good method to reduce the amount of data, and is a good method for the first analysis of data. When the images have been analyzed, and the most important dimensions found, one can reduce the dimensionality by reducing the number of dimensions (wavelength-bands). In a scatter plot made by two PC's, similar samples (pixels) tend to cluster together. Figure 2.10 shows two PC's made in a two-dimensional space. The first PC has the greatest variance, while the second (in a two-dimensional case) is orthogonal to the first component.

To understand how PCA works, some background mathematics will be presented. In the mathematics $\mathbf{x}$ and $\mathbf{y}$ presents one-dimensional data sets, $\mathbf{X}$ and $\mathbf{Y}$ data set matrices, and $\mathbf{P}$ a matrix. The mean of a data set $\mathbf{x}$ in one dimension could be written as:[79]

$$\bar{x} = \frac{1}{n}\sum_{i=1}^{n} x_i \tag{2.6}$$

where $\bar{x}$ is the mean value of vector $\mathbf{x}$ and n the number of elements in $\mathbf{x}$. The mean is used further to find the standard deviation, the variance and the covariance.

The standard deviation gives a measure of how spread out the data set is from the mean. The standard deviation is found through:[79]

$$s = \sqrt{\frac{1}{n-1}\sum_{i=1}^{n}(x_i - \bar{x})^2} \tag{2.7}$$

where $s$ is the standard deviation. The closer the standard deviation is to zero, the less spread the data is. The variance is the square of the standard deviation and is as follows:[79]

$$Var(\mathbf{x}) = s^2 = \frac{1}{n-1}\sum_{i=1}^{n}(x_i - \bar{x})^2 = \frac{1}{n-1}\sum_{i=1}^{n}(x_i - \bar{x})(x_i - \bar{x}) \tag{2.8}$$

where Var($\mathbf{x}$) is the variance of $\mathbf{x}$.

The covariance looks at the relationship between two dimensions. Unlike the mean, the standard deviation and the variance explained above, which only holds in one dimension. The covariance gives the correlation between dimensions. The covariance between data set $\mathbf{x}$ and $\mathbf{y}$ is given by the formula:[79]

$$Cov(\mathbf{x},\mathbf{y}) = \frac{1}{n-1}\sum_{i=1}^{n}(x_i - \bar{x})(y_i - \bar{y}) \tag{2.9}$$

For the covariance, the sign is the most important, it tells us if the data sets change together (positive sign) or change opposite to each other (negative sign).

In hyperspectral imaging the data acquired is multidimensional. Since covariance only takes two dimensions, a covariance matrix is necessary to express the covariance for more than two dimensions. A data set matrix $\mathbf{X}$ with dimensions $m$-by-$n$, where $m$ is the number of variables (wavelength-bands) and $n$ is the number of samples (pixels). The covariance could be written as follows:[80]

$$Cov(\mathbf{X}) = \mathbf{C_X} = \frac{1}{n-1}\mathbf{X}\mathbf{X}^T = \frac{1}{n-1}\begin{pmatrix} \mathbf{x}_1\mathbf{x}_1^T & \mathbf{x}_1\mathbf{x}_2^T & \cdots & \mathbf{x}_1\mathbf{x}_m^T \\ \mathbf{x}_2\mathbf{x}_1^T & \mathbf{x}_2\mathbf{x}_2^T & \cdots & \mathbf{x}_2\mathbf{x}_m^T \\ \vdots & \ddots & \vdots & \\ \mathbf{x}_m\mathbf{x}_1^T & \mathbf{x}_m\mathbf{x}_2^T & \cdots & \mathbf{x}_m\mathbf{x}_m^T \end{pmatrix} \tag{2.10}$$

where $\mathbf{x}_i$ is the row vector of $\mathbf{X}$ at $i$, where $i$ is a number in the range *1* to $n$. Some of the properties of $\mathbf{C}_X$ is that it is a square matrix (m-by-m), the diagonal terms are the variances and the off-diagonal entries are the covariance's.

Square matrices might have eigenvalues and eigenvectors, which are found by solving the characteristic equations of the square matrix. An eigenvector, $\mathbf{v}$, of a linear transformation is a non-zero vector that does not change its direction when that linear transform is applied to it. The eigenvalue is associated with the eigenvector, and denoted $\lambda$.[81]

PCA converts the data set into a new basis by calculating the covariance matrix, finding the eigenvalues and eigenvectors and transforming the data into a new basis. By doing this, one can observe some characteristics of the principal components (PC). The first PC contains the largest amount of variance possible, while the second PC contain the most variance that is orthogonal to the first PC. This also yields for all the succeeding PC's.[82,83]

When performing a PCA, a new basis for the data is formed. To do that, the data set $\mathbf{X}$ ($m$-by-$n$-matrix), will be linearly transformed into another matrix $\mathbf{Y}$, with the dimensions ($m$-by-$n$), with a matrix $\mathbf{P}$ of dimensions $m$-by-$m$ to fulfill the equation:[80]

$$\mathbf{Y} = \mathbf{P}\mathbf{X} \tag{2.11}$$

which represents a change of basis. $\mathbf{X}$ is projected on to the columns of $\mathbf{P}$. PCA seeks to de-correlate the original data by finding the directions in which the variance is maximized, and then use those directions to define a new basis.[80]

To construct the covariance matrix of $\mathbf{Y}$, $\mathbf{C_Y}$, the diagonal entries must be maximized (close to one), and the off-diagonal entries minimized (close to zero). The transformation matrix $\mathbf{P}$ has to be chosen such that $\mathbf{C_Y}$ becomes diagonal for the objectives to be met. $\mathbf{C_Y}$ could then be written:[84]

$$\mathbf{C_Y} = \frac{1}{n-1}\mathbf{Y}\mathbf{Y}^T = \frac{1}{n-1}(\mathbf{P}\mathbf{X})(\mathbf{P}\mathbf{X})^T = \frac{1}{n-1}(\mathbf{P}\mathbf{X})(\mathbf{X}^T\mathbf{P}^T) = \frac{1}{n-1}\mathbf{P}\mathbf{A}^T\mathbf{P}^T \tag{2.12}$$

where $\mathbf{A} = \mathbf{X}\mathbf{X}^T$, a symmetric $m$-by-$m$ matrix. $\mathbf{A}$ could then be written:[84]

$$\mathbf{A} = \mathbf{E}\mathbf{D}\mathbf{E}^T \tag{2.13}$$

where $\mathbf{D}$ is a diagonal matrix, and $\mathbf{E}$ is an orthonormal matrix of eigenvectors of $\mathbf{A}$. $\mathbf{P}$ is selected to be a matrix where each row is an eigenvector of $\mathbf{A}$, making $\mathbf{P} \equiv \mathbf{E}^T$, and substituting into Equation 2.13 and then into Equation 2.12 we obtain:[80,84]

$$\mathbf{C_Y} = \frac{1}{n-1}\mathbf{P}\mathbf{A}^T\mathbf{P}^T = \frac{1}{n-1}\mathbf{E}^T(\mathbf{E}\mathbf{D}\mathbf{E}^T)\mathbf{E} = \frac{1}{n-1}\mathbf{D} \tag{2.14}$$

since $\mathbf{E}\mathbf{E}^T = \mathbf{I}$, the identity matrix. Then the choice of $\mathbf{P}$ has diagonalized $\mathbf{C_Y}$, which was the goal.

To illustrate how much variance the first principal components contain, the first then PC's are plotted in Figure 2.11. The first principal component has the highest variances in both cases, as expected due to the criteria of PCA. The two first components in both cases stands for approximately 85% of the total variance, and the three first for approximately 90% of the variance. The fist bands contains the most variance, and therefore the most information. The later bands have lower variance, and mostly contains noise.

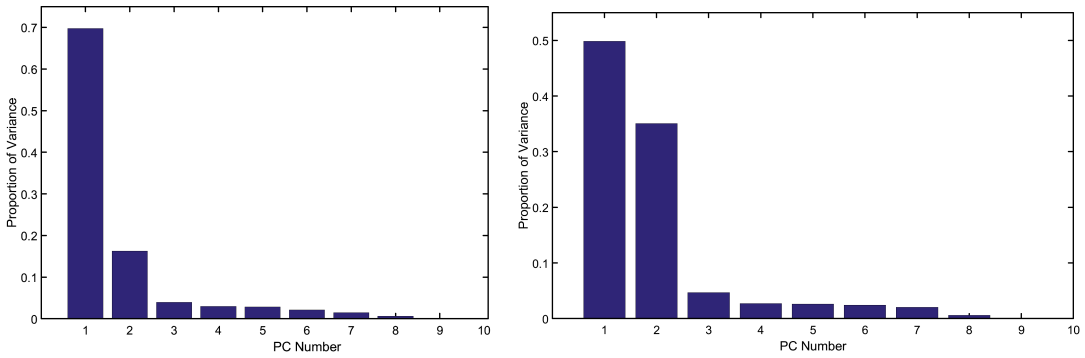


Figure 2.11: The proportional variance of the first ten PC's of a HSI. (a) Sample 1 (b) sample 2.

### 2.4.2 Minimum Noise Fraction (MNF)

Minimum noise fraction, MNF, is used to reduce the noise in images. It is a modified two PC-transform, which takes the quality of the signal into account. The PC-images of an MNF transformation are ordered in terms of signal quality. In hyperspectral images, it is desirable to have less and more evenly distributed noise throughout the different bands. MNF reduces the level of noise by reducing the dimensionality, by filtering out the higher PC's, as described in subsection 2.4.1.[85]

The linear transformation consists of the two following PCA rotations:[86]

- The first rotation uses the principal components of the covariance matrix to decorrelate and rescale the noise in the data (noise whitening), resulting in transformed data with unit variance and no band-to-band correlation
- The second rotation uses the PC derived from the original image data after noise-whitening by the first rotation and rescaled by the noise standard deviation. The data is divided into two groups, one with eigenvalues close to one and noise-dominated images, and another with great eigenvalues and coherent images.

After the MNF is performed, an inverse MNF is applied on the bands with the best signal quality. The inverse MNF transform utilizes the coherent images and filters the non-coherent images to reproduce a full image cube (original data space). The number of bands to include in the inverse MNF is decided through visual inspection of the bands and looking at the eigenvalues of the bands.[86]

### 2.4.3 Spectral Angle Mapper (SAM)

The spectral angle mapper, SAM, resolves spectral similarity by calculating the spectral angle between two spectral vectors that have a common origin. SAM attempts to obtain the angles between a reference spectrum and image spectrum. They are treated as vectors in a space with a dimensionality equal to the number of bands.[87] The equation for this angle is:[88]

$$\alpha = \arccos \frac{\sum \mathbf{XY}}{\sqrt{\sum \mathbf{X}^2 \sum \mathbf{Y}^2}} \tag{2.15}$$

where $\alpha$ is the calculated angle (radians), $\mathbf{X}$ the test spectrum, and $\mathbf{Y}$ the reference spectrum. See Figure 2.12 for visual interpretation.

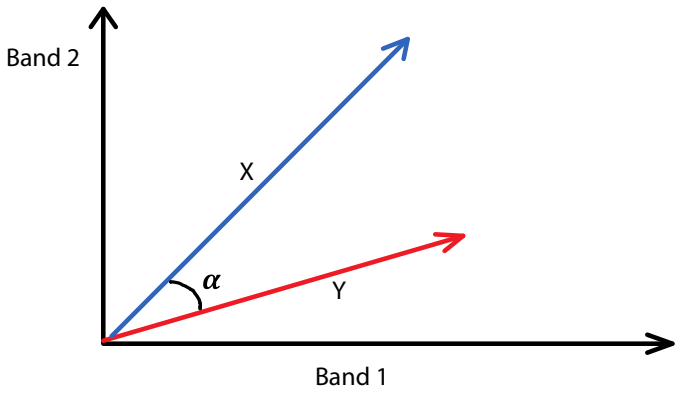


Figure 2.12: Plot showing the test spectra vector, $\mathbf{X}$, and the reference spectra vector, $\mathbf{Y}$, in a two-band image.

SAM is a supervised classification method; uses a reference spectrum. A training stage is the first step to perform a SAM analysis. In the training stage known samples are used to categorize the materials and obtain a numerical description of their spectra. The second stage is classification, where Equation 2.15 is used, to give each pixel a value for the calculated angle. The third stage is the output, where the image is displayed according to the classification angle. In the output stage, a threshold angle is normally set, and the pixels below the threshold are classified and pseudo-colored to form the new image.

Since SAM uses vectors, only the direction is important. Difference in strength/length between the vectors is neglected.

### 2.4.4 Partial Least Squares-Discriminant Analysis

Partial least squares-discriminant analysis, PLS-DA, is performed in order to sharpen the separation between groups of observations. This is done by rotating PCA components to obtain a maximum separation between classes.[89]

PLS-DA is a variant of partial least squares regression where the $\boldsymbol{Y}$-data is categorical (dummy variables describing the categories.[89] It is an algorithm that is used in a series of steps in a classification procedure. The aim of PLS-DA is to find a discriminator, which can separate the variables. The dimensionality of the discriminator will depend on the amount of variables.[90]

$$\mathbf{X} = \mathbf{T}\,\mathbf{P} + \mathbf{E} \tag{2.16}$$

$$\mathbf{Y} = \mathbf{T}\,\mathbf{q} + \mathbf{f} \tag{2.17}$$

Where $\mathbf{X}$ is the data matrix containing $n$ samples and $m$ analytical measurements (spectra of the samples, e.g. PP). $\mathbf{y}$ is a vector with length $n$, and is a numerical label for the samples. If there are more than two samples, i.e. $N$ samples, $\mathbf{y}$ becomes a matrix with dimensions $n$-by-$N$. The labelling denotes whether the specific vector in $\mathbf{X}$ with length $m$ is within the group. If it is a part of the group, it is marked +1. If it is not a part of that group it is denoted 0 (or -1 in some literature). $\boldsymbol{E}$ and $\mathbf{f}$ are residuals. $\mathbf{P}$ is the $\mathbf{X}$-loadings, and $\mathbf{q}$ the $\mathbf{Y}$-loadings. $\mathbf{T}$ is the $\mathbf{X}$-scores.[90,91]

Once the model is built, it is possible to predict the value of $\mathbf{Y}$. The relationship between $\mathbf{X}$ and $\mathbf{Y}$ can be expressed by:[90]

$$\mathbf{Y} = \mathbf{X}\,\mathbf{b} + \mathbf{f} = \mathbf{T}\,\mathbf{q} + \mathbf{f} \tag{2.18}$$

where $\boldsymbol{b}$ is a regression coefficient (dimension $m$-by-1). An unknown sample value of $\boldsymbol{c}$ can then be predicted by:[90]

$$\hat{c} = \mathbf{X}\,\mathbf{b} \tag{2.19}$$

then $\boldsymbol{b}$ could be written:[90]

$$\mathbf{b} = \mathbf{W}\,(\mathbf{PW})^{-1}\mathbf{q} \tag{2.20}$$

where $\boldsymbol{W}$ is the PLS weight vector. $\hat{c}$ determines the class the sample belongs to. The simplest, but not always best, is to assign the value to a class depending on if it is above or below zero.[90]

### 2.4.5 Comparison of the Three Models

Table 2.3: Pros of the three methods. PCA,[2] SAM,[3] and PLS-DA[4]

| PCA | SAM | PLS-DA |
|---|---|---|
| • spatial information is well preserved<br>• low computational complexity<br>• easy implementation | • quick labeling of data<br>• insensitive to gain<br>• illuminations treated equally<br>• can be used on single pixels | • can be used to predict either continuous or categorical variables<br>• ranks variables<br>• reduces dimensionality<br>• resistant to multi-collinearity and a much larger number of variables than observations<br>• handles noisy data |

Table 2.4: Cons PCA,[3] SAM,[2] and PLS-DA[4]

| PCA | SAM | PLS-DA |
|---|---|---|
| • low performance for HS images<br>• significant spectral distortion<br>• very sensitive to different illumination<br>• most variance is not always the most important | • fails if the vector magnitude is important<br>• requires high spectral resolution<br>• need for training data | • model validation is essential and often overlooked<br>• scores plot may present an overoptimistic view of the separation between classes<br>• tendency to overfitting<br>• need reference spectra |

# Chapter 3: Methods

In this chapter the methods for collecting the samples as well as the test setup and implementation of analyses are described.

## 3.1 Collection of Materials

The collection of the plastic samples came from household waste. A list of the most common products made of each type of plastic was set up beforehand (products described in subsection 2.3.8). Most plastic packaging in Norway contains a recycling symbol, to tell the consumer where to recycle the product.


Figure 3.1: Recycling symbols of plastic.

The symbols are either a plastic symbol or a form of the symbols shown in Figure 3.1. Only plastics with one of the indicated symbols (as shown in the figure) for the most predominant plastic material should be collected and used to ensure correct classification of the materials. In addition, some producers were contacted for the PVC-samples, as they were not marked. PETE is another short form of polyethylene terphthalate and V for polyvinyl chloride. HDPE and LDPE were put in the category PE.

The seawater should be taken from the ocean, as the goal is to use HSI to identify plastics in water.

## 3.2 Test

Measurements were carried out on the samples, and three separate tests were set up. To achieve reproducible results, setups and schemes for testing have been made, and are presented in this section.

### 3.2.1 Test 1

The first laboratory test is important to get an overview of the samples, such as their spectral characteristics and how to treat the samples with respect to specular reflection and addition of water. In Table 3.1 the first test matrix is shown. All samples will be inspected in combination without water, with water, and with water with seaweed to get information of how the sample spectra react to the different conditions.

Table 3.1: Test matrix scheme for test 1. All the plastic samples are set up to be imaged in the Petri dish with no water, 20 ml seawater, 20 ml seawater with seaweed.

| Sample Content | PE | PP | PET | PVC | PS |
|---|---|---|---|---|---|
| Fragments in petri dish | ✓ | ✓ | ✓ | ✓ | ✓ |
| Fragments in petri dish, and 20 ml seawater | ✓ | ✓ | ✓ | ✓ | ✓ |
| Fragments in petri dish, and 20 ml seawater with seaweed | ✓ | ✓ | ✓ | ✓ | ✓ |

In addition to the test scheme in Table 3.1, 20 ml of NaCl-water, 20 ml of seawater, and 20 ml of seawater with seaweed were set up to be tested.

### 3.2.2 Test 2

The second test scheme is shown in Table 3.2. This test scheme was set up after some analysis (mean spectra, SAM and PCA) and knowledge about the samples was used. From test 1, the spectral features for most of the samples were found, and the different intensities of reflectance depending on the thickness and color of the material were found.

The second test matrix compare samples from the same source (e.g. PP yogurt container) to samples of the same material but from different sources (e.g. PP). The effect changing the thickness of the water layer has on the combined spectra of the material and the water will be measured as well.

Before the second test was performed, more plastics were collected and sorted according to material to obtain a more diverse basis to test on.

Table 3.2: Test matrix scheme for test 2. All samples are to be imaged in the petri dish from one source (e.g. PP rice-bag) and from all sources (e.g. PVC member card and PVC wire insulation) with and without water.

| Sample<br>Content | PE | PP | PET | PVC | PS |
|---|---|---|---|---|---|
| Fragments in petri dish, one source | ✓ | ✓ | ✓ | ✓ | ✓ |
| Fragments in petri dish, one source, 10 ml seawater | ✓ | ✓ | ✓ | ✓ | ✓ |
| Fragments in petri dish, all sources | ✓ | ✓ | ✓ | ✓ | ✓ |
| Fragments in petri dish, all sources, 20 ml seawater | ✓ | ✓ | ✓ | ✓ | ✓ |

| Content<br>Sample | 0 ml | 10 ml | 20 ml | 30 ml | 40 ml | 50 ml |
|---|---|---|---|---|---|---|
| PS | ✓ | ✓ | ✓ | ✓ | ✓ | ✓ |
| PE, PP, PET, PVC, PS | ✓ | | ✓ | | | |

### 3.2.3 Test 3

Due to specular reflection in most of the images acquired in test 2, most of them were retaken in test 3, and are therefore set up in Table 3.3. To reduce specular reflection, relatively flat (no bends) and less shiny plastic were used. In addition, the edge of the Petri dish was marked with a black marker and a matte sticky tape was applied to reduce specular reflection.

Table 3.3: Test matrix scheme for test 3. Retake of most samples from test 2 due to specular reflection. In addition the change in thickness of water level was applied to PE plastic.

| Sample Content | PE | PP | PET | PVC | PS |
|---|---|---|---|---|---|
| Fragments in petri dish, one source | ✓ | | ✓ | ✓ | ✓ |
| Fragments in petri dish, one source, 10 ml seawater | ✓ | | ✓ | | ✓ |
| Fragments in petri dish, all sources | ✓ | ✓ | ✓ | | ✓ |
| Fragments in petri dish, all sources, 20 ml seawater | ✓ | | ✓ | | ✓ |
| Water Sample | 0 ml | 20 ml | 30 ml | 40 ml | 50 ml |
| PE | ✓ | ✓ | ✓ | ✓ | ✓ |

In addition to the test scheme in test 3, a similar appearance (all white in VIS) fragment cardboard-matrix was imaged. White plastic fragments from the five groups of plastic were placed on black cardboard, as shown in Figure 3.2 (b), according to the matrix in (a). This setup was chosen to have a more controlled environment with a different background. The circular shape and limited space in a Petri dish made it harder to set up a control matrix for all five plastic types.

## 3.3 Experimental Setup

The test setup described in section 3.2 is shown in Figure 3.3. The camera (HySpex SWIR-320m-e, see subsection A.2.2) and the light source (Norsk Elektro Optikk,

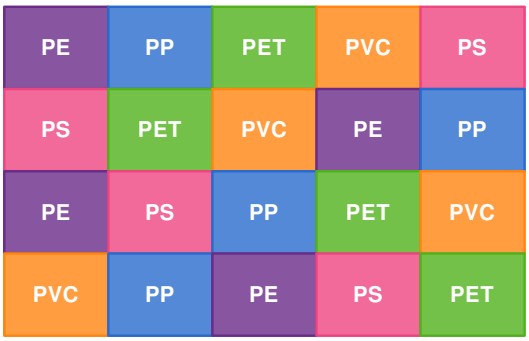


(a) Colored placement of plastic

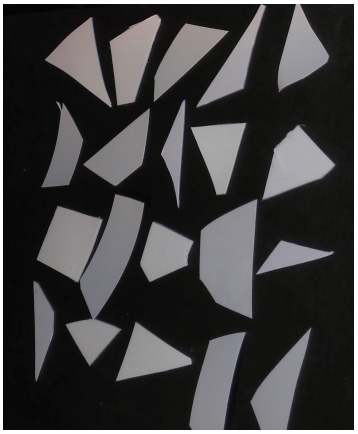

(b) Plastic-matrix (RGB-image)

Figure 3.2: Plastic placed in a matrix for classification. (a) Setup, (b) RGB-image, white fragments of plastic on top of black cardboard.

Skedsmokorset, Norway) were both mounted on the translation stage (8MT195-540-10, Long-travel Motorized Linear Stage, Standa, Lithuania), to ensure as uniform lighting along the image as possible. After the mounting, the light source was finely tuned to be positioned in the angle giving the highest detected intensity. The intensity of the light source affects the ability to distinguish features.

A sample was placed in a Petri dish made of borosilicate glass to avoid similar absorption of the Petri dish and the samples. The Petri dish was placed below the camera on top of a piece of black cardboard together with a white standard (Spectralon Ocean Optics, Duiven, the Netherlands).

The Petri dish had a diameter of 95 mm and a height of 12 mm. See subsection A.2.1 for more specifications.[92] This means 10 ml of water in the Petri dish will give a water layer with a thickness of 1.41 mm.

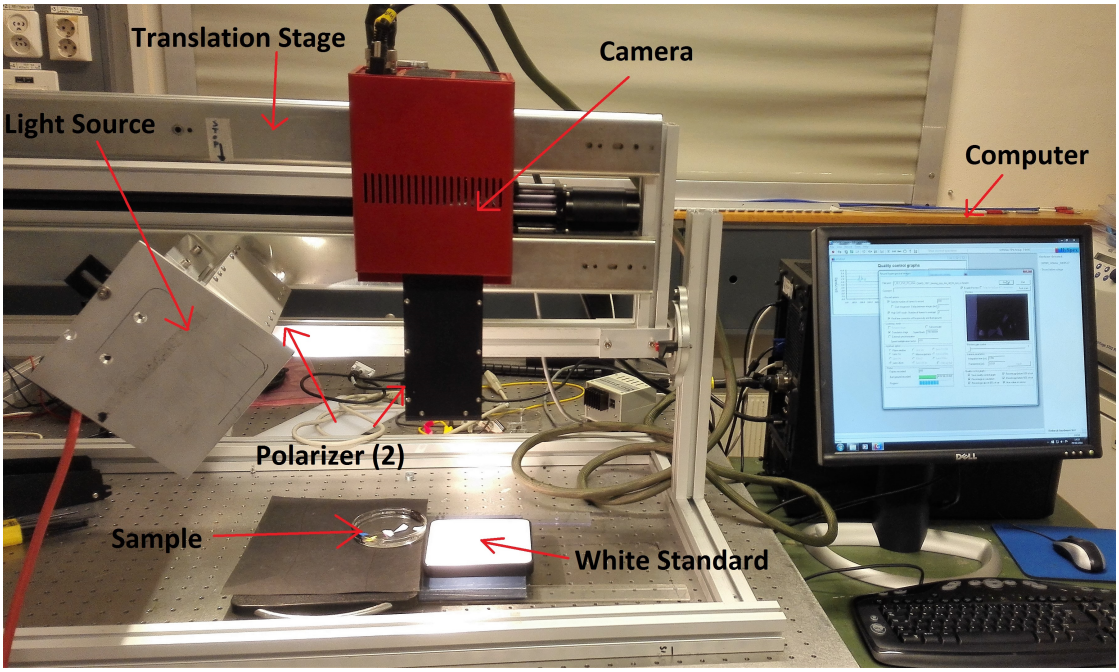


Figure 3.3: Setup in the laboratory

The intensity spectrum of the light source (NEO) for the wavelengths between 0.95 µm to 2.5 µm before the calibration is shown in Figure 3.4. The light source intensity spectra has a slope and some spikes.

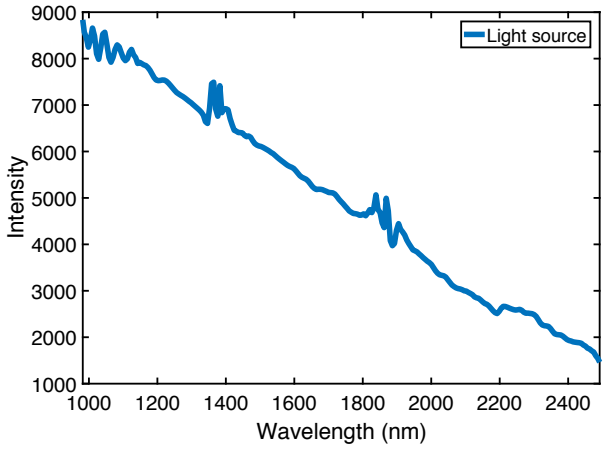


Figure 3.4: Light source intensity spectrum, uncalibrated.

In front of the light source a polarizer (Versalight Polarizer IR, Meadowlark

Optics, CO, U.S.) was mounted to reduce specular reflection and for eye safety. To reduce specular reflection further, a polarizer (Versalight Polarizer IR, Meadowlark Optics, CO, U.S.) was mounted in front of the camera lens. Specifications of the polarizers are found in subsection A.2.4

The hyperspectral camera used in this project (HySpex SWIR-320m-e), has a spectral range from 1.0 µm to 2.5 µm, 320 spatial pixels and 256 wavelength bands.[93] For this experiment 256 bands within the spectral range and 320 spatial pixels were used. The spectral range was chosen from known spectral features of C-H-bonds. See subsection A.2.2 for more specifications of the camera. The camera imaged spatially across the sample (pushbroom-line), and moved with the translation stage along the sample.

The integration time used varied between the experiments, due to specular reflection problems which made the integration time shorter. The integration time affects the SNR, the lower integration time, the lower SNR. For test 1, the integration time was set to 13.5 ms, test 2 at 7.2 ms, and test 3 at 8.5 ms.

A 20 ml measuring cylinder and a 1 ml pipette were used to measure the amount of water added to the plastic samples within the Petri dish.

A closer image of the placement of the Petri dish and the white standard is shown in Figure 3.5.

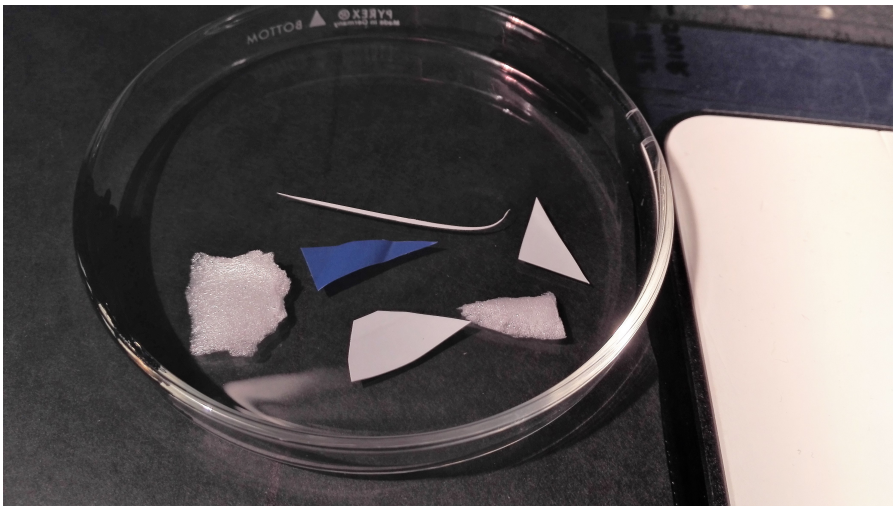

Figure 3.5: RGB-image of the placement of the sample and the white standard.

To reduce the specular reflections at the edge of the Petri dish, a black marker and matte sticky tape was applied for some of the tests.

## 3.4 Analysis

Computation and analysis are important to extract the wanted information. The raw data collected from the testing has therefore been processed according to the theory in section 2.4. Different image analyses were applied to identify the best algorithm for this application. A flowchart of the order of calibration and analysis is shown in Figure 3.6.

First, the raw data was corrected, and dark current was removed through specific software for the hyperspectral camera (ENVI 4.8) to create a hyperspectral image. There is a shutter in the camera that blocks all incoming light, in order to measure the dark current. The dark current is removed according to Equation 2.1.

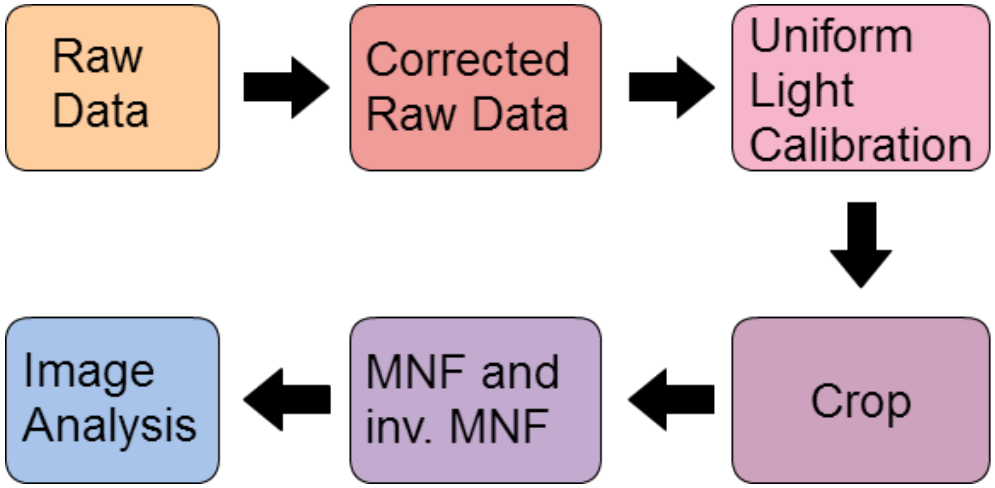


Figure 3.6: Flowchart showing the order of execution of the image chain from raw data to image analysis.

The light distribution in an image is not necessarily uniform. The light distribution in the x-direction varied across the sample, due to an uneven light distribution. The light distribution along the image (y-direction) was uniform, due to the movement of the light source and the camera in the y-direction (along translation stage). The spectral dimension was shown to not be uniform in Figure 3.4.

A white standard (srt-99-050, Spectralon Ocean Optics, Duiven, the Netherlands[94]) was used as a reference to measure the average amount of incoming light, both in the spectral dimension and in the x-direction. The white standard had reference values for each wavelength.

For the process of uniform light calibration, see Figure 3.7. The measured white standard values for a particular $x$ was taken the average of (b). The average of that particular $x$ was compared to the reference value of the white standard

for each wavelength. Then the whole column of that particular $x$, was corrected to make the measured white standard-average match the white standard reference spectra (c). The rest of the image was column-wise corrected for this mean value to obtain more uniform images and spectra (d).

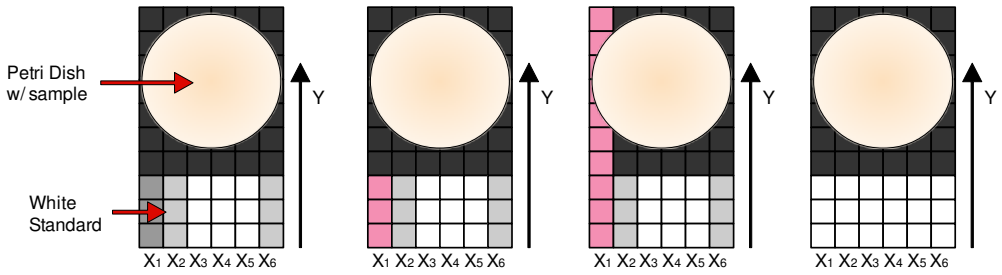


Figure 3.7: Correction of uneven light distribution across the sample. (a) Placement of components in image, (b) comparing the average of the white standard in column $X_1$, (c) correcting the whole column $X_1$ for the deviation from average lightning and (d) corrected image.

This calibration method is known as flat-field calibration, and is used to normalize the intensities in an image to reflectance. The spectra of the samples used for analysis were in relative reflectance, as it was measured relative to the white standard.[95] The relative reflectance shown in the results are a combination of the absorption and the scattering properties of a material. If a medium has high absorption at a wavelength, the reflectance will be low, as described in section 2.2.

After the calibration, the images were cropped, leaving out the white standard and the edges of the Petri dish. The plastics and the medium around were kept for further analysis. The cropping function is shown in subsection A.1.6.

Then an MNF was performed, followed by an inverse MNF, as described in subsection 2.4.2. This was performed to reduce the overall noise-level. Only the five to ten first bands were used in the inverse MNF for the images in this project, as decided through visual inspection of each image. The visual inspection was performed by looking at the band-images, and the cut-off band was chosen where there was little information left, and the image was heavily dominated by noise. Since higher bands have a lower variance, a cut-off level for the variance could have been used (see the proportional variance plot in Figure 2.11). A cut-off level for the variance needed, would be good for automation of the process.

After the MNF and inverse MNF were performed, the images were ready to be analyzed by the chosen algorithms PCA, SAM and PLS-DA.

### 3.4.1 MATLAB and Evince

The image analyses performed for this project were principal component analysis (PCA), spectral angle mapper (SAM) and partial least squares discriminant analysis (PLS-DA).

To get a first impression of the images, an image viewer was used. The script and describing figure is shown in subsection A.1.1. In the image viewer one can explore the image in terms of spectral features at a certain pixel or the image intensities for a certain wavelength. The image viewer also contained the possibility to mark interesting pixels and save them as a region of interest (ROI) (e.g. PE).

The ROI containing several pixels from the same sample (e.g. PE fragment) were used for plotting the mean spectra and as the reference spectra in SAM. The function for plotting the mean spectra is shown in subsection A.1.7.

The SAM-analysis tool is shown in subsection A.1.2. The reference spectra was created the same way as the mean spectra. There the code is represented, as well as a figure of how to set the threshold.

The function for performing the PCA is shown in subsection A.1.3, together with an illustrating figure of the user-interface.

PLS-DA was done with the help of the software Evince (version 2.7.5, Prediktera, Umeå, Sweden). The input in Evince is the same as in MATLAB, the image data files that have been corrected according to Figure 3.6. How the process works in Evince is explained by images and text in subsection A.1.4.

# Chapter 4: Results and Discussion

This chapter will show the accuracy of the different types of classification algorithms, the spectra dependency on color and water depth and spectral features of the materials will be thoroughly explained through results and discussion.

## 4.1 Collection of Samples

The seawater was collected in Ilsvika, Trondheim, Norway the $29^{th}$ of February. The seawater was very clear, most likely due to the low algae production during winter, as seen in Figure 4.1 (a).[96,97] The plastic was collected from household waste (HW) in Trondheim, Norway, and separated with respect to content. The plastic was then cut into smaller fragments and placed in individual containers, as seen in Figure 4.1b.


(a) Collected water and seaweed

(b) Plastic collected and labeled

Figure 4.1: (a) Collected seawater from Ilsvika, Trondheim, Norway and (b) collected, sorted and labeled plastics from household waste (HW). The plastic is placed as follows starting in upper left corner: PE, PP, PET, PVC, PS, and plastic collected from the ocean

Most of the plastic came from food preservation, like yogurt containers, cling wrap, chocolate wrapping and similar. The full list of the origin of the plastics is shown in Table 4.1.

Table 4.1: Table showing the sources of the different types of plastic.

| PE | PP | PET | PVC | PS |
|---|---|---|---|---|
| cling wrap<br>plastic bag (thin)<br>zip-lock bag<br>hand lotion tub<br>grocery bag | chocolate wrap<br>sour cream tub<br>yogurt tub<br>rice-bag<br>meat container<br>Nutella lid | soda bottle<br>sriracha bottle<br>tomato box<br>quark tub | member card<br>wire insulation | food container<br>coffee cup<br>mushroom box<br>yogurt container<br>strawberry box |

The tests were performed on three different days. The first test was performed on March $7^{th}$, 2016, the second test on April $25^{th}$, 2016, and the third test on May $9^{th}$, 2016. See section 3.2 for the test matrices made for the three tests.

## 4.2 Results of Pre-Process Correction

The effect of uniform light calibration as described in section 3.4, is shown in Figure 4.2. Looking at the white standard in the top of the image in (a) the intensity measured across the image varies, with the highest intensity in the middle. In (b), one can see that the calibration has made the light distribution uniform across the image (solid red).

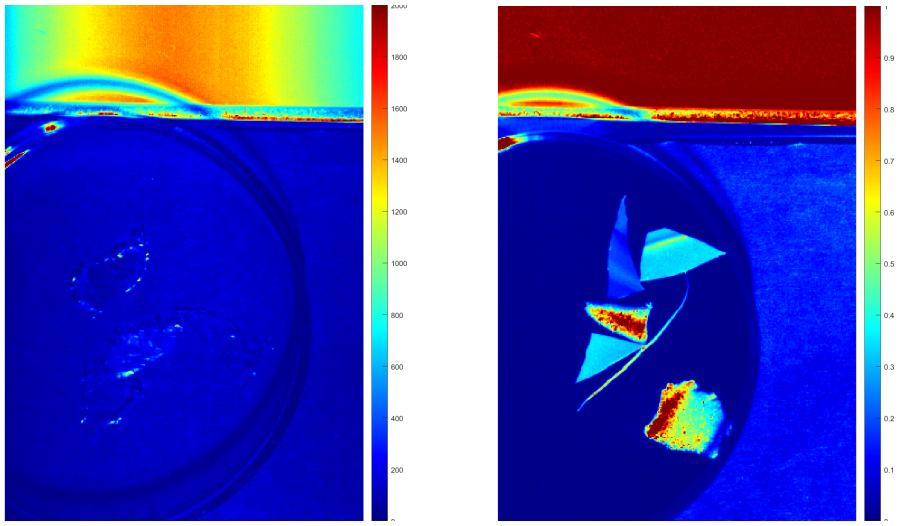

(a) Uncalibrated (b) Calibrated

Figure 4.2: Calibration of the image, using the white standard as a reference. Note the different scaling before and after calibration, (a) shows measured intensity, while (b) shows relative reflectance.

The scaling has changed from intensity in Figure 4.2 (a) to relative reflectance in Figure 4.2 (b). The calibrated reflectance of the white standard illuminated with the light source is shown in Figure 4.3. Comparing this to Figure 3.4, the reflectance of the light source is flattened out, and stays flat around one until 2000 nm. After 2000 nm the reflectance deviates from one and fluctuates. The features of the reflectance comes from the properties of the white standard. The reflectance in this thesis refers to relative reflectance.

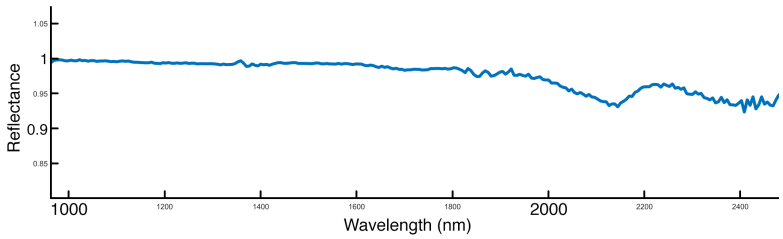


Figure 4.3: The reflectance of the light source.

## 4.3 Spectral Analysis

In this section the spectra of the different samples will be discussed and analyzed. The impact of the thickness of the water layer, difference in reflectance from different samples and the absorption features of plastic will be presented. How the reflectance plots were made is described in subsection 3.4.1.

### 4.3.1 Absorption in Water

Looking at the absorption spectrum for water in the SWIR-region, absorption peaks were identified in subsection 2.3.10, and were expected at 970 nm, 1200 nm, 1450 nm and 1950 nm.[73] By taking the mean spectrum of pure salt water, the reflectance troughs from the literature fits quite well for the measured water reflectance, see Figure 4.4.

Water has a high absorption coefficient for the longer wavelengths, as shown in Figure 4.4. After 2000 nm the spectrum fluctuates, which likely is due to the calibration to the white standard, as mentioned in section 4.2. The reflectance graph was taken from the thinnest layer of water (only 10 ml added to the Petri dish), which gave clearer spectral features for the longer wavelengths.

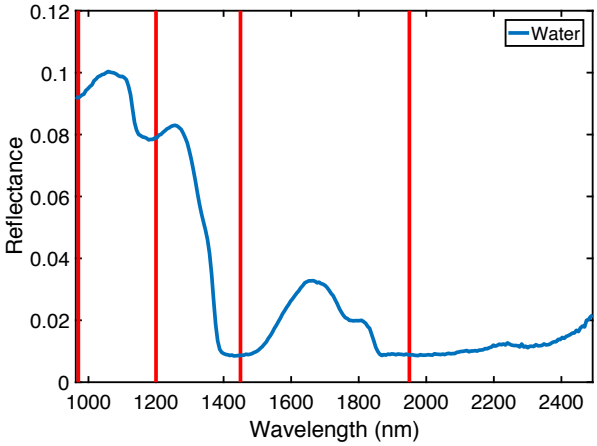


Figure 4.4: Reflectance spectra of salt water. The four reflectance troughs are taken from the literature,[73] and are marked in red.

### 4.3.2 Comparison of NaCl-Water and Seawater

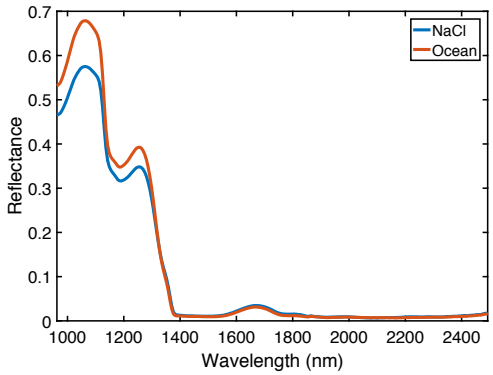


Figure 4.5: Comparison of sterilized NaCl-water and water collected from the ocean. The spectral features are similar.

For the laboratory experiments, water obtained from the ocean was used to ensure closer conditions to the plastic in the ocean for the hyperspectral imaging. The spectrum of water from the ocean has been compared to the spectra of sterilized NaCl-water (see subsection A.2.3), as shown in Figure 4.5. The two spectra are very similar, the spectral features are observed in both, and the only difference observed is the value of the reflectance. This difference could be due to a small difference in the thickness of the water layer, difference in scattering and absorption

due to particles in the seawater (microplastics, sediments, sand, but probably not algae, as mentioned in section 4.1). The similarity between the spectra, allows them to be interchanged in this thesis.

### 4.3.3 Comparison of PE, PP, PET, PVC, and PS Spectra for Wavelengths between 1000nm and 2000nm

Comparing the acquired spectra of the samples to previous literature is important to give a first confirmation of valid data. The spectra from the literature (presented in subsection 2.3.10) is compared to the acquired spectra in Figure 4.6. The main features such as reflectance peaks and troughs are present in both spectra.

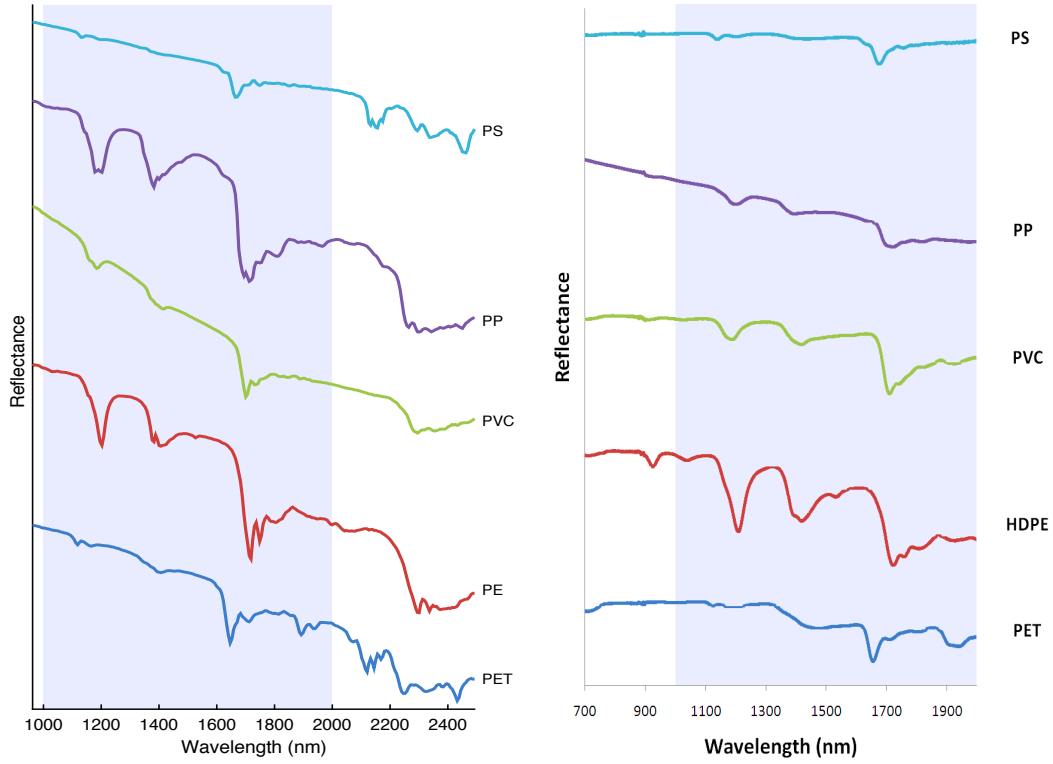


(a) Acquired spectra

(b) Spectra from literature[76]

Figure 4.6: Comparison of the mean spectra of the acquired data, (a), to spectra from the literature, (b). Shaded areas marks the overlapping wavelengths. Note: different scaling.

The acquired spectra in Figure 4.6 (a) are more detailed than the spectra from the literature in (b). According to the data sheet of the spectrometer used in the literature, the spectral bandwidth could be set at different lengths.[98] From

the figure, one can assume that the HySpex camera used in this thesis has used a higher spectral resolution than the one from the literature. In addition, the slope of the spectra acquired in this test are steeper. Looking at Figure 4.3, the reflectance for the wavelengths between 1000 nm and 2000 nm is close to one. This means the acquired data are correctly calibrated for those wavelengths, and the literature might have a calibration that is off.[32]

### 4.3.4 Effect of the Thickness of Water Layer

Different amounts of added water resulted in different thicknesses of the water layer which changed the reflectance intensity of both water and plastics. The water was measured with a measuring cylinder and a pipette and added to the Petri dish, as described in section 3.3. According to Beer's law in section 2.2 for absorption (water has little scattering), the intensity is negatively dependent on the distance propagated. With a thicker layer of water, it is therefore expected to observe higher absorption (lower reflectance) in water. This dependency was well confirmed from the spectrum analysis, and shown for five different water levels ranging from 10 ml to 50 ml in Figure 4.7 (a). For thicker layers of water (20 ml and above) the absorption in water above 1400 nm is substantial, and most of the light is absorbed.

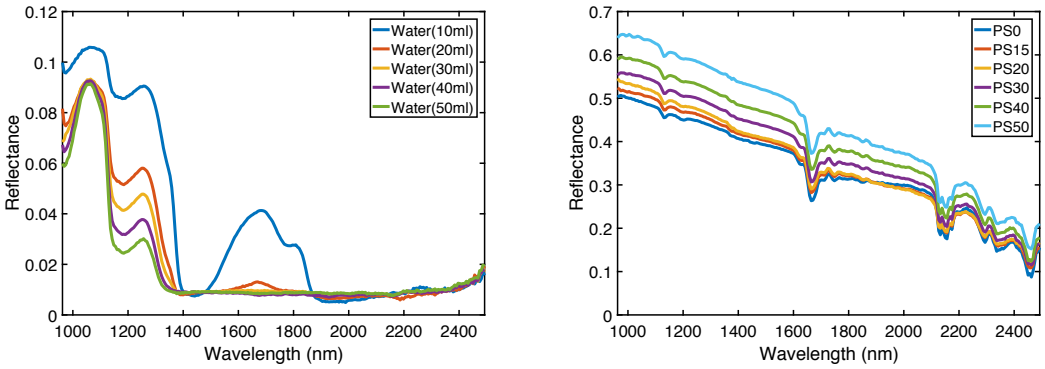


(a) Water (b) Plastic (PS)

Figure 4.7: The effect of different thicknesses of the water layer on (a) water reflectance and (b) plastic reflectance.

The thickness of the water layers also affected the reflectance of plastic, as shown in Figure 4.7 (b). In this case, the reflectance increased as the water level increased, which is opposite of the reflectance of water. This phenomenon is further explained in subsection 2.2.4.

### 4.3.5 Spectral Features

The red lines in Figure 4.8 mark the absorption peaks (reflectance troughs) observed for each material. The positions of the absorption peaks are listed in Table 4.2. Both the graph and the listed peaks are similar for the different materials. This was expected, as all the materials are plastics and contain a C-H bond.

Table 4.2: Observed absorption peaks for the different types of plastics and the absorption peaks from the literature.[74,75]

| Material | $1^{st}$ peak [nm] | $2^{nd}$ peak [nm] | $3^{rd}$ peak [nm] | $4^{th}$ peak [nm] |
|---|---|---|---|---|
| PE | 1202 | 1382 | 1718 | 2301 |
| PP | 1178 | 1382 | 1694 | 2265 |
| PET | 1118 | 1406 | 1646 | 2247 |
| PVC | 1184 | 1418 | 1700 | 2295 |
| PS | 1130 | 1370 | 1664 | 2295 |
| Literature | 1100-1225 | 1300-1420 | 1650-1800 | 2200-2450 |

Comparing the absorption peaks of the samples in Figure 4.8 to the literature in subsection 2.3.10 shows a clear correlation to the C-H bond absorption. The absorption observed comes from combination-, first overtone- and second overtone-stretching.

### 4.3.6 Low Reflectance Materials

Different levels of reflectance are observed for different products from the same type of plastics (e.g. PET) with different added fillers (pigmentation, scattering fillers, flame retardants etc.). Different color (in VIS) was the main reason for change in reflectance level observed during the laboratory experiment.

The impact different pigments can have on the reflectance spectrum is seen in Figure 4.9, where (a) is from the literature,[99] and (b) from the analysis. In this case, two extremes are shown, to the left black and white PP are compared, while to the right black and transparent PET are compared. This change in reflectance intensity has during the analysis proven to be a challenge when it comes to classification. According to the literature the same challenges have been observed.[99] Black pigmentation absorbs most of the light in the visible wavelengths, this shows that black plastic also absorbs most of the light in NIR. Low reflectance leads to a low signal to noise ratio (SNR).

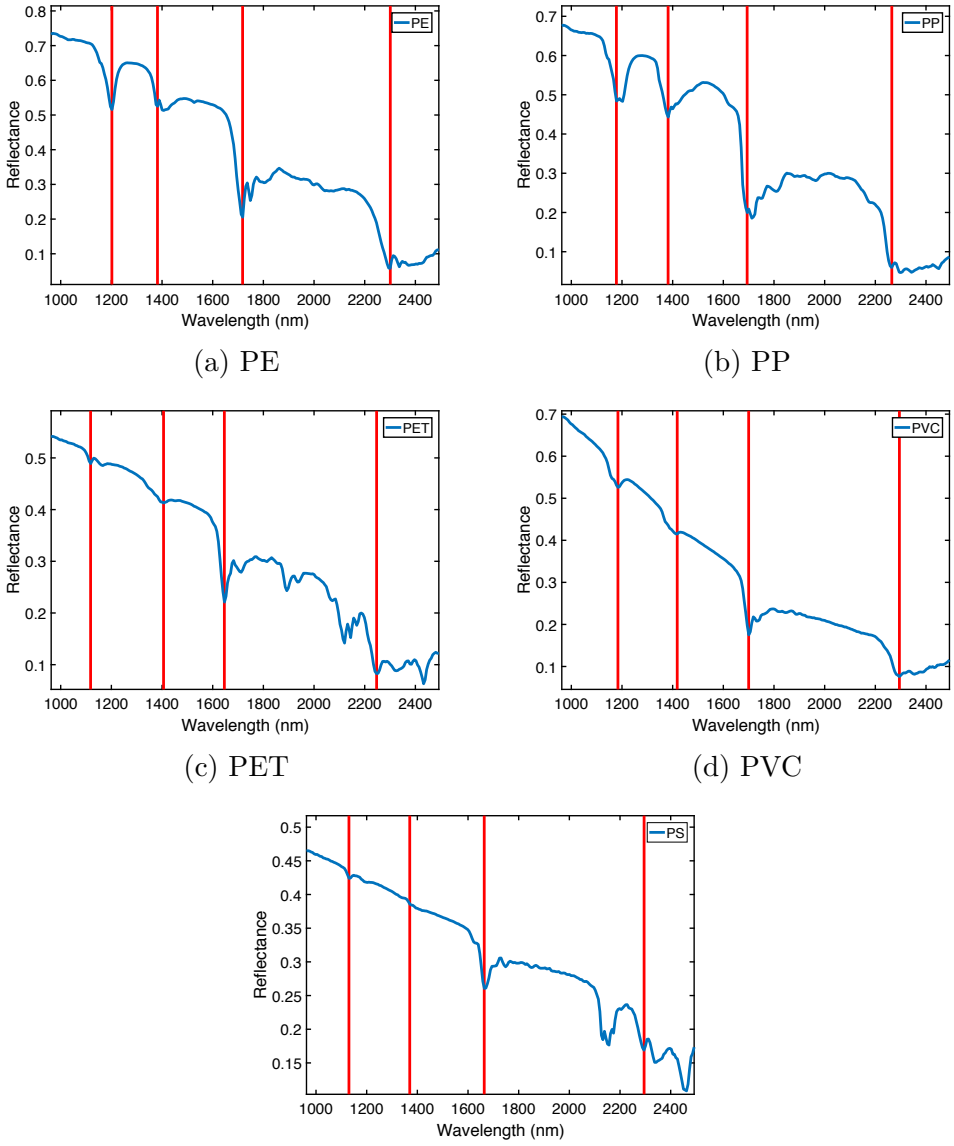


(a) PE (b) PP

(c) PET (d) PVC

(e) PS

Figure 4.8: Reflectance spectra of (a) PE, (b) PP, (c) PET, (d) PVC and (e) PS. The spectral features are marked with red lines. They mark the reflectance troughs (absorption peaks) of the materials.

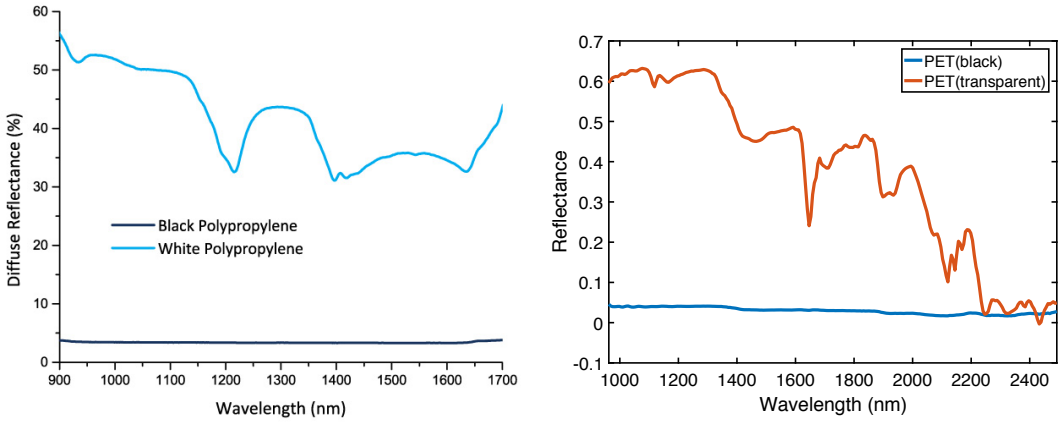


(a) $PP^{99}$ (b) PET

Figure 4.9: Comparison of the reflectance spectra of two different colored plastics for the wavelengths between 962 nm and 1700 nm. The measured reflectance for the black plastic is flat, and has a low SNR. Note: different scaling.

Increasing the integration time will give a higher SNR, and might help to detect the spectral features for plastics with black pigmentation. Increasing the integration time can cause the saturation in the pixels of the standard used for calibration. A standard with lower reflectance than the white standard (close to 100%), like a grey standard (e.g. 30%), will increase the maximum integration time before saturation.

Absorption can differ by pigmentation as mentioned above. PP was collected and analyzed from seven different sources, and a combination spectra plot is shown in Figure 4.10. The plot shows the differences in reflectance within the same material, but from different sources. Even though the reflectance changes, the main spectral features are still intact, and can be detected, except for $PP_2$, where the only reflectance trough that can be observed is the one at 1382 nm. $PP_2$ also contained black pigmentation (in VIS). This supports the theory given in subsection 2.2.4, where different factors cause change in the level of reflectance. The spectral features will be further discussed in the next section.

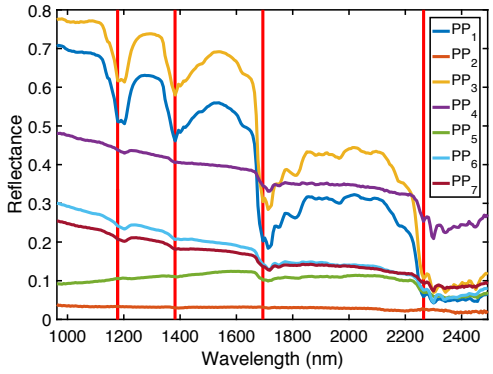


Figure 4.10: Comparing the reflectance spectra of PP from different sources. The sources are numbered for easier read-off. The sources are listed in Table 4.1. The red lines represent the position of the main spectral features described in subsection 4.3.5.

## 4.4 Spectral Angle Mapper

In this section the results of the SAM-analysis will be presented and discussed. The difference between ocean water and NaCl-water, accuracy of the method, importance of correct threshold and dependent factors will be further explored.

How the SAM was performed is explained in subsection 3.4.1. At least one ROI (e.g. PP) was used as a reference spectrum. In this thesis the classification for different ROI's were set by a threshold-value, $t$, which represented the maximum allowed angle between the reference spectra and the test spectra. Image enhancement by pseudo-coloring is described in subsection 2.1.5.

### 4.4.1 White Plastic Fragments on Black Cardboard

Similar shaped plastic and plastic with similar appearance were placed in a five-by-four matrix on top of black cardboard (as described in section 3.2) is shown in Figure 4.11. In (a) an RGB-image of the plastics shows the similarity in shape and color of the fragments in VIS. Due to a difference in the strength in spectra between different pigmentation's, all fragments used were chosen to be white. (b) Shows the classification by SAM. With a low threshold, $t = 0.05$, the amount of classified pixels is high enough to separate between the different types of plastic and the cardboard.

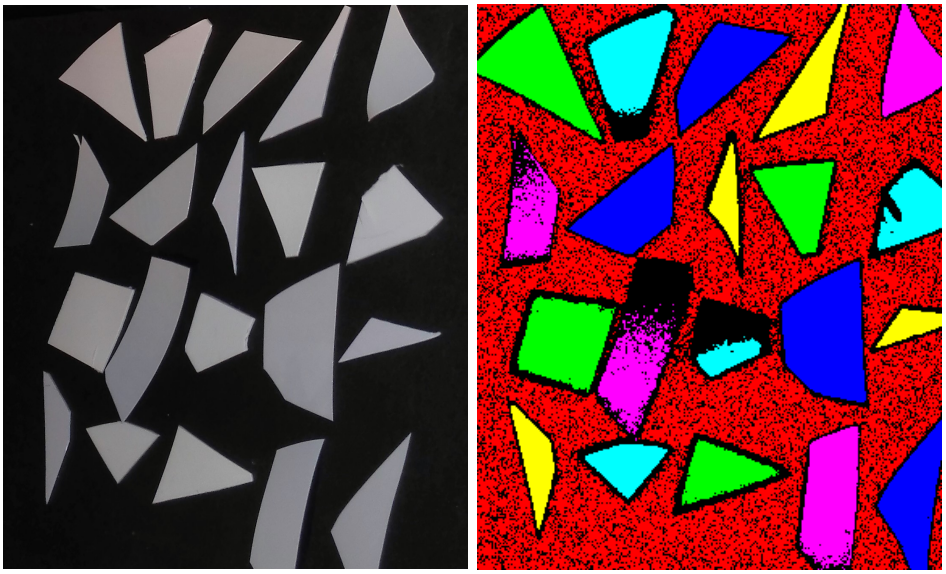

(a) Plastic-matrix (RGB-image) (b) Colorized by SAM.

Figure 4.11: Images of white plastic fragments placed directly on black cardboard. (a) RGB-image, (b) SAM with $t = 0.05$ for PE (green), PP(cyan), PET(blue), PVC(yellow), PS(magenta), cardboard(red) and unclassified(black).

Table 4.3: Classified pixels according to material and color by SAM for Figure 4.11 (b).

| Material | Color | Number of pixels |
|---|---|---|
| PE | Green | 7916 |
| PP | Cyan | 5016 |
| PET | Blue | 9628 |
| PVC | Yellow | 3502 |
| PS | Magenta | 6998 |
| Cardboard | Red | 48 756 |
| Unclassified | Black | 23 835 |
| Total | | 105 651 |

### 4.4.2 Different Types of Plastic on Glass

It is important to evaluate what threshold values to set. For recognition of plastic and which type of material the plastic is from, it is important to keep the threshold value low enough to prevent overlap between classes, and high enough threshold

to identify the material. Classifying all pixels are of less importance the bigger the samples being imaged are.

The reflectance of the material plays an important role in identifying the material. As shown in Figure 4.12, with the exception of (c) PET, the samples have been classified. The PET-sample contained transparent fragments, which had a lower absorption, and the spectra was influenced by the background.

Increasing the threshold increases the amount of classified pixels, as shown in Figure 4.13. More background pixels and pixels at the edge of the plastic-fragment are classified. The background and the samples have quite different spectra, and increasing the threshold did not result in any overlap.

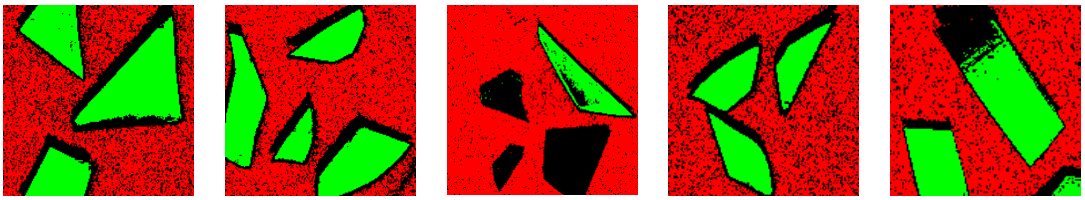

(a) PE (b) PP (c) PET (d) PVC (e) PS

Figure 4.12: SAM of plastic on glass. The threshold was set to $t = 0.05$ for all plastics and the glass. Plastic(green), glass/background(red) and unclassified pixels(black).

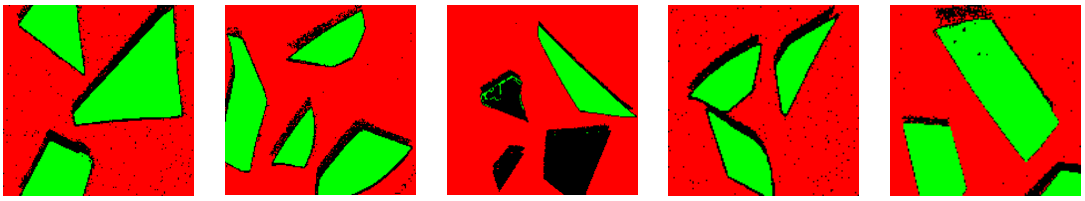

(a) PE (b) PP (c) PET (d) PVC (e) PS

Figure 4.13: SAM of plastic on glass. The threshold was set to $t = 0.10$ for all plastics and the glass. Plastic(green), glass/background(red) and unclassified pixels(black).

### 4.4.3 Plastics with Added Water

In Figure 4.14 20 ml of seawater has been added to the Petri dish with the plastic. Each sample contains plastic fragments of the same material (e.g. PE) from several sources. The different sources have different levels of absorption, and with a low threshold of $t = 0.05$, the spectra differs too much to be classified by SAM.

Increasing the threshold to $t = 0.10$, more of the fragments are classified as plastics, as seen in Figure 4.15. This is valid especially for (b), PP.

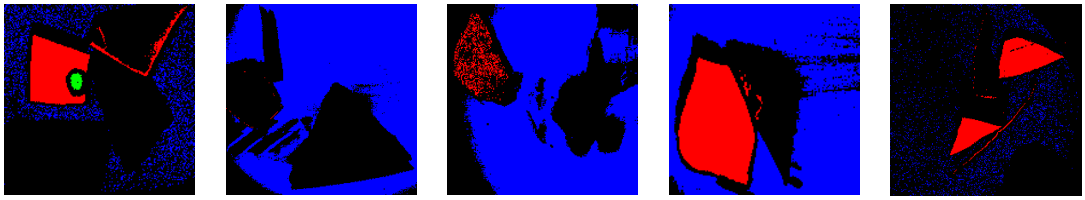

(a) PE (b) PP (c) PET (d) PVC (e) PS

Figure 4.14: SAM of plastic and 20 ml water. The threshold was set to $t = 0.05$ for all types of plastic and the water. Plastic(red), water(blue), unclassified(black). The green in (a) represents a water droplet on top of the plastic.

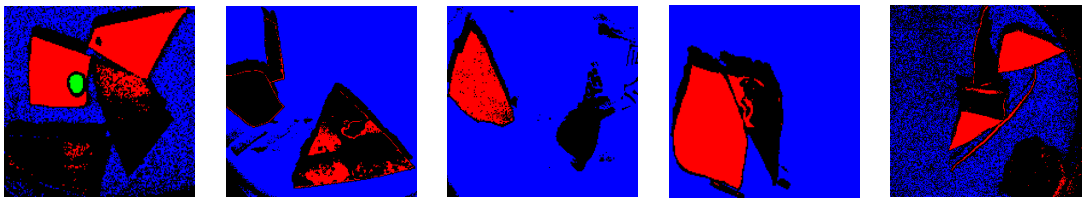

(a) PE (b) PP (c) PET (d) PVC (e) PS

Figure 4.15: SAM of plastic and 20 ml water. The threshold was set to $t = 0.10$ for all types of plastic and the water. Plastic(red), water(blue), unclassified(black). The green in (a) represents a water droplet on top of the plastic.

### 4.4.4 Effect of the Changing Thickness of Water Layer

The thickness of the water layer has little influence on the classification by SAM, when changing the thickness of the water layer for plastics that float (lower density than water). The result is shown for two different thresholds, $t = 0.05$ in Figure 4.16 and $t = 0.10$ in Figure 4.17. Adding water to the Petri dish caused the fragments to move, which is seen in the figures. In (a) there are PE fragments from two different sources, but adding water made them drift to the edge of the Petri dish, where edge-effects occur. Edge effects are not taken into account, and the fragments from a different source is therefore not present in (b)-(d).

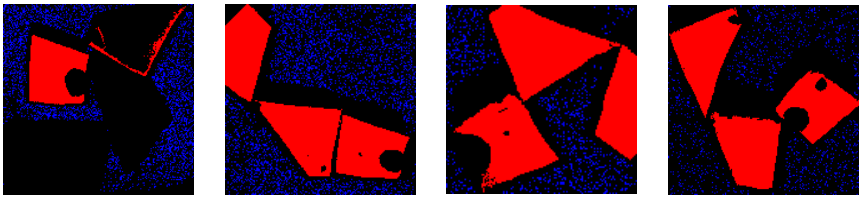

(a) 20 ml (b) 30 ml (c) 40 ml (d) 50 ml

Figure 4.16: SAM of PE and 20 ml, 30 ml, 40 ml and 50 ml water. The threshold was set to $t = 0.05$ for PE and water. Plastic in red, water in blue.

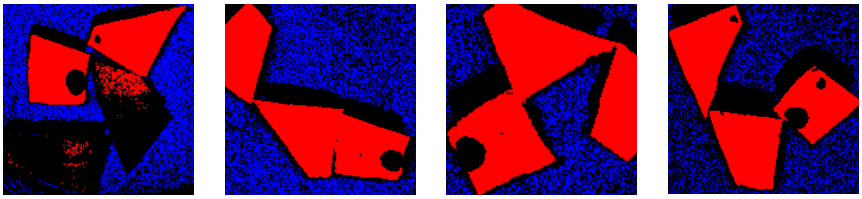

(a) 20 ml (b) 30 ml (c) 40 ml (d) 50 ml

Figure 4.17: SAM of PE and 20 ml, 30 ml, 40 ml and 50 ml water. The threshold was set to $t = 0.10$ for PE and water. Plastic in red, water in blue.

### 4.4.5 PP from Different Sources

PP from seven different sources were tested to check the versatility of the method. It is important that the analyzing method chosen is able to sort out different types of PP, not only the PP of a certain size and source. The result of SAM on the seven sources of PP is shown in Figure 4.18. (a)-(d) shows different thresholds for PP and glass. The spectrum used for PP in SAM is an average of the all the plastic fragments present. Therefore, a higher threshold is needed to classify the PP.

In Figure 4.18(e), the reference spectra used are taken from each one of the fragments. This gives a lower threshold for classifying the PP, and several of the fragments are marked as an overlap between spectra (in white).

(a) $t_{PP} = 0.05$ (b) $t_{PP} = 0.1$ (c) $t_{PP} = 0.2$ (d) $t_{PP} = 0.3$ (e) $t = 0.05$

Figure 4.18: SAM of PP from seven different sources. The threshold for PP and glass is set to (a) $t_{PP} = 0.05$ and $t_g = 0.05$, (b) $t_{PP} = 0.10$ and $t_g = 0.10$, (c) $t_{PP} = 0.20$ and $t_g = 0.10$, (d) $t_{PP} = 0.30$ and $t_g = 0.10$ and in (e) all the different types of PP had a threshold of $t_{PP} = 0.05$. (a)-(d) PP in green, glass in red. (e) PP colorized.

In the ocean, the sources of the plastics will be unknown, such that a reference spectrum made up of the mean of several different spectra of the same material is needed. Another option is to make several reference spectra for the same material, to ensure a low enough threshold to not overlap with other material types.

Table 4.4: Angles between the different materials, as calculated by SAM. The white plastic fragments of the materials were used for the calculation.

| | PE | PP | PET | PVC | PS |
|---|---|---|---|---|---|
| PE | | 0.0658 | 0.1292 | 0.1250 | 0.2036 |
| PP | 0.0658 | | 0.1506 | 0.1412 | 0.2290 |
| PET | 0.1292 | 0.1506 | | 0.1575 | 0.1503 |
| PVC | 0.1250 | 0.1412 | 0.1575 | | 0.2483 |
| PS | 0.2036 | 0.2290 | 0.1503 | 0.2483 | |

Calculated angles between the different samples are shown in Table 4.4. The table presents a quick overview of which sample's spectra are the closest. PE and PP have the smallest angle between them, while PS differs the most from the other samples overall. With a threshold of $t = 0.1$, SAM will classify PE and PP in the same category for the angles given. Comparing this with the result in Figure 4.18, a threshold of at least $t = 0.1$ is needed for a mean reference spectrum. To classify the highest amount of pixels in Figure 4.18, a threshold of $t = 0.3$ was needed, with that threshold, SAM would have classified different types of plastics as PP.

Table 4.5: Angles between $PP_1$ and the rest of the PP's, as calculated by SAM.

| | $PP_2$ | $PP_3$ | $PP_4$ | $PP_5$ | $PP_6$ | $PP_7$ |
|---|---|---|---|---|---|---|
| $PP_1$ | 0.3786 | 0.0838 | 0.3214 | 0.4125 | 0.1488 | 0.2199 |

The spectral angles between $PP_1$ and the rest of the PP's are shown in Table 4.5. The table shows greater angles between two types of PP than Table 4.4 showed between two different types of plastic. The angles vary a lot within PP, which shows that fillers, pigmentation and thickness are important for the observed spectra.

## 4.5 Principal Component Analysis

In this section the results of the PCA will be presented and discussed. How different types of plastic and water thickness affect the analysis will be investigated.

### 4.5.1 White Plastic Fragments on Black Cardboard

PCA works well for separating plastic from cardboard for PC 1 against PC 3, but struggles to differentiate between the different types of plastic for the sample shown in Figure 4.19 (a) and (b). The plastic fragments of PE, PP, PET, PVC, and PS are placed according to Figure 3.2. The resulting spectra in (c) shows the combined mean-spectra of all the pixels marked in blue.

By making a scatter plot of PC 2 against PC 3, as seen in (e), some of the plastics are separated, but the cardboard is spread out. The plastics are separated into three, as seen in (d). PE and PP are clustered together, PET and PS are clustered together, while PVC stands out the most. Similar spectra will cluster together, which is observed for PE and PP.

PCA distinguished between plastic and cardboard, but was unable to distinguish between different types of plastic. The pixel count is shown in Table 4.6 for PC 1 against PC 3.

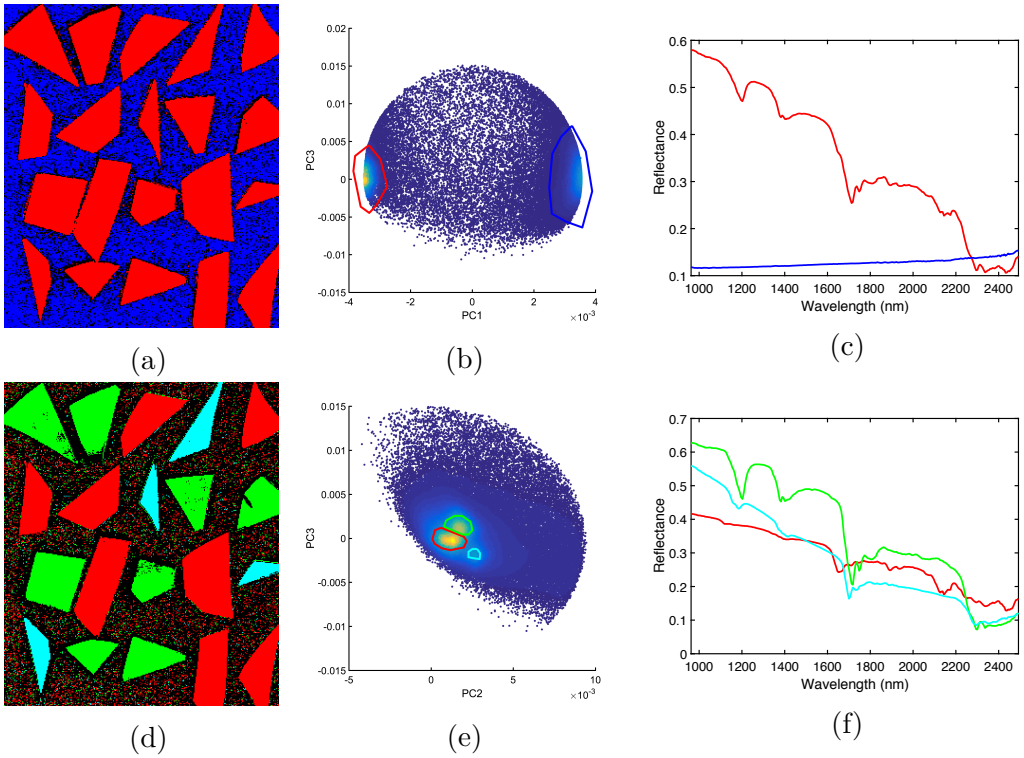


Figure 4.19: PCA of the white fragments of PE, PP, PET, PVC and PS placed on white cardboard. (a) Resulting image, (b) scatter plot (c) spectra plot of PC 1 against PC 3. (d) Resulting image, (e) scatter plot (f) spectra plot of PC 2 against PC 3. Scatter plot plotted in colors of density (yellow is most dense while dark blue is least dense).

Table 4.6: Classified pixels according to material and color by PCA

| Material | Color | Number of pixels |
|---|---|---|
| Plastic | Red | 44 133 |
| Cardboard | Blue | 47 140 |
| Unclassified | Black | 14 378 |
| Total | | 105 651 |

### 4.5.2 Plastics with Added Water

The results of doing PCA on the plastics with 20 ml added water is shown in Figure 4.20. The samples were divided by material (PE, PP, PET, PVC, PS), but within an image the sample came from different sources (e.g. wrapping, boxes,

bottles). The clusters of the different sources of the same material tended to cluster separately as seen in (f)-(j), and the plastics are therefore pseudo-colored accordingly in (a)-(e). In (d) two of the fragments sank, and only their shadows are visible as black pixels. The clusters marking the water (in blue), does not have a clear tendency of where it is placed in the scatter plot. The clusters of water are the most densely populated, and could be found that way.

### 4.5.3 Effect of the Changing Thickness of Water Layer

Changing the thickness of the water layer by adding more water to the Petri dish with PE does not have big impact of the PCA, see Figure 4.21. The water is represented in the lower right corner of the scatter plot with a positive value for PC 2 (principal component number 2) and a negative PC 3 value. The PE is placed to the left and has a negative PC 2 value and a positive PC 3 value. Therefore it is possible to separate the components for this sample by a simple threshold.

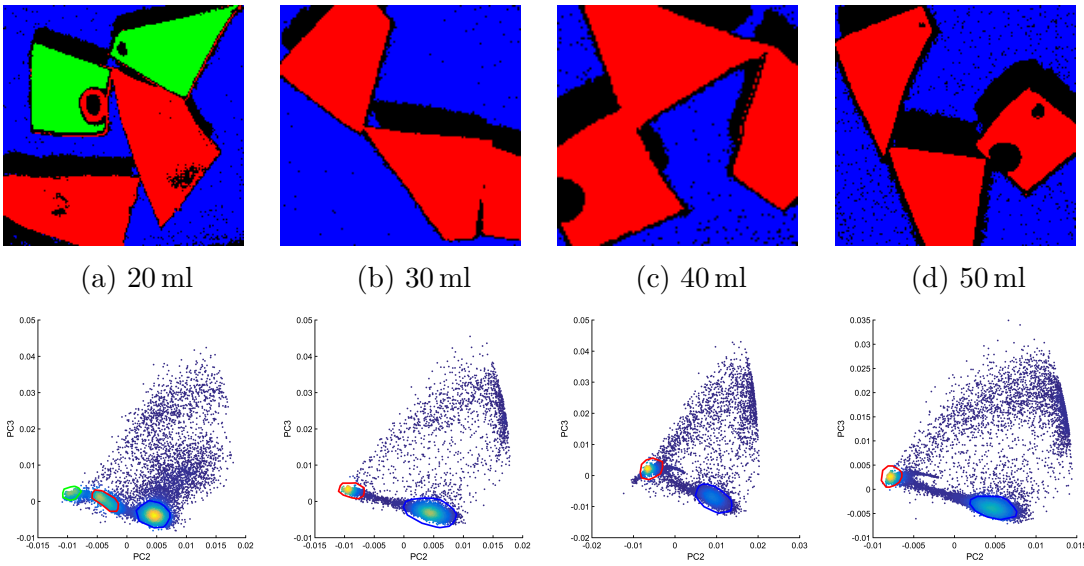


(a) 20 ml (b) 30 ml (c) 40 ml (d) 50 ml

(e) 20 ml (f) 30 ml (g) 40 ml (h) 50 ml

Figure 4.21: PCA of PE with changing level of water. (a)-(d) shows the resulting images of the marked clusters in (e)-(h). (e)-(h) shows the scatter-plots of PC 2 vs. PC 3. Scatter plots plotted in colors of density (yellow is most dense while dark blue is least dense).

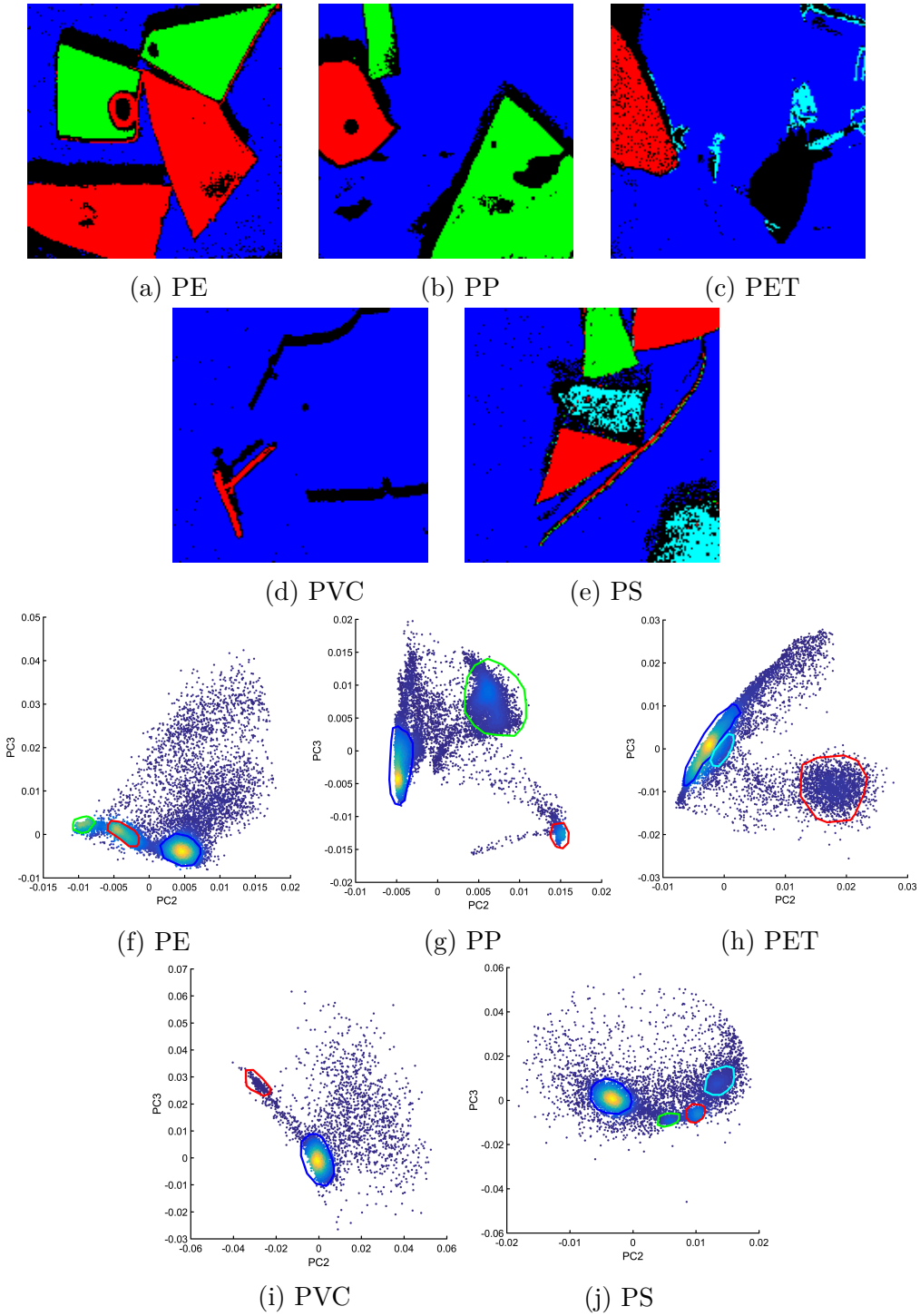


(a) PE (b) PP (c) PET

(d) PVC (e) PS

(f) PE (g) PP (h) PET

(i) PVC (j) PS

Figure 4.20: PCA of the samples with 20 ml added water in the Petri dish. (a)-(e) shows the resulting images of the marked clusters (according to color) in (f)-(j). (f)-(j) shows the scatter-plots of PC 2 vs. PC 3. Scatter plots plotted in colors of density (yellow is most dense while dark blue is least dense).

### 4.5.4 PP from Different Sources

The PCA of the sample containing PP from the different sources collected is shown in Figure 4.22. The scatter plot was chosen to compare PC 2 against PC 3 for all the other samples, as it separated the components of the image the best. For this sample, the scatter plot of PC 2 against PC 3 only showed a single cluster (b), and was therefore not a good choice. PC 1 against PC 3 shows two clusters well separated in (d). Several of the fragments are not classified, and shown in black. This makes PCA more unstable as one has to use different PC for different materials.

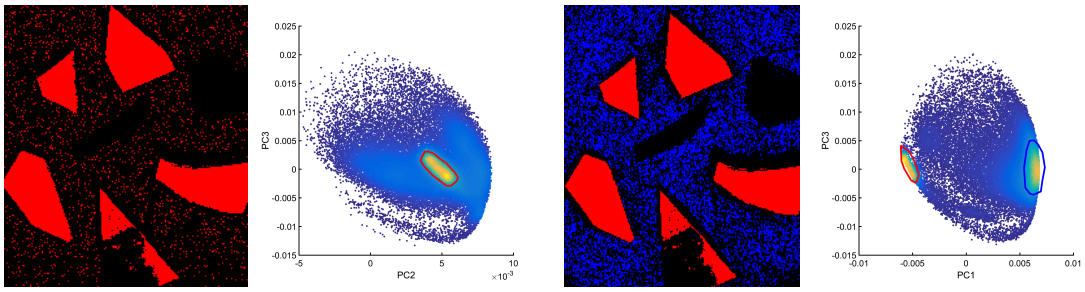


(a) PC 2 vs. PC 3 (b) PC 2 vs. PC 3 (c) PC 1 vs. PC 3 (d) PC 1 vs. PC 3

Figure 4.22: PCA of PP from seven different sources. (a) and (c) shows the resulting images of the clusters in (b) and (d) respectively. (b) shows a scatter plot of PC 2 vs. PC 3, while (d) shows PC 1 vs. PC 3.Scatter plots plotted in colors of density (yellow is most dense while dark blue is least dense).

PCA is dependent on spectra strength and the contents of the image, and have through this presentation of results proved to not be the right tool for classification of materials.

## 4.6 Partial Least Squares-Discriminant Analysis

The results of the PLS-DA will be presented in this section. The categories for the PLS-DA were PE, PP, PET, PVC, PS and water. The categories were set from a combination of several images, to have more samples to train on. The images combined to set the categories (classification categories) were the cardboard-matrix and 20 ml of water added to either PE, PP, PET, PVC or PS.

### 4.6.1 White Plastic Fragments on Black Cardboard

All the types of white plastic fragments placed on the cardboard were identified correctly according to the test-matrix in Figure 3.2, see Figure 4.23 (a). The

fragments have nicely defined edges, and most of the pixels of the plastics are classified. (b) Shows the scatter plot made by the PLS-DA, where the clusters are more separated than the scatter plot by the PCA (Figure 4.19).

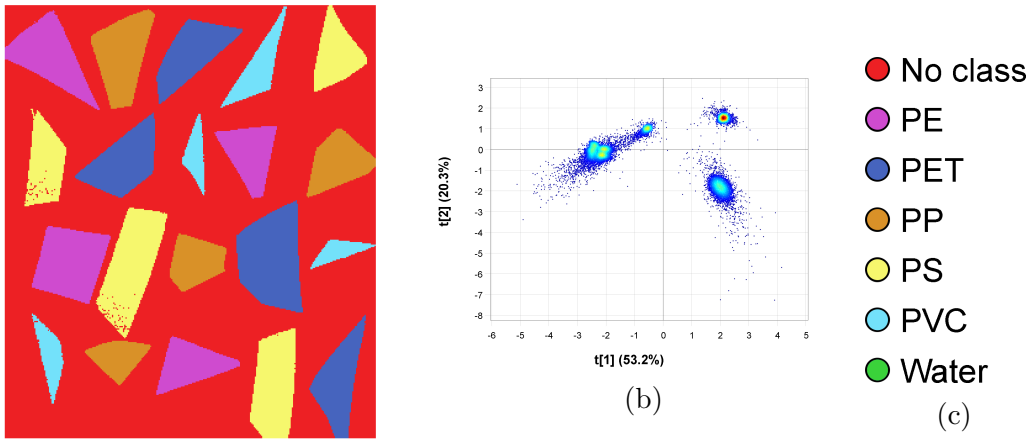


(a) (b) (c)

Figure 4.23: PLS-DA results of the plastic fragments of PE, PP, PET, PVC and PS placed on a cardboard. (a) Pseudo-colored image, as set by PLS-DA, (b) PLS-DA scatter plot, (c) legends for the coloring.

Table 4.7: Classified pixels according to material and color by PLS-DA on the black cardboard with white fragments of PE, PP, PET, PVC and PS. In the PLS-DA, the cardboard was left out as a class, and therefore is a part of the unclassified red pixels.

| Material | Color | Number of pixels |
|---|---|---|
| PE | Purple | 8642 |
| PP | Orange | 6838 |
| PET | Blue | 10 072 |
| PVC | Light Blue | 3303 |
| PS | Yellow | 9140 |
| Unclassified | Red | 67 656 |
| Total | | 105 651 |

### 4.6.2 Plastics with Added Water

PLS-DA's ability to classify different materials varied a lot, as seen in Figure 4.24. (b) Contained PP from two different sources, and only one of the sources were

classified by PLS-DA. In (c) which contained PET and water, none of the PET were classified. The PET were also hard to classify with SAM (Figure 4.15) and PCA (Figure 4.20). One of the reasons is the high density of PET, which caused one of the fragments to sink below the water.

The PVC in (d) were not classified at all, but the PLS-DA found the difference in spectra (shown in red). The greatest fragments had sunk as well in (d). PS in (e) were well classified, and PLS-DA classified all the PS-fragments as PS, despite the different sources (yogurt container and Styrofoam food container).

(a) PE (b) PP (c) PET (d) PVC (e) PS

Figure 4.24: PLS-DA of PE, PP, PET, PVC and PS with 20 ml added water to the Petri dish. PE(purple), PP(orange), PET(dark blue), PVC(light blue), PS(yellow), water(green) and non-classified(red).

### 4.6.3 Effect of the Changing Thickness of Water Layer

Changing the layer of water did not change the outcome of the PLS-DA remarkably. The classification of PE with a varying thickness of water in the Petri dish is shown in Figure 4.25. In (a) there is PE from two different sources (hand lotion container and plastic bag), and the plastic bag was either not classified or classified as water. Neither SAM or PCA were able to classify both types of PE plastic either. The reason for this might be the thickness, as the plastic bag was much thinner and had a different reflectance intensity than the plastic from the hand lotion.

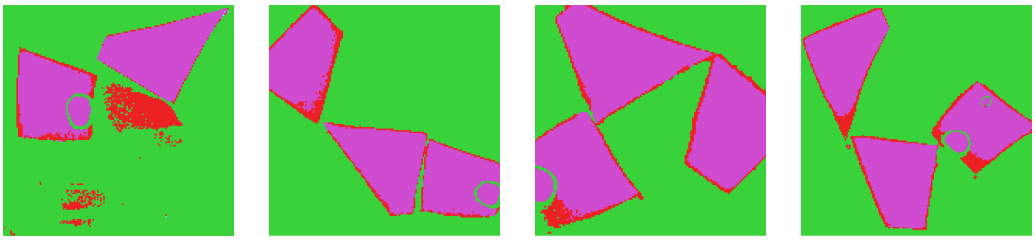

(a) 20 ml (b) 30 ml (c) 40 ml (d) 50 ml

Figure 4.25: PLS-DA of PE with 20 ml, 30 ml, 40 ml and 50 ml water respectively. PE in purple, water in green, red marks unclassified pixels.

### 4.6.4 PP from Different Sources

With PP from seven different sources (see Table 4.1), PLS-DA only classified two out of the seven samples, as seen in Figure 4.26 (a). One of the plastic fragments was classified as water and some of the shadows from the fragments were classified as water as well. The fragments were placed in a Petri dish with no added water. The PLS-DA probably had too few samples to train on, as it is a method that gets better and better the more training samples are used to form the categories.

In (b) the five types of plastic (PE, PP, PET, PVC and PS) were placed in a Petri dish and 10 ml water were added. PLS-DA worked for four out of five samples of plastic. The PVC was not classified, which was the case in Figure 4.24 (d) as well.

An interesting thing to look at, is whether PLS-DA can work as a classification tool between water and plastic. This was done in (c), where PE, PP, PET, PVC and PS were all were categorized together as "plastic". In this case even the fragment of PVC was classified.

(a) PP, (from seven sources)

(b) PE, PP, PET, PVC, PS, 10 ml water

(c) PE, PP, PET, PVC, PS, 20 ml water

Figure 4.26: PLS-DA of (a) seven different types of collected PP (b) PE, PP, PET, PVC, PS and 10 ml and (c) PE, PP, PET, PVC, PS and 20 ml. (a) and (b) are colored according to Figure 4.23(c), while (c) pseudo-colors plastic blue and water green.

## 4.7 Accuracy

Table 4.8: PLS-DA classification matrix

| Material Classification | PE | PP | PET | PVC | PS | Water | Row total |
|---|---|---|---|---|---|---|---|
| PE | **17** | | | | | | 17 |
| PP | | **12** | | | | | 12 |
| PET | | | **4** | | | | 4 |
| PVC | | 2 | 2 | **7** | 1 | | 12 |
| PS | | | | | **14** | | 14 |
| Water | | | | | | **12** | 12 |
| No class | 3 | 7 | 4 | 5 | | | 19 |
| Column total | 20 | 21 | 10 | 12 | 15 | 12 | 90 |
| Accuracy | 85% | 57% | 40% | 58% | 93% | 100% | 73% |

In the previous sections (subsection 4.4.1, subsection 4.5.1 and subsection 4.6.1), the pixel count of the image containing white plastic fragments on a black cardboard has been shown. In Table 4.9, a greater amount of pixels were classified by PCA than SAM, but the classification by PCA is highly dependent on the area marked by visual inspection, and SAM by the set threshold. PCA marked all types of plastic together, and was able to classify more of the plastic. SAM had some troubles with PP and PS for a low threshold ($t = 0.05$). PLS-DA was not trained to predict cardboard (no class was defined by the cardboard), which made all the cardboard unclassified. PLS-DA classified (predicted) more plastic by percentage than SAM. In all three cases the cardboard and the edges between plastic and cardboard were the least classified.

Table 4.9: The classified pixels by SAM, PCA and PLS-DA in the image containing white plastic fragments on a black cardboard compared by percentage. PLS-DA was not trained to predict cardboard, and therefore no pixels were classified as cardboard by PLS-DA.

| Material | SAM [%] | PCA [%] | PLS-DA [%] |
|---|---|---|---|
| Plastic | 31.3 | 41.8 | 36.0 |
| Cardboard | 46.1 | 44.6 | - |
| Unclassified | 22.6 | 13.6 | 64.0 |

Even though SAM performed poorest measured in percentage classified, the

SAM classified all fragments correctly, and in a classification process it would be enough to separate the plastics. PCA performed best by percentage, but the classification depended on the choice of compared principal components. PLS-DA would have performed better with more training.

## 4.8 Three Band Analysis

In reality, using 256 wavelengths gives great characteristics, but takes a lot of processing power and much storage space. One way to reduce the amount of data is to reduce the number of bands. The analysis in this section has therefore been performed using only three wavelengths. The wavelengths were chosen according to the results of the mean spectra-features of the plastics, as given in Table 4.2. The four wavelengths chosen, were the mean of the absorption troughs (1162 nm, 1392 nm, 1684 nm and 2281 nm).

From the four chosen wavelengths, only three were used. The results of using the bands at 1392 nm, 1684 nm and 2281 nm are shown in Figure 4.27.

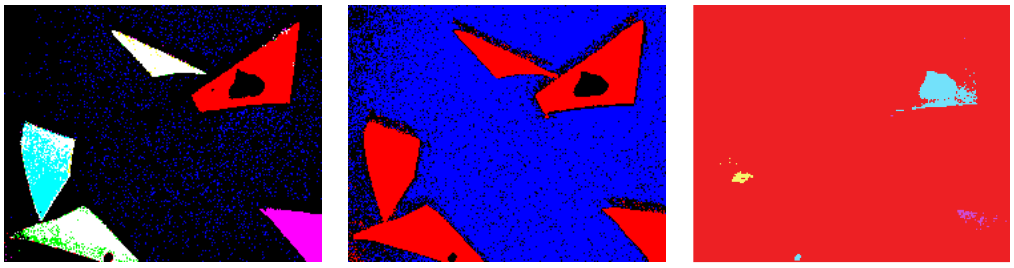

(a) SAM (b) PCA (c) PLS-DA

Figure 4.27: Analysis of the image containing PE, PP, PET, PVC, PS and added 10 ml added water. The bands used for analysis were 1392 nm, 1684 nm and 2281 nm. (a) SAM with a threshold for all components of $t = 0.05$, (b) resulting PCA-image, (c) resulting PLS-DA prediction. Coloring for the image in (a) PE(red), PP(cyan), PET(green), PVC(yellow), PS(magenta) and water (blue), white is overlap by at least two classifications, in (b) plastic (red), water (blue), and in (c) PE(light blue), PP(yellow), PS(pink) and unclassified(red).

SAM works quite well for the three chosen bands, and the method is able to classify most of the plastic. With a low threshold of $t = 0.05$, SAM classifies several pixels as below the threshold for more than one reference spectra (marked white in (a)). Many of the water pixels are still unclassified(black). The clusters in the PCA was spread on each side of zero for PC 2, and the resulting image is shown in (b). There were only two clusters, hence all the plastics were marked red. The PLS-DA did not work quite as well, only a few pixels were predicted.

From this result, using three wavelengths is a possibility, especially by using SAM. PLS-DA would probably need a greater set of training data to be able to predict more pixels. PCA would work to separate the plastic from the water. Using different wavelengths of the ones mentioned above, the result was quite similar. The analysis showed that the second wavelength (1392 nm) is the most important wavelength to distinguish the water from the samples, and within the samples. As seen in Figure 4.4, the reflectance of water at this wavelength is very low.

Another image, classifying the white plastic fragments placed on black cardboard is shown in Figure 4.28. SAM was able to classify all of the plastic fragments as plastic, but PE and PP had a lot of overlapping pixels(white). PCA was able to distinguish between cardboard and plastic. PLS-DA was able to predict more pixels than in Figure 4.27.

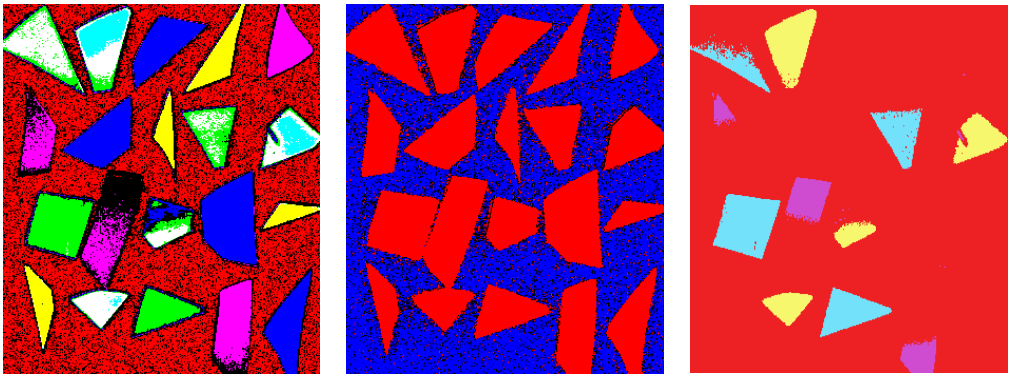

(a) SAM (b) PCA (c) PLS-DA

Figure 4.28: Analysis of the image containing PE, PP, PET, PVC, PS and added 10 ml added water. The bands used for analysis were 1162 nm, 1392 nm and 2281 nm. (a) SAM with a threshold for all components of $t = 0.05$, (b) resulting PCA-image, (c) resulting PLS-DA prediction. Coloring for the image in (a) PE(green), PP(cyan), PET(blue), PVC(yellow), PS(magenta) and cardboard(red), white is overlap by at least two classifications, in (b) plastic(red), cardboard(blue), and in (c) PE(light blue), PP(yellow), PS(pink) and unclassified(red).

## 4.9 Discussion

In reality if the method of HSI of plastics in water will be used, it will most likely be used as the first step of characterization. This means it will be more important for this method to distinguish between plastics and other types of materials one might find in the ocean or on shore, such as seaweed, glass and wood, instead of

between different types of plastics. A result of how the three different methods have dealt with the task of classifying plastics in water is shown in Figure 4.29. In SAM the reference spectra were made up of the mean from the ROI of PE, PP, PET, PVC, and PS, and so was the categories in the PLS-DA.

As seen in Figure 4.29, all three methods were able to distinguish plastics (in general) from water.

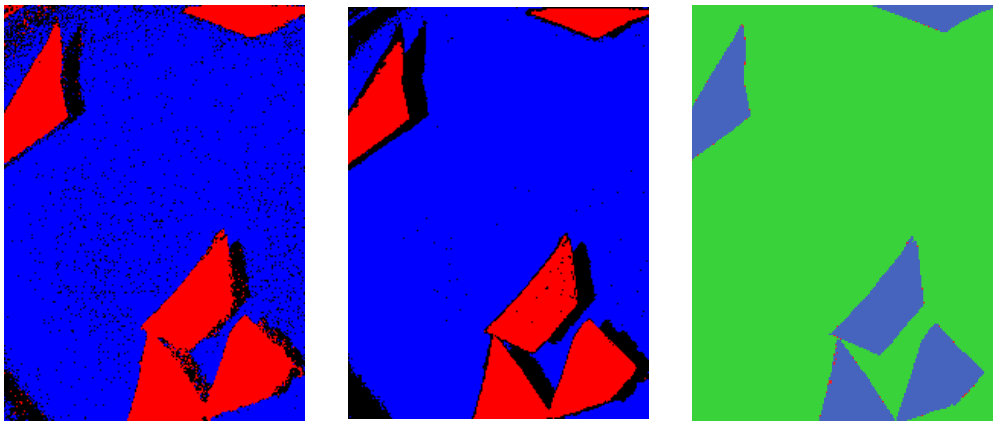

(a) SAM (b) PCA (c) PLS-DA

Figure 4.29: Comparison of (a) SAM (water, blue, plastic, red), (b) PCA (water, blue, plastic, red) and (c) PLS-DA (water, green, plastic, red) of plastics (PE, PP, PET, PVC and PS) in water.

For SAM, the angles between samples were presented in Table 4.4 and Table 4.5. The angles between different types of PP were shown to be greater than between different types of white plastic fragments of PE, PP, PET, PVC, and PS. This proves the additives to the plastics play a big role in the calculation of the spectral angle. Even though the spectra looked quite different and the angles calculated were quite big, the main spectral features were intact for the different PP's (see Figure 4.10). Reducing the amount of bands, only including bands close to the absorption features might reduce the spectral angle between different types of PP, as calculated by SAM.

From the experiments performed, the mean spectra of glass, cardboard, seaweed and water was obtained, and are shown in Figure 4.30 together with the spectra of vegetation.

As seen in Figure 4.30, the spectra of grass, soil, vegetation, glass, water, cardboard, and seaweed are relatively different from the spectra of the plastics in (d). For a three-band analysis it is important to choose the wavelengths that makes the plastics spectra stand out the most from the other material spectra.

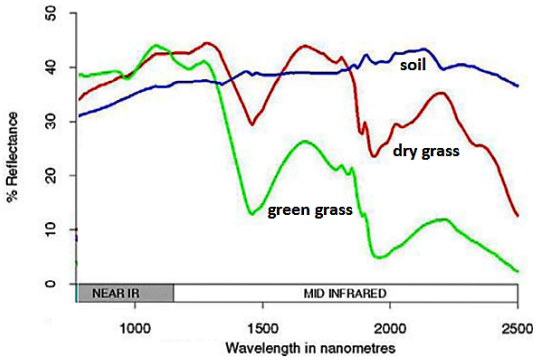


(a) Soil, green grass, and dry grass[100]

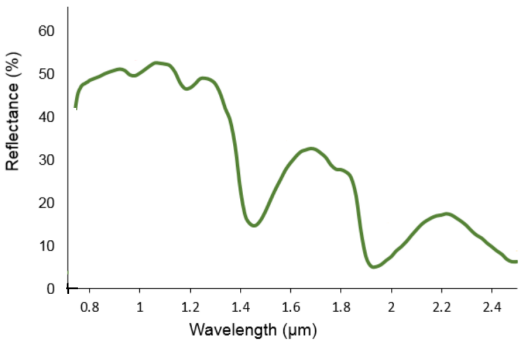


(b) Vegetation[101]

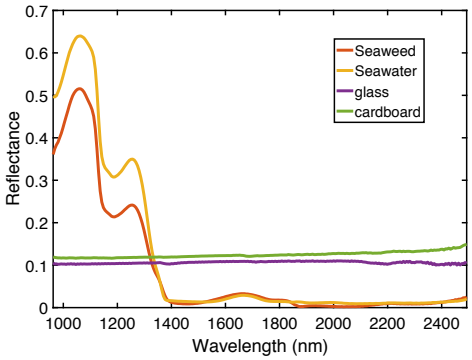


(c) Glass, cardboard, seaweed, and water

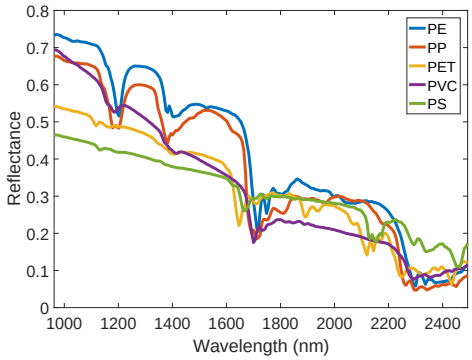


(d) PE, PP, PET, PVC, and PS

Figure 4.30: The spectra of (a) soil, green grass, and dry grass,[100] (b) vegetation,[101] (c) glass, cardboard, seaweed, and water, and (d) PE, PP, PET, PVC, and PS. (a) and (b) modified from literature. Note: different scaling.

In the laboratory setup, the imaging process was controlled. Bringing the imaging system outdoors, aspects like weather and illumination source must be taken into account. The lamp used in the experiment emitted light in the desired wavelengths. An illumination source is needed outside as well. The sun emits light in the NIR region, but the absorption in water reduces the incoming light substantially for some of the wavelengths chosen in the three-band method. Therefore, an illumination source might be needed.

Outside weather is another factor to take into account. Due to the high absorption in water, rainy days are not optimal for NIR-imaging. The performance of SAM, PCA, and PLS-DA for the results presented in this chapter is presented in Table 4.10.

SAM proved to be the most consistent method of the three of them. For the three band imaging, SAM performed well, and as mentioned in subsection 4.4.5, the three band images might improve SAM's classification ability of different PP.

The analysis using PCA was not consistent, and the best PC's used in the PC scatter plot varied. The placement of the clusters was not consistent, except for the sample with changing water thickness with PE.

PLS-DA worked well for some samples. It was experienced during the analysis that the greater the data basis used during training were, the better the prediction made by PLS-DA was. Further acquiring of images would increase the data basis, and improve the training, such that PLS-DA would be able to give consistently good predictions.

Table 4.10: Comparison of SAM, PCA, and PLS-DA on the performance and the results in this thesis.

| Sample type | SAM | PCA | PLS-DA |
|---|---|---|---|
| White plastic fragments on cardboard | ✓ | (✓) | ✓ |
| Plastics in water | ✓ | ✓ | |
| Changing water level | ✓ | ✓ | ✓ |
| PP, different sources | | | |
| Three bands | ✓ | ✓ | |

The type of plastics that float ashore on beaches is highly dependent on the location. Close to plastic industries, plastic pellets are common, close to fishing industry, fishing nets and lines are common. If this method proves to work at identifying plastics in the ocean, it would be interesting to distinguish between similar products. If it was possible to distinguish between different types of e.g.

plastic pellets, and find the guilty industry for the contamination, that would be a way to enforce the law of littering. Maybe further analysis would be enough, or maybe a increase in the spectral resolution would be needed to distinguish between e.g. plastic pellets.

# Chapter 5: Conclusion

An introductory examination of the use of hyperspectral imaging to characterize plastics in the ocean has been performed. Plastics collected from household waste has been imaged in a laboratory setup. The results of the measurements have shown that hyperspectral imaging is an applicable method to classify plastics in the ocean.

The classification methods SAM, PCA and PLS-DA have been used on the hyperspectral images. The classification methods were used to identify the plastic samples. To validate the classification methods a known set of plastic samples of known plastic material and a measured amount of seawater were used. The plastics used during the experiments were PE, PP, PET, PVC and PS.

For SAM and PLS-DA, ROI's from the samples were used to classify/predict the contents of the hyperspectral images. SAM worked well on most samples, by adjusting the threshold. For samples of one sample material (e.g. PP), but from different sources (yogurt container, strawberry container etc.), which might contain different fillers and pigmentation to achieve the wanted appearance, the threshold needed to be much higher than for same source materials.

The classification method PLS-DA worked quite well for distinguishing between plastic and water. The prediction made by the PLS-DA was proved during analysis to work better the more samples it used in its categories (during training).

PCA proved to be able to cluster different groupings together. The placement of the clusters made by comparing the values of two principal components were not consistent between water and plastic. The method was found to be highly dependent on spectral intensity. Due to the lack of consistency of the cluster placement, PCA should not be used as the classification method.

Different fillers, especially black pigmentation have been proved to be hard to classify, as the SNR is very low, due to the spectral features of the samples being approximately the same size as the noise. Neither of the methods were able to classify the black plastic as a part of a classification group. Only if the black plastic was used as a reference spectrum, SAM managed to classify the black plastics. It was probably classified due to the lack of absorption features, rather than due to the absorption features.

The main absorption features for PE, PP, PET, PVC, PS and water were found. The main absorption features arose from combination, first- and second-overtone C-H stretching in the plastics, and from combinations of asymmetric and symmetric stretch and symmetric bending of H-O-H for the water.

For plastics with higher densities than water, such as PVC, this method will

not work in the ocean, as the samples will sink and the NIR absorption in water is too big. On shorelines on the other hand, the plastic is not covered by water but is most likely mixed with water, seaweed, and other trash, where the method will most likely work, according to section 4.9. The spectra of seaweed, vegetation, grass, cardboard, soil and glass are found to be substantially different from plastics, and the identification/classification of plastics should work.

Analysis based on three of the spectral bands showed promising results of classifying the plastics from the water. The bands were chosen from the mean wavelengths of the main absorption features of the plastics. The wavelengths were found to be at 1162 nm, 1392 nm, 1684 nm and 2281 nm. The most important band for classification between plastic and water was at 1392 nm.

During the literature study on plastic contamination, it has shown to be important to find a way to detect and clean up the plastics from the ocean as soon as possible. The increasing amount of microplastics and plastics in the ocean is put on the agenda to several environmental organizations. Being in contact with "Bellona" through emails and a phone call, and an evening seminar with "Miljøvernforbundet", has shown how important this is for them.

## 5.1 Recommendations for Further Work

In further work it is important to validate the findings found in this thesis, to ensure the results and the conclusion have been made correctly. Reference spectra from a larger variation of the different plastic types should be made for SAM, and more training and ROI's should be used in the categories PLS-DA uses for prediction.

A goal for further work with hyperspectral imaging of plastic particles in the ocean would be to bring the technology out of the laboratory. The size of the plastics will vary, and high spatial resolution is needed. Especially if the goal is to find microplastics. To ease the need of processing power the spectral dimension should be reduced. Further tests should be performed with fewer wavelengths (e.g. three, as proposed in section 4.8).

The method is well known in the plastic recycling industry, and the same technology could most likely be used on plastics in water as long as they are not covered by water. In addition the illumination source for outdoor recording should be looked into.

A different classification method could also be used for further experiments, and compare them with the methods used in this analysis.

Finding the best three wavelengths should be put weight on. The three best wavelengths should take into account the absorption of wavelengths in water (lower illumination from the sun, impact of changing humidity etc.). Other materials one

might expect to be found in or around the ocean should be compared with the spectra of water for those three wavelengths as well.

Being able to find the exact source for the plastics found would be an advantage for the law enforcement to charge industries guilty for littering. To be able to do this, a spectral library is needed, and comparison of weathered products (teared, partly decomposed, grown by algae) and brand new products needs to be taken into account for this to possible.

# Bibliography


[1] S. Bogfjellmo, *Field-Deployable Hyperspectral Analysis*. Norwegian University of Technology and Science, Department of Electronics and Telecommunications, Project Report, 2016.

[2] J. A. Richards, X. Jia, *Remote Sensing Digital Image Analysis - An Introduction(Third Edition)*. Springer, 1996.

[3] L. Loncan , L. B. Almeida , J. M. Bioucas-Dias , X. Briottet , J. Chanussot , N. Dobigeon , S. Fabre , W. Liao , G. A. Licciardi , M. Simões , J.-Y.s Tourneret , M. A. Veganzones , G. Vivone , Q. Wei , N. Yokoya, "Hyperspectral pansharpening: a review," *CoRR*, vol. abs/1504.04531, 2015.

[4] P. S. Gromski, H. Muhamadali, D. I. Ellis, Y. Xu, E. Correa, M. L. Turner, R. Goodacre, "A tutorial review: Metabolomics and partial least squares-discriminant analysis – a marriage of convenience or a shotgun wedding," *Analytica Chimica Acta*, vol. 879, pp. 10 – 23, 2015.

[5] R. Vannela, "Are we "Digging Our Own Grave" under the oceans?" *Environmental Science & Technology*, vol. 46, no. 15, pp. 7932–7933, 2012.

[6] M. A. Browne, A. Dissanayake, T. S. Galloway, D. M. Lowe, R. C. Thompson, "Ingested microscopic plastic translocates to the circulatory system of the mussel, mytilus edulis (l.)," *Environmental Science & Technology*, vol. 42, no. 13, pp. 5026–5031, 2008.

[7] I. E. Napper, A. Bakir, S. J. Rowland, R. C. Thompson, "Characterization, quantity and sorptive properties of micoplastics extracted from cosmetics," *Marine Pollution Bulletin*, 2015.

[8] C. M. Boerger, G. L. Lattin, S. L. Moore, C. J. Moore, "Plastic ingestion by planktivorous fishes in the North Pacific Central Gyre," *Marine Pollution Bulletin*, vol. 60, no. 12, pp. 2275 – 2278, 2010.

[9] DG Environment Newsalert Service, "Plastic waste: Ecological and human health impacts," Science for Environment Policy, European Commission, Tech. Rep., 2011.

[10] C. Jordan (U.S. Fish and Wildlife Service Headquarters), "Albatross at midway atoll refuge." [Online]. Available: https://commons.wikimedia.org/w/index.php?curid=26762401

[11] C. Moore, C. Phillips, *Plastic ocean: How a sea captain's chance discovery launched a determined quest to save the oceans.* Avery, 2011.

[12] J. G. B. Derraik, "The pollution of the marine environment by plastic debris: a review," *Marine Pollution Bulletin*, vol. 44, no. 9, pp. 842 – 852, 2002.

[13] P. Sundt, P-E. Schulze, F. Syversen, "Sources of microplastics-pollution to the marine environment," Norwegian Environment Agency (MiljØdirektoratet), Tech. Rep., 2014.

[14] *UN scientists call for action on marine microplastics*, 2015. [Online]. Available: http://www.theguardian.com/environment/2015/apr/29/un-scientists-call-for-action-on-marine-microplastics

[15] M. Chang, "Microplastics in facial exfoliating cleansers," 2013. [Online]. Available: http://nature.berkeley.edu/classes/es196/projects/2013final/ChangM_2013.pdf

[16] NOAA. Noaa's marine debris blog. [Online]. Available: https://marinedebrisblog.wordpress.com/category/microplastics/

[17] C. Z. Yang, S. I. Yaniger, V. C. Jordan, D. J. Klein, G. D. Bittner, "Most plastic products release estrogenic chemicals: A potential health problem that can be solved," *Environmental health perspectives*, vol. 119, no. 7, pp. 989–996, 2011. [Online]. Available: http://search.proquest.com/docview/880949183?accountid=12870

[18] K. Tanaka, H. Takada, R. Yamashita, K. Mizukawa, M. A. Fukuwaka, Y. Watanuki, "Accumulation of plastic-derived chemicals in tissues of seabirds ingesting marine plastics," *Marine Pollution Bulletin*, vol. 69, no. 1–2, pp. 219 – 222, 2013. [Online]. Available: http://www.sciencedirect.com/science/article/pii/S0025326X12005942

[19] R. Sussarellu, M. Suquet, Y. Thomas, C. Lambert, C. Fabioux, M. E. J. Pernet, N. Le Goïc, V. Quillien,C. Mingant, Y. Epelboin, C. Corporeau, J. Guyomarch, J. Robbens, I. Paul-Pont, P. Soudant, A. Huvet, "Oyster reproduction is affected by exposure to polystyrene microplastics," *Proceedings of the National Academy of Sciences*, vol. 113, no. 9, pp. 2430–2435, 2016. [Online]. Available: http://www.pnas.org/content/113/9/2430.abstract

[20] C. Stevenson, "Plastic devris in the california marine ecosystems: A ssummary of current research, solution efforts and data groups," University of Southern California, Sea Grant, Los Angeles, CA, U.S.A, Tech. Rep., 2011.

[21] Y. Mato, T. Isobe, H. Takada, H. Kanehiro, C. Ohtake, T. Kaminuma, "Plastic resin pellets as a transport medium for toxic chemicals in the marine environment," *Environmental Science & Technology*, vol. 35, no. 2, pp. 318–324, 2001.

[22] K. L. Law, S. E. Morèt-Ferguson, D. S: Godwin, E. R: Zettler, E. DeForcee, T. Kukulka, G. Proskurowski, "Distribution of surface plastic debris in the eastern pacific ocean from an 11-year data set," *Environmental Science & Technology*, vol. 48, pp. 4732–4738, 2014.

[23] R. C. Thompson, Y. Olsen, R. P. Mitchell, A. Davis, S. J. Rowland, A. W. G. John, D. McGonigle, A. E. Russell, "Lost at sea: Where is all the plastic," *Science Mag*, vol. 304, p. 838, 2004.

[24] J. M. Amigo, H. Babamoradi, S. Elcoroaristizabal, "Hyperspectral image analysis. a tutorial," *Analytica Chmica Acta*, vol. 896, pp. 34–51, 2015.

[25] S. Serranti, V. Luciani, G. Bonifazi, B. Hu, P. C. Rem, "An innovative recycling process to obtain pure pe and pp from houshold waste," *Waste Management*, vol. 35, pp. 12–20, 2015.

[26] Researchgate. Mathias bochow. [Online]. Available: https://www.researchgate.net/profile/Mathias_Bochow/publications

[27] L. A: Paluchowski, E. Misimi, L. Grimsbo, L. L. Randeberg, "Towards automated sorting of atlantic cod (gadus morhua) roe, milt, and liver – spectral characterization and classification using visible and near-infrared hyperspectral imaging," *Food Control*, vol. 62, pp. 337–345, 2016.

[28] Y. Naoyuki, S. Tsubasa, O. Satoru, I. Ichiro, "Middle infrared (wavelength range: 8 µm to 14 µm) 2-dimensional spectroscopy (total weight with electrical controller: 1.7 kg, total cost: less than 10,000 usd) so-called hyperspectral camera for unmanned air vehicles like drones," pp. 984 028–984 028–7, 2016.

[29] D.-W. Sun, *Hyperspectral Imaging for food quality analysis and control.* Elsevier Inc., 2010, ch. 4, Hyperspectral Image Processing Techniques.

[30] D-W. Sun, *Hyperspectral Imaging for food quality analysis and control.* Elsevier Inc., 2010, ch. 1, Principles of Hyperspectral Imaging Technology.

[31] J. Hernandez-Palacios, L.L. Randeberg, I. Baarstad, T. Løke, T. Skauli, "Hyperspectral low-light camera for imaging of biological samples," in *2010 2nd Workshop on Hyperspectral Image and Signal Processing: Evolution in Remote Sensing*, 2010, pp. 1–4.

[32] L. L. Randeberg, "Personal written and oral communication."

[33] Investopdeia. Multicollinearity. [Online]. Available: http://www.investopedia.com/terms/m/multicollinearity.asp

[34] G. Lu, B. Fei, "Medical hyperspectral imaging: a review," *Journal of Biomedical Optics*, vol. 19, no. 1, p. 010901, 2014.

[35] D.-W. Sun, *Hyperspectral Imaging for food quality analysis and control*. Elsevier Inc., 2010, ch. 3, Hyperspectral Image Classification Methods.

[36] T. Skauli, T. Haavardsholm, I. Kåsen, T. Opsahl, A. Kavara, A. Skaugen, "Hyperspectral imaging technology and systems, exemplified by airborne real-time target detection," *CLEO:2011 - Laser Applications to Photonic Applications*, p. CMG5, 2011. [Online]. Available: http://www.osapublishing.org/abstract.cfm?URI=CLEO_SI-2011-CMG5

[37] LaserFocusWorld. Hyperspectral imaging: One-shot camera obtains simultaneous hyperspectral data. [Online]. Available: http://www.laserfocusworld.com/articles/print/volume-47/issue-3/world-news/hyperspectral-imaging-one-shot-camera-obtains-simultaneous-hyperspectral-data.html

[38] ABB, "Hyperspectral imaging ft-spectroradiometers: Radiometric accuracy for infrared signature measurements." [Online]. Available: https://library.e.abb.com/public/f680cc90e1ad1c3a852578cb006b1034/4567%20MR-i%206%20pages%20V2%20.pdf

[39] L. Ziph-Schatzberg. Hyperspectral imaging enables industrial applications. [Online]. Available: http://www.photonics.com/Article.aspx?AID=56804

[40] M. Schlerf, G. Rock, P. Lagueux, F. Ronellenfitsch, M. Gerhards, L. Hoffmann, T. Udelhoven, "A hyperspectral thermal infrared imaging instrument for natural resources applications," *Remote Sensing*, vol. 4, pp. 3995–4009, 2012.

[41] C. D: Tran, "Principles, instrumentation, and applications of infrared multispectral imaging, an overview," *Analytical Letters*, vol. 38, pp. 735–752, 2005.

[42] N. Gat, "Imaging spectroscopy using tunable filters: A review," *Proc. SPIE*, vol. 4056, pp. 50–64, 2000.

[43] S. E: Umbaugh, *Digital Image Processing and Analysis: Human and Computer Vision*. Taylor & Francis Group, LLC, 2011.

[44] B. Bhanu, S. Lee, *Genetic Learning for Adaptive Image Segmentation*. Springer Science & Business Media, LLC, 1994.

[45] M. E. Thomas, *Optical Propagation in Linear Media: Atmospheric Gases and Particles, Solid-State Components, and Water*. Oxford University Press, 2011.

[46] the Physics Classroom. Light absorption, reflection, and transmission. [Online]. Available: http://www.physicsclassroom.com/class/light/Lesson-2/Light-Absorption,-Reflection,-and-Transmission

[47] U. ChemWiki. Combination Bands, Overtones and Fermi Resonances. [Online]. Available: http://chemwiki.ucdavis.edu/Core/Physical_Chemistry/Spectroscopy/Vibrational_Spectroscopy/Vibrational_Modes/Combination_Bands,_Overtones_and_Fermi_Resonances

[48] L. V. Wang, H. Wu, *Biomedical Optics, Principles and Imaging*. John Wiley & Sons, 2007.

[49] B. E. A. Saleh, M. C. Teich, *Fundamentals of Photonics, second edition*. John Wiley & Sons, 2007.

[50] Z. Otremba, "The influence of an oil-film covered sea surface on the reflection and upward transmission of light," *Oceanologia*, vol. 36, pp. 137–154, 1994.

[51] M. Kutz, *Applied Plastics Engineering Handbook: Processing and Materials*. William Andrews (imprint of Elsevier), 2011.

[52] A. Small S. Hong, D. Pine, "Scattering properties of core–shell particles in plastic matrices," *Journal of Polymer Science Part B: Polymer Physics*, vol. 43, no. 24, pp. 3534–3548, 2005.

[53] U. Fritz Albregtsen. Reflection, refraction, diffraction, and scattering. [Online]. Available: https://www.uio.no/studier/emner/matnat/ifi/INF-GEO4310/h09/undervisningsmateriale/imaging-kap2.pdf

[54] R. N. Clark, G. A. Swayze, I. Leifer, K. E. Livo, R. Kokaly, T. Hoefen, S. Lundeen, M. Eastwood, R. O. Green, N. Pearson, C. Sarture, I. McCubbin, D. Roberts, E. Bradley, D. Steele, T. Ryan, R. Dominguez, and the Airborne Visible/Infrared Imaging Spectrometer (AVIRIS) Team , "A method for quantitative mapping of thick oil spills using imaging spectroscopy," USGS (U.S. Geological Survey), Tech. Rep., 2010.

[55] I. Scientific Polymer Products. Refractive index of polymers by index. [Online]. Available: http://scientificpolymer.com/technical-library/refractive-index-of-polymers-by-index/

[56] Plastemart. (2014) Global demand for polyethylene to rise 4% pa to almost 100 mln tons in 2018. [Online]. Available: http://www.plastemart.com/Plastic-Technical-Article.asp?LiteratureID=2189&Paper=Global-demand-polyethylene-4-percent-to-100-million-tons-in-2018

[57] Ceresana, Market Intelligence Consulting. (2014) Market study: Poypropylene (3rd edition). [Online]. Available: http://www.ceresana.com/en/market-studies/plastics/polypropylene/

[58] T. Somheil. (2014) Study: global pvc demand grow 3.2% annualy through 2021. [Online]. Available: http://www.plasticstoday.com/articles/study-global-pvc-demand-grow-32-annually-through-2021-140825

[59] (2014) Global pet supply to exceed 24.39 mln tonnes in 2015. [Online]. Available: http://mcgroup.co.uk/news/20140117/global-pet-supply-exceed-2439-mln-tonnes-2015.html

[60] The Essential Chemical Industry, University of York. Poly(phenylethene) (polystyrene). [Online]. Available: http://www.essentialchemicalindustry.org/polymers/polyphenylethene.html

[61] Encyclopædia Britannica Online. (2016) Polyethylene (pe). [Online]. Available: http://global.britannica.com/science/polyethylene

[62] K. Batra, "Role of additives in linear low density polyethylene (lldpe) films," Master's thesis, Department of Chemistry, Indian Institute of Technology Kharagpur, Kharagpur, West Bengal-721302, 2013-14.

[63] D. Tripathi, *Practical Guide to Polypropylene*. Shawbury, Shrewsbury, Shropshire, UK: Rapra Technology Limited, 2002.

[64] C. Maier, T. Calafut, *Polypropylene: The Definitive User's Guide and Databook*. Norwich, NY, USA: Plastics Design Library, 1998.

[65] Plastic Moulding. Polyvinyl chloride (pvc). [Online]. Available: http://www.plasticmoulding.ca/polymers/pvc.htm

[66] Wikipedia. Polyethylene terephtalate. [Online]. Available: https://en.wikipedia.org/wiki/Polyethylene_terephthalate

[67] AZO Materials. Polystyrene(ps)(c8h8) plastic recycling. [Online]. Available: http://www.azom.com/article.aspx?ArticleID=7915

[68] MSNBC. New york city's 'styrofoam' ban goes into effect. [Online]. Available: http://www.msnbc.com/msnbc/new-york-citys-styrofoam-ban-goes-effect

[69] P. M. Inc. Fillers. [Online]. Available: http://www.plasticmaterials.net/fillers/fillers.html

[70] A. M. van Hank, *Chemistry and Technology of Emulsion Polymerisation*. John Wiley & Sons, 2013.

[71] K. Sleigh. (2011). [Online]. Available: http://algeinfo.imr.no/index.php?side=visinfo&id=513

[72] W. H. S. G. NOAA. Hvor lang tid tar det fr det brytes ned? [Online]. Available: http://www.miljostatus.no/tema/avfall/forsopling-av-havet/

[73] S: Jacquemoud, S. L. Ustin. Application of radiative transfer models to moisture content estimation and burned land mapping. [Online]. Available: http://www.ipgp.jussieu.fr/~jacquemoud/publications/jacquemoud2003.pdf

[74] B. H. Stuart, *Analytical Techniques in the Sciences (AnTs)*: Infrared Spectroscopy: Fundamentals and Applications*. John Wiley & Sons, 2004.

[75] N. Parthiban, S. S: Ghosh, D. Banji, "Near infra red spectroscopy- an overview," *International Journal of ChemTech Research*, vol. 3, pp. 831–832, 2011.

[76] H. Masoumi, S. M. Safavi, Z. Khani, "Identification and classification of plastic resins using near infrared reflectance spectroscopy," *International Journal of Mechanical, Industrial, Mechatronic and Manufacturing Engineering*, vol. 6, pp. 877–884, 2012.

[77] C. Rodarmel, J. Shan, "Principal component analysis of hyperspectral image classification," *Surveying and Land Information Systems*, vol. 62, no. 2, p. 115, 2002.

[78] , "An application of image processing techniques for enhancement and segmentation of bruises in hyperspectral images," Master's thesis, Norwegian University of Science and Technology Department of Computer and Information Science, 2005.

[79] L. I. Smith, "A tutorial on principal component analysis," 2002.

[80] M. Richardson, "Principal component analysis," 2009.

[81] Wikipedia. Eigenvalues and eigenvectors. [Online]. Available: https://en.wikipedia.org/wiki/Eigenvalues_and_eigenvectors

[82] D.-W. Sun, *Hyperspectral Imaging for food quality analysis and control*. Elsevier Inc., 2010, ch. 5, Spectral Preprocessing and Calibration techniques.

[83] V. Powell, L. Lehe. (2015) Principal component analysis; explained visually. [Online]. Available: http://setosa.io/ev/principal-component-analysis/

[84] J. Shlens, "A tutorial on principal component analysis," 2005.

[85] E. P. University. [Online]. Available: ftp://ftp.ecn.purdue.edu/jshan/86/help/html/spectral_analysis/minimum_noise_fraction.htm

[86] ENVI. Minimum noise fraction transform. [Online]. Available: https://www.harrisgeospatial.com/docs/minimumnoisefractiontransform.html

[87] P. E. Dennison, K. Q. Halligan, D. A. Roberts, "A comparison of error metrics and constraints for multiple endmember spectral mixture analysis and spectral angle mapper," *Remote Sensing of Environment*, vol. 93, pp. 359–367, 2004.

[88] O. A. de Carvalho Jr, P. R. Meneses, "Spectral correlation mapper (scm): An improvement of the spectral angle mapper (sam)," *Summaries of the 9th JPL Airborne Earth Science Workshop, JPL Publication 00-18*, vol. 9, 2000.

[89] C. B. data to life. Pls-da. [Online]. Available: http://www.camo.com/resources/pls-da.html

[90] R. G. Brereton, G. R. Llod, "Partial least squares discriminant analysis: taking the magic away," *Journal of Chemometrics*, vol. 28, pp. 213–225, 2014.

[91] S. Wold, L. Eriksson, J. Trygg, N. Kettaneh, "The pls method – partial least squares projections to latent structures – and its applications in industrial rdp (research, development, and production)." 2004. [Online]. Available: http://citeseerx.ist.psu.edu/viewdoc/download?doi=10.1.1.87.8287&rep=rep1&type=pdf

[92] Amazon. Corning Pyrex Borosilicate Glass Petri Dish Bottom. [Online]. Available: http://www.amazon.com/Corning-Borosilicate-Bottom-Diameter-Height/dp/B004DGII7O/

[93] HySpex. [Online]. Available: http://www.hyspex.no/products/swir_384.php

[94] labsphere. Diffuse reflectance targets. [Online]. Available: http://www.pro-lite.co.uk/File/LAB_Targets_Product_Sheet.pdf

[95] J-L. A. Hegstad, "Hyperspektral avbildning av in vitro sårmodeller fra menneskehud," Master's thesis, Norwegian University of Science and Technology Department of Electronics and Telecommunications, Master Thesis, 2013.

[96] Store norske leksikon. (2015). [Online]. Available: https://snl.no/alger

[97] Algeinfo. [Online]. Available: http://algeinfo.imr.no/index.php?side=visinfo&id=513

[98] Jasco. Model v.550/560/570 spectrophotometer. [Online]. Available: http://www.orgchm.bas.bg/~i2mp/V_550560570.pdf

[99] Y. Mattley. Sorting Plastic Resins Using NIR Spectroscopy. [Online]. Available: http://oceanoptics.com/wp-content/uploads/App-Note-Sorting-Plastic-Resins-Using-NIR-Spectroscopy2.pdf

[100] M. A. Ashraf, M. J. Maah, I. Yusoff, *Biomass and Remote Sensing of Biomass*. InTech, 2011.

[101] H. S. University. Vegetation spectral reflectance curves. [Online]. Available: http://gsp.humboldt.edu/olm_2015/Courses/GSP_216_Online/lesson2-1/vegetation.html

[102] Versalight polarizer. [Online]. Available: http://www.meadowlark.com/versalight-trade-polarizer-p-79?mid=6#.V0XCipGLTgk

# Appendix A: Attachments

## A.1 Matlab-files

The main Matlab-files used for analyzing the data. The wavelengths listed in the code are taken from the information about the camera, and are not fully shown in the attachments due to length.

### A.1.1 Image Viewer

The code makes an image viewer to inspect the spectral features and wavelength intensities of the data.

```
function showshowshow
    FilterSpec = {'C:\Users\Silja\Desktop\Master\matlab\files\Reflected\*.hdr'};
    %Retrieve file ending with .hdr
    [FileName,PathName,~] = uigetfile(FilterSpec);
    %Split FileName to make a .mat-file for quicker access later
    file = regexp(FileName, '\.', 'split');
    matfile = strcat(PathName, file{1}, '.mat');
    if exist(matfile, 'file')
        load(matfile);
    else
        HSI = enviread(strcat(PathName, file{1}));
        save(matfile, 'HSI', '-v6'); % Fast save and load
    end

    %The wavelengths for the spectral bands:
    wavelengths = [962.401794          968.402344          974.402893          980.403

    %Making an empty figure, preallocating
    curx = 1; cury = 1; curz = 1;
    ifig = figure();
    ifig.Pointer = 'crosshair';
    imageHandle = plotImage(curz);
    hold on;
    %Makes it possible to mark an area, specified x and y
    scatterHandle = scatter([],[], 30, 'black', 'o');
```

```
hold off;
sfig = figure();
[plotHandle, vmarkerHandle] = plotSpectrum(curx,cury);

%Plots the image in x-y for a specified wavelength
function imageHandle = plotImage(z)
    z = round(z);
    figure(ifig);
    imageHandle = imshow(HSI.z(:,:,z),'Border','tight');
    colormap jet; colorbar;
    %Set the max. value for the strength to 1 (choosen after
    %evaluation)
    caxis([0 1]);
    set(ifig,'WindowButtonDownFcn',@ImageClickCallback);
    set(ifig,'KeyReleaseFcn',@ImageKeyUpCallback);
    %Shows the wavelength dispalyed in the figure in the header
    set(ifig,'Name',num2str(wavelengths(curz)),'NumberTitle','off');
end

%Replots the image for the choosen wavelength z
function rePlotImage(z)
    curz = round(z);
    set(imageHandle, 'CData', HSI.z(:,:,curz));
    set(ifig,'Name',num2str(wavelengths(curz)),'NumberTitle','off');
end

%Plots the spectrum initially
function [plotHandle,vmarkerHandle] = plotSpectrum(x,y)
    x = round(x); y = round(y);
    figure(sfig);
    spectrumData = squeeze(HSI.z(y,x,:));
    plotHandle = plot(wavelengths, spectrumData);
    hold on;
    plotx = wavelengths(1);
    vmarkerHandle = plot([plotx,plotx],[-1,1]);
    hold off;
    set(sfig, 'WindowButtonDownFcn', @PlotClickCallback);
    if max(HSI.z(:))>1
        maxy = 10000;
    else
```

```
            maxy = max(HSI.z(:));
        end
        ylim([0, maxy]); xlim([wavelengths(1), wavelengths(end)]);
        set(sfig,'Name',sprintf('(%u,%u)',curx,cury),'NumberTitle','off');
    end

    %Replots the spectrum for a choosen x-y coordinate
    function rePlotSpectrum(x,y)
        curx = round(x); cury = round(y);
        data = squeeze(HSI.z(cury,curx,:));
        set(plotHandle, 'YData', data);
        set(sfig,'Name',sprintf('(%u,%u)',curx,cury),'NumberTitle','off');
    end

    function ImageClickCallback ( objectHandle , ~ )
        axesHandle  = get(objectHandle, 'Children');
        coordinates = get(axesHandle(end),'CurrentPoint');
        coordinates = coordinates(1,1:2);
        coordinates(1) = clamp(coordinates(1), 1, HSI.info.samples);
        coordinates(2) = clamp(coordinates(2), 1, HSI.info.lines);
        rePlotSpectrum(coordinates(1), coordinates(2));
        objectHandle.WindowButtonMotionFcn = @ImageClickCallback;
        objectHandle.WindowButtonUpFcn = @StopDragging;
    end

    function ImageKeyUpCallback ( objectHandle, event )
        if strcmp(event.Key, 'space')
            fprintf('(%d, %d, %d) - (%.6f nm)\n', curx, cury, curz, wavelengths(curz)
            ydata = get(scatterHandle, 'YData');
            set(scatterHandle, 'YData', [ydata cury]);
            xdata = get(scatterHandle, 'XData');
            set(scatterHandle, 'XData', [xdata curx]);
        end

        if strcmp(event.Key, 'return')
            fileName = inputdlg('Enter filename:');
            folderName = strcat(PathName, file(1));
            newfile   = strcat(folderName, '/', fileName, '.mat');
            ydata = get(scatterHandle, 'YData');
            xdata = get(scatterHandle, 'XData');
```

```
            if ~exist(folderName{1}, 'dir')
                mkdir(folderName{1})
            end
            save(newfile{1}, 'xdata', 'ydata');

            set(scatterHandle, 'XData', []);    %Removes set points in image
            set(scatterHandle, 'YData', []);
        end
    end

    function PlotClickCallback ( objectHandle , ~ )
        axesHandle  = get(objectHandle, 'Children');
        coordinates = get(axesHandle(1),'CurrentPoint');
        coordinates = coordinates(1,1:2);

        coordinates(1) = clamp(coordinates(1), min(wavelengths), max(wavelengths
        plotx = coordinates(1);
        set(vmarkerHandle, 'XData', [plotx,plotx]);

        x = interp1(wavelengths, 1:length(wavelengths), coordinates(1));
        rePlotImage(x);
        objectHandle.WindowButtonMotionFcn = @PlotClickCallback;
        objectHandle.WindowButtonUpFcn = @StopDragging;
    end

    function StopDragging ( objectHandle, ~ )
        objectHandle.WindowButtonMotionFcn = '';
        objectHandle.WindowButtonUpFcn = '';
    end

    function res = clamp(x, bottom, top)
        res = max(min(x,top),bottom);
    end
end
```

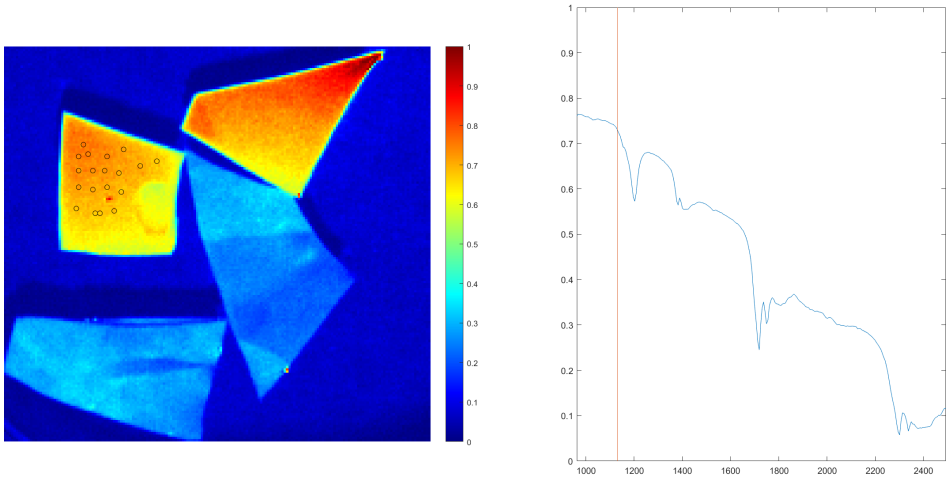


(a) (b)

Figure A.1: Image viewer in MATLAB. (a) False colored image according to spectral intensity at a certain wavelength. (b) spectral features at a certain pixel.

### A.1.2 Spectral Angle Mapper

Calculates the spectral angle, and gives the user the opportunity to false color an image by setting a threshold value for the maximum angle allowed. Illustarted in Figure A.2.

```
function sam_master
    FilterSpec = {'C:\Users'};
    [FileNames,PathName,FilterIndex] = uigetfile(FilterSpec, 'MultiSelect', 'on');
    FileNames = cellstr(FileNames); % If only one file
    motherfile = strcat(PathName(1:end-1), '.mat');
    file = regexp(PathName, 'Reflected\', 'split'); %split where needed
    file1 = regexp(file{2}, '_SWIR', 'split');
    load(motherfile, 'HSI');

    s = size(HSI.z);
    im2d = double(reshape(HSI.z, s(1)*s(2), [])); % Reshape hypercube
    lqs = zeros(s(1),s(2), length(FileNames));

    colors = 'rgbcmy';
```

```
for j = 1:length(FileNames)
    load(strcat(PathName, FileNames{j}), 'ydata', 'xdata');
    spectra = zeros(length(xdata), s(3));
    for i = 1:length(xdata)
        spectra(i,:) = HSI.z(ydata(i), xdata(i), :);
    end
    meanspectra = double(mean(spectra));

    im2d = im2d';
    meanspectra = meanspectra';

    for k=1:s(3) %calculate angle
        tmp = im2d(:,k);
        sam(k) = acos(dot(tmp, meanspectra)/ (norm(meanspectra) * norm(tmp))
    end

    lqs(:,:,j) = reshape(sam, s(1), s(2));

    figure('Name',FileNames{j},'NumberTitle','off')
    imshow(lqs(:,:,j));
    colormap jet; colorbar;
    caxis([0 0.5]);

    limitslider = uicontrol('Style', 'slider',...
                    'Min', min(sam(:)), 'Max', max(sam(:)), 'Value', 0.5,
                    'SliderStep', [0.0001 0.0001],... % (Normalized)
                    'Units', 'normalized',...
                    'Position', [0.1 .9 0.8 .05],...
                    'Callback', @(s,~) caxis([0 s.Value]));
    addlistener(limitslider,'ContinuousValueChange',@(s,~) caxis([0 s.Value]

    cutoffinput = uicontrol('Style', 'edit',...
                        'Min', 0, 'Max', 0,... % Single line input
                        'String', '0.05',...
                        'Units', 'normalized',...
                        'Position', [0.4 .05 0.2 .05],...
                        'Callback', @max_val,...
                        'Tag', num2str(j));
```

```
    end

    rgb_image = zeros(s(1),s(2), 3);
    rgb_figure = figure('Name','rgb_image','NumberTitle','off');
    rgb_im = imshow(rgb_image);
    masks = false(s(1),s(2), length(FileNames)+1);
    colors(length(FileNames)+1) = 'w';

    function max_val(event, ~)
        tag = str2double(event.Tag);
        val = str2double(event.String);
        rgb_image = zeros(s(1),s(2), 3);
        masks(:,:,tag) = lqs(:,:,tag) <= val;
        masks(:,:,end) = sum(masks(:,:,1:end-1),3) > 1;
        for k = 1:(length(FileNames)+1)
            C = colors(k);
            C = rem(floor((strfind('kbgcrmyw', C) - 1) * [0.25 0.5 1]), 2);
            for l = 1:3
                tmp = rgb_image(:,:,l);
                tmp(masks(:,:,k)) = C(l);
                rgb_image(:,:,l) = tmp;
            end
        end

        rgb_im.CData = rgb_image;
        savesam;
    end

    function savesam(~,~)
        set(gca,'fontsize',22);
        q = {'Filename:'}; %Creates user input dialog box (inputdlg)
        PathName = 'C:\Users\Silja\Desktop\Master\matlab\SAM\';

        savename = strcat(PathName, file1{1}, '/', inputdlg(q));
        savename = savename{1};
        if ~exist(strcat(PathName, file1{1}, '/'), 'dir')
            [~] = mkdir(strcat(PathName, file1{1}, '/'));
        end

        imwrite(rgb_image, strcat(savename, '-image.png'));
```

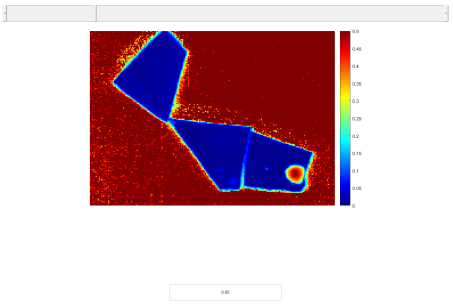

Figure A.2: An example of how one can set the threshold in SAM. The number in the bottom is changed to set the threshold, while the slider at the top changes the scaling of the color bar.

```
    end
end
```

### A.1.3 Principal Component Analysis

The MATLAB-function performs a PCA with a user-interface for setting the PC's to be plotted against each other. Interface shown in Figure A.3.

```
function pkaint4
    wavelengths = [962.401794          968.402344          974.402893          9
    FilterSpec = {'*.hdr'};
    [FileName,PathName,FilterIndex] = uigetfile(FilterSpec);
    file = regexp(FileName, '\.', 'split');
    matfile = strcat(PathName, file{1}, '.mat');

    if exist(matfile, 'file')
        load(matfile);
    else
        HSI = enviread(strcat(PathName, file{1}));
        save(matfile, 'HSI', '-v6'); % Fast save and load
    end

    cropped = cropHSI(HSI.z);
    s = size(cropped);

    pic2d = reshape(cropped, s(1)*s(2), [])';
    B = zscore(pic2d);
```

```
coeff = pca(B);

figure;
image = zeros(s(1), s(2), 3);
new_image = zeros(s(1), s(2), 3);
colim = imshow(image); % Initialialize colorimage
figure;

xpoly = [];
ypoly = [];
recthandle = 0;

sp = uipanel('Title','Scatter plot','FontSize',12,...
             'Position', [.01 .01 .69 .98 ]);%,'Clipping','on');
ax = axes('Parent',sp);
c = zeros(length(coeff(:,1)), 3);
scatterhandle = scatter(coeff(:,1), coeff(:,2), [], c, '.');
hold on;
set(gcf, 'windowbuttondownfcn', @get_info)

function get_info(~, ~)
    pos = get(ax,'CurrentPoint');
    pos = pos(1,1:2);
    x = pos(1); y = pos(2);
    if (x > ax.XLim(1)) && (x < ax.XLim(2)) && (y > ax.YLim(1)) && ...
            (y < ax.YLim(2))
        xpoly = [xpoly x]; ypoly = [ypoly y];
        if recthandle == 0
            recthandle =  plot(xpoly, ypoly);
        else
            recthandle.XData = [xpoly xpoly(1)];
            recthandle.YData = [ypoly ypoly(1)];
        end
    end
end

cp = uipanel('Title','Control','FontSize',12,...
             'Position', [.71 .01 .28 .98]);

xcomp = uicontrol(cp, 'Style', 'popupmenu',...
```

```
                    'String', num2cell(1:size(coeff,2)),...
                    'Units', 'normalized',...
                    'Position', [0 .9 1 .10],...
                    'Callback', @changecoefficient,...
                    'Tag', 'xcomp');
ycomp = uicontrol(cp, 'Style', 'popupmenu',...
                    'String', num2cell(1:size(coeff,2)),...
                    'Value', 2,...
                    'Units', 'normalized',...
                    'Position', [0 .8 1 .10],...
                    'Callback', @changecoefficient,...
                    'Tag', 'ycomp');

uicontrol(cp, 'Style', 'pushbutton',...
              'String', 'What is inside?',...
              'Units', 'normalized',...
              'Position', [0 .72 1 .08],...
              'Callback', @showinpoly);

uicontrol(cp, 'Style', 'pushbutton',...
              'String', 'Clear polygon',...
              'Units', 'normalized',...
              'Position', [0 .64 1 .08],...
              'Callback', @clearpoly);

uicontrol(cp, 'Style', 'pushbutton',...
              'String', 'Red', 'Tag', '1',...
              'Units', 'normalized',...
              'Position', [0 .5 1 .07],...
              'Callback', @colorize);
uicontrol(cp, 'Style', 'pushbutton',...
              'String', 'Green', 'Tag', '2',...
              'Units', 'normalized',...
              'Position', [0 .43 1 .07],...
              'Callback', @colorize);
uicontrol(cp, 'Style', 'pushbutton',...
              'String', 'Blue', 'Tag', '3',...
              'Units', 'normalized',...
              'Position', [0 .36 1 .07],...
              'Callback', @colorize);
```

```
uicontrol(cp, 'Style', 'pushbutton',...
              'String', 'Cyan', 'Tag', '4',...
              'Units', 'normalized',...
              'Position', [0 .29 1 .07],...
              'Callback', @colorize);
uicontrol(cp, 'Style', 'pushbutton',...
              'String', 'Magenta', 'Tag', '5',...
              'Units', 'normalized',...
              'Position', [0 .22 1 .07],...
              'Callback', @colorize);
uicontrol(cp, 'Style', 'pushbutton',...
              'String', 'Yellow', 'Tag', '6',...
              'Units', 'normalized',...
              'Position', [0 .15 1 .07],...
              'Callback', @colorize);

uicontrol(cp, 'Style', 'pushbutton',...
              'String', 'Save',...
              'Units', 'normalized',...
              'Position', [0 .0 1 .07],...
              'Callback', @save_pca);

function changecoefficient(source,~)
    if source.Tag == 'xcomp'
        scatterhandle.XData = coeff(:,source.Value);
    elseif source.Tag == 'ycomp'
        scatterhandle.YData = coeff(:,source.Value);
    end
end

function showinpoly(~,~)
    inside = inpolygon(scatterhandle.XData, scatterhandle.YData,...
                       [xpoly xpoly(1)], [ypoly ypoly(1)]);
    figure();
    imshow(reshape(inside, s(1), s(2)));
end

function clearpoly(~,~)
    xpoly = []; ypoly = [];
    recthandle.XData = xpoly;
```

```
        recthandle.YData = ypoly;
    end

    function colorize(so, ~)
        rgbcmy = str2double(so.Tag);
        inside = inpolygon(scatterhandle.XData, scatterhandle.YData,...
                           [xpoly xpoly(1)], [ypoly ypoly(1)]);
        switch rgbcmy
            case 1
                rgbcmy = [1 0 0];
            case 2
                rgbcmy = [0 1 0];
            case 3
                rgbcmy = [0 0 1];
            case 4
                rgbcmy = [0 1 1];
            case 5
                rgbcmy = [1 0 1];
            case 6
                rgbcmy = [1 1 0];
        end

        if (rgbcmy(1)>0)
            new_image(:,:,1) = reshape(inside, s(1), s(2));end
        if (rgbcmy(2)>0)
            new_image(:,:,2) = reshape(inside, s(1), s(2));end
        if (rgbcmy(3)>0)
            new_image(:,:,3) = reshape(inside, s(1), s(2));end

        mask = new_image ~= 0;
        image(mask) = new_image(mask);
        colim.CData = image;

        sz = size(image);

        scatterhandle.CData(:,1) = reshape(image(:,:,1),1, sz(1)*sz(2));
        scatterhandle.CData(:,2) = reshape(image(:,:,2),1, sz(1)*sz(2));
        scatterhandle.CData(:,3) = reshape(image(:,:,3),1, sz(1)*sz(2));
    end
```

```
function save_pca(~,~)
    % Scatter
    hfig = figure('Visible', 'off');
    scatta = scatter(scatterhandle.XData, scatterhandle.YData,...
                     250, scatterhandle.CData, '.');
    set(gca,'fontsize',22);
    hfig.PaperUnits = 'inches';
    hfig.PaperPosition = [0 0 10 10];
    hfig.PaperPositionMode = 'manual';
    xlabel(['PC' num2str(xcomp.Value)]);
    ylabel(['PC' num2str(ycomp.Value)]);
    q = {'Filename:'};
    path_save = 'C:\Users\Silja\Desktop\Master\matlab\PCA\';
    folder_name = regexp(FileName, '_SWIR', 'split');
    savename = strcat(path_save, folder_name{1}, '/', inputdlg(q));
    savename = savename{1};
    if ~exist(strcat(path_save, folder_name{1}, '/'), 'dir')
        [~] = mkdir(strcat(path_save, folder_name{1}, '/'));
    end

    saveas(scatta, strcat(savename, '-scatter.png'));
    close(hfig);

    % Mean spectra
    if any(scatterhandle.CData(:))
        hfig = figure('Visible', 'off');
        for i = 1:3
            color = [0 0 0];
            color(i) = 1;
            pickus = scatterhandle.CData(:,i);
            if any(pickus)
                picked = pic2d(:, logical(pickus));
                m = mean(picked,2);
                plot(wavelengths, m, 'Color', color, 'LineWidth', 2);
                hold on;
            end
        end

        xlim([wavelengths(1), wavelengths(end)]);
        xlabel('Wavelength (nm)'); ylabel('Reflectance');
```

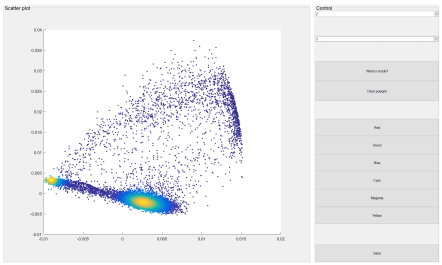

Figure A.3: Thee MATLAB-representation of the PCA-analysis. To the right is a control panel, where one can set the PC one want to use. One can also make a polygon in the scatter plot and check what has been marked, and color the surrounded pixels with the color buttons. The two last options are to clear polygon, were one removes the line of the marked polygon, or save, which saves the scatter plot and the image as PDF-files.

```
            set(gca,'fontsize',22);
            hfig.PaperUnits = 'inches';
            hfig.PaperPosition = [0 0 10 7];
            hfig.PaperSize = [10 7];
            hfig.PaperPositionMode = 'manual';
            saveas(hfig, strcat(savename, '-spectra.pdf'));
            close(hfig);
        end

        % RGB
        imwrite(image, strcat(savename, '-image.png'));
        % Original
        imwrite(cropped(:,:, round(s(3)/10)), strcat(savename, ...
            '-original.png'));
    end
end
```

### A.1.4 Partial Least Squares-Discriminant Analysis

Figure A.4 shows the steps of predicting the data in an image. First the image file is chosen, and area selection, wavelength selection and other options are available in (a). After loading the data, a PCA is performed, and the result is shown in (b) loading plot, (c) intensity plot and (d) PC scatter plot.

Then one can choose the classes/categories to use for the prediction. In (e) the chosen cluster is marked (dark area), and the marked cluster is marked in the

image as well, see (f). After saving the different clusters in classes (e.g. water and PE), one can compose a PLS-DA model.

The result of doing a PLS-DA model is shown as a scatter plot in (g). When the PLS-DA model is made, the image one want to do the prediction on is loaded and then predicted. The prediction is shown in (h).

In this example the sample with PE and 20 ml water was chosen to make the model. The prediction was made on the sample with PE and 30 ml water.

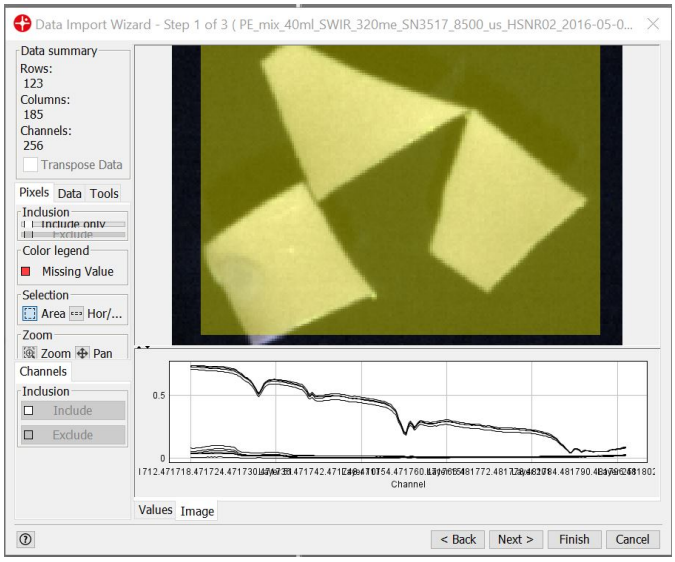


(a) Options after choosing the image file

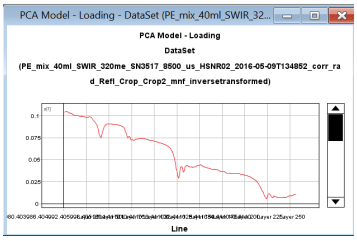


(b) Loading

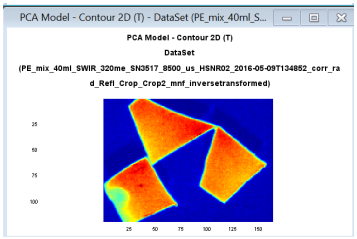


(c) Intensity

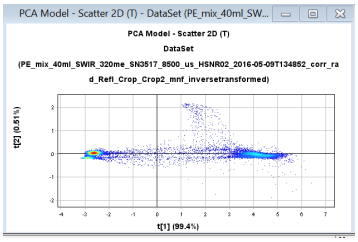


(d) PC scatter plot

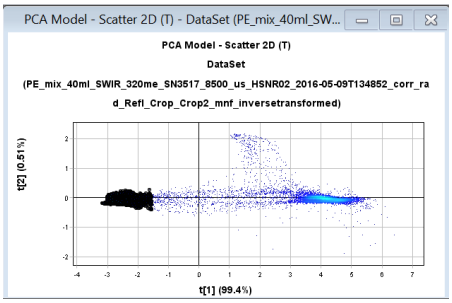


(e) Selected cluster

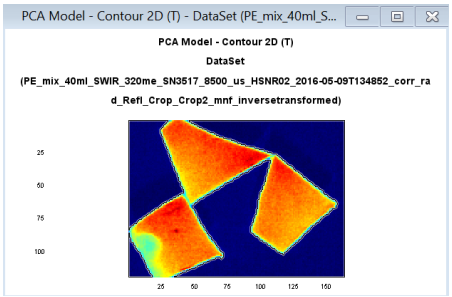


(f) Image from marked cluster

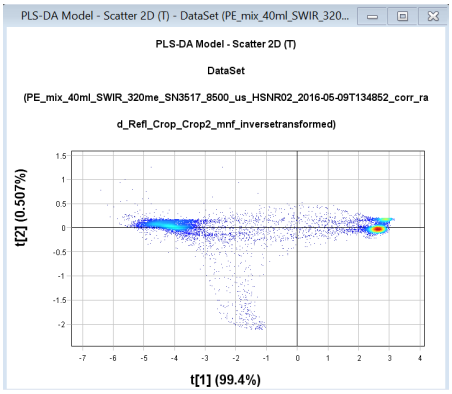


(g) PLS-DA scatter plot

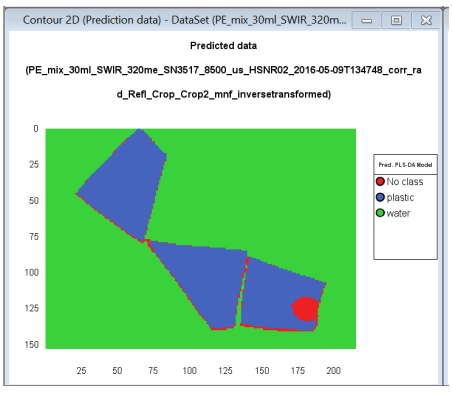


(h) Predicted data

Figure A.4: The steps of PLS-DA in evince. (a) choose what part of the image to use, (b),(c) and (d) loading, intensity and scatter plot from the resulting PCA, (e) selcted cluster in scatter plot, (f) image of the selceted cluster from (e), (g) PLS-DA scatter plot and (h) Predicted data of a chosen image.

### A.1.5 Joiner

Can join images from several files together.

```
function joiner
    FilterSpec = {'*.hdr'};
    [FileNames,PathName,FilterIndex] = uigetfile(FilterSpec, ...
        'MultiSelect', 'on');
    FileNames = cellstr(FileNames); % If only one file
    joined = [];
    for j = 1:length(FileNames)
        file = regexp(FileNames{j}, '\.', 'split');
        matfile = strcat(PathName, file{1}, '.mat');
        if exist(matfile, 'file')
            load(matfile);
        else
            HSI = enviread(strcat(PathName, file{1}));
            save(matfile, 'HSI', '-v6');
        end

        if j == 1
            cropped = cropHSI(HSI.z);
            dimensions = size(cropped);
        else
            cropped = cropHSI(HSI.z, dimensions);
        end

        s_cropped = size(cropped);
        s_joined = size(joined);
        joined(1:s_cropped(1), s_joined(2)+1:s_joined(2)+s_cropped(2), :)...
            = cropped;
    end
    s = size(joined);
    imshow(joined(:,:, round(s(3)/10)))

    HSI.z = joined;
    HSI.info.lines = s(1);
    HSI.info.samples = s(2);
    HSI.info.description = 'Joined files';

    [file,path] = uiputfile('*.mat','Save joined file as');
    matfile = strcat(path, file);
```

```
    save(matfile, 'HSI', '-v6')
end
```

### A.1.6 Crop Image

Crops the image in a chosen rectangular shape.

```
function [ cropped ] = cropHSI( img, dimensions )
    image_fig = figure();
    s = size(img);
    im_handle = imshow(img(:,:, round(s(3)/10)));
    if nargin < 2
        h = imrect(gca,[10 10 s(2)-20 s(1)-20 ]); % initial border of rect
    else
        h = imrect(gca,[10 10 dimensions(2) dimensions(1) ]);
        setResizable(h, 0);
    end

    fcn = makeConstrainToRectFcn('imrect',get(gca,'XLim'),get(gca,'YLim'));
    setPositionConstraintFcn(h,fcn);
    pos = wait(h);
    pos = round(pos);
    cropped = img(pos(2):pos(2)+pos(4), pos(1):pos(1)+pos(3), :);
    close(image_fig);
end
```

### A.1.7 Mean Plotter

Plots the mean spectra of the chosen ROI.

```
    col = 1;
    mainfig = figure();

    while col > 0

        FilterSpec = {'*.mat'};
        [FileName,PathName,~] = uigetfile(FilterSpec, 'MultiSelect', 'on');
        FileName = cellstr(FileName); % If only one file
        motherfile = strcat(PathName(1:end-1), '.mat');
        load(motherfile);

        wavelength = [962.401794          968.402344          974.402893
```

```
        plots = zeros(1, length(FileName));
        load(strcat(PathName, FileName{1}));
        spectra = zeros(length(xdata),size(HSI.z, 3));
            for i = 1:length(xdata)
                spectra(i, :) = HSI.z(ydata(i), xdata(i), :);
            end

        color = get(groot, 'DefaultAxesColorOrder');
        m = mean(spectra);
        figure(mainfig);
        plots(1) = plot(wavelength, m, 'color', color(col,:), ...
            'LineWidth', 4);
        hold on

        q(col) = inputdlg({'Name: '});
        col = col + 1;

        a = inputdlg({'Continue? (y/n)'});
        if a{1} == 'n'
            col = 0;
        end
    end

        set(gca,'fontsize',22);
        xlabel('Wavelength (nm)');
        ylabel('Reflectance');
        legend(q);
        f = {'Filename:'};
        path_save = 'C:\Users\Silja\Desktop\Master\matlab\Mean\';
        savename = strcat(path_save, '/', inputdlg(f));
        savename = savename{1};

        xlim([wavelength(1), wavelength(end)]);
        mainfig.PaperUnits = 'inches';
        mainfig.PaperPosition = [0 0 10 7];
        mainfig.PaperSize = [10 7];
        mainfig.PaperPositionMode = 'manual';
        saveas(mainfig, strcat(savename, '-spectra.pdf'));
        close(mainfig);
```

```
        % a = 1392; makes red vertical line
% line([a a], [m(256)-0.1 m(20)+0.1], 'Color', [1 0 0], 'LineWidth', 4)
```

## A.2 Instrumentation

### A.2.1 Petri Dish

Specifications of the petri dish are found in Table A.1.

Table A.1: Petri Dish Specifications[92]

| Specification | |
|---|---|
| Brand Name | Corning |
| Part Number | 3160-100BO |
| Material Type | Borosilicate Glass |
| Inside Diameter | 95 mm |
| Inside Height | 12 mm |
| Outside Diameter | 95 mm |
| Outside Height | 12 mm |
| UNSPSC Code | 41122101 |

### A.2.2 HySpex SWIR-320m-e

Specifications of the hyperspectral camera used during the experiments are given in Table A.2.

Table A.2: HySpex SWIR-320m-e Main Specifications[93]

| Specification | |
|---|---|
| Spectral Range | 1.0 µm to 2.5 µm |
| Spatial Pixels | 320 |
| F-Number | F2.0 |
| FOV across track | 13.5° |
| Pixel FOV across/along track | 0.75 mrad/0.75 mrad |
| Spectral sampl. | 6 nm |
| # of bands | 256 |
| Binning modes | - |
| Noise floor | - |
| Peak SNR | - |
| Dynamic range | - |
| Digitization | 14 bit |
| Max frame rate | 100 fps |
| Sensor head weight | 7.5 kg |
| Sensor head dimension (l*w*h in cm) | 36x14x15.2 |
| Sensor head power consumption | ∼100 W |
| FPA cooling T | ∼195 K |

### A.2.3 Salt Water

Image of the pure NaCl-water used to compare the collected salt water from the ocean is shown in Figure A.5.

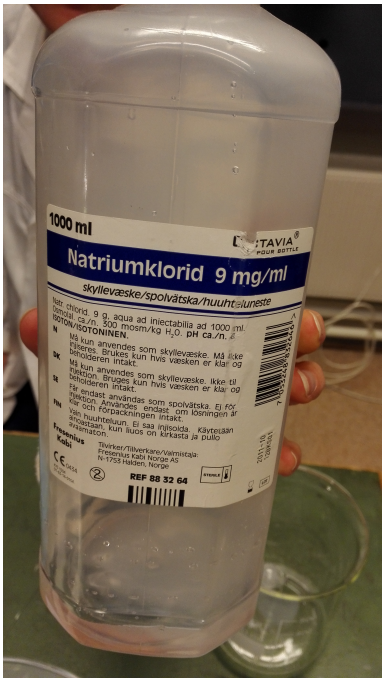


Figure A.5: Salt water used during experiment.

### A.2.4 Versalight$^{TM}$Polarizer IR

The specifications of the polarizers used in the experiments are shown in Table A.3.

Table A.3: Versalight$^{TM}$Polarizer IR[102]

| Specification | |
|---|---|
| Wavelength Range | 1000 nm to 2000 nm |
| Substrate Material | Eagle XG® |
| Transmitted Wavefront Distortion | ~5$\lambda$ per in. |
| Surface Quality (scratch-dig) | 80-50 |
| Beam Deviation | $\leq$ 1arc-min |
| Contrast ratio | Refection > 80:1<br>Typ. Transmission > 2000:1 |
| Maximum Temperature | 200 °C |
| Laser Damage Threshold | 10 kW/cm$^2$, CW, 1540 nm |